REPUBLIC OF TURKEY

YILDIZ TECHNICAL UNIVERSITY

GRADUATE SCHOOL OF SCIENCE AND ENGINEERING

WASTE WATER HEAVY METAL TREATMENT BY THE USE OF CHITOSAN OBTAINED FROM CARIDEA AND BRACHYURA SHELLS

Zehra Özden ÖZYALÇIN

MASTERS OF CHEMICAL ENGINEERING THESIS

Department of Chemical Engineering

Chemical Engineering Program

Supervisor

Assoc. Prof. Dr. Azmi Seyhun KIPÇAK

June, 2022

REPUBLIC OF TURKEY

YILDIZ TECHNICAL UNIVERSITY

GRADUATE SCHOOL OF SCIENCE AND ENGINEERING

WASTE WATER HEAVY METAL TREATMENT BY THE USE OF CHITOSAN OBTAINED FROM CARIDEA AND BRACHYURA SHELLS

A thesis submitted by Zehra Özden ÖZYALÇIN in partial fulfillment of the requirements for the degree of MASTERS IN CHEMICAL ENGINEERING is approved by the committee on 09.06.2022 in Department of Chemical Engineering, Chemical Engineering Program.

Assoc. Prof. Dr. Azmi Seyhun KIPÇAK
Yıldız Technical University
Supervisor

Approved By the Examining Committee

Assoc. Prof. Dr. Azmi Seyhun KIPÇAK, Supervisor
Yildiz Technical University _____

Prof. Dr. Emek MÖRÖYDOR DERUN, Member
Yildiz Technical University _____

Prof. Dr. Tülin Banu İYİM, Member
Istanbul University - Cerrahpaşa _____

I hereby declare that I have obtained the required legal permissions during data collection and exploitation procedures, that I have made the in-text citations and cited the references properly, that I haven't falsified and/or fabricated research data and results of the study, and that I have abided by the principles of the scientific research and ethics during my Thesis Study under the title of Waste Water Heavy Metal Treatment by The Use of Chitosan Obtained from Caridea and Brachyura Shells supervised by my supervisor, Assoc. Prof. Dr. Azmi Seyhun KIPÇAK. In the case of a discovery of a false statement, I am to acknowledge any legal consequence.

Zehra Özden ÖZYALÇIN

Signature

This study was supported by the project number FYL-2020-3933 of Yıldız Technical University Scientific Research Project Coordination.

Dedicated to my family

and my beloved friends

ACKNOWLEDGEMENTS

I would like to express my deepest gratitude to my supervisor Assoc. Prof. Dr. Azmi Seyhun KIPÇAK for his invaluable patience and everlasting support. I would like to extend my sincere thanks to Prof. Dr. Emek DERUN and Assoc. Prof. Dr. Nurcan TUĞRUL for generously providing me with plentiful opportunities and immense knowledge. I would also like to thank Assist. Prof. Dr. Ekin KIPÇAK for her unceasing encouragement and moral support throughout my academic research. In addition, I would like to thank Yıldız Technical University Scientific Research Projects Coordination Unit for financially supporting this study research.

Lastly, words cannot express my gratitude to my beloved parents, sister, and spouse who have never given up on moral support. I would also like to thank my friends and colleagues for keeping my motivation high throughout my journey.

.

Zehra Özden ÖZYALÇIN

TABLE OF CONTENTS

LIST OF SYMBOLS

%	Percentage
°C	Degree Celsius
a*	Redness
Al	Aluminium
b*	Yellowness
cm	Centimeter
dL	Deciliter
g	Gram
h	Hour
kDa	Kilodalton
kg	Kilogram
L	Liter
L*	Lightness
mg	Milligram
min	Minute
mL	Milliliter
Pb	Lead
s	Second
Sb	Antimony
W	Watt
w/v	Weight Per Volume
ΔE	Total Color Change
µg	Microgram
µm	Micrometer

LIST OF ABBREVIATIONS

ATSDR	Agency for Toxic Substances and Disease Registry
CCD	Charge Coupled Device
DNA	Deoxyribonucleic acid
EFSA	European Food Safety Authority
FAO	Food and Agriculture Organization of the United Nations
FT-IR	Fourier-Transform Infrared Spectroscopy
IARC	International Agency for Research on Cancer
ICP-OES	Inductively Coupled Plasma Atomic Emission Spectroscopy
IR	Infrared
JECFA	The Joint FAO/WHO Expert Committee on Food Additives
mRNA	Messenger Ribonucleic Acid
N.D.	Not Detected
ppm	Parts-per-million
RF	Radio Frequency
rpm	Revolutions per Minute
RT	Room Temperature
US	United States of America
USD	United States Dollar
WHO	The World Health Organization

LIST OF FIGURES

LIST OF TABLES

ABSTRACT

Waste Water Heavy Metal Treatment by the Use of Chitosan Obtained from Caridea and Brachyura Shells

Zehra Özden ÖZYALÇIN

Department of Chemical Engineering

Masters of Chemical Engineering Thesis

Supervisor: Assoc. Prof. Dr. Azmi Seyhun KIPÇAK

At the forefront of the major issues of the modern world is the waste problem and therefore pollution. Heavy metals, one of the leading pollutants, often cause irreversible damage to living life by contaminating spring waters and soil. Therefore, the removal of heavy metals is becoming an increasingly essential concern. Millions of tons of chitin-rich shellfish that take many years to biodegrade are caught every year in the fisheries and aquaculture industries, a sector that finds a very limited place in recycling. The industrial applications of chitin, which has an important economic value, are limited due to its physicochemical properties. Chitosan, obtained by deacetylation of chitin molecules in an alkaline medium, is not only the cheapest and simplest chitin derivative but also one of the most widely utilized biopolymers for adsorption of a wide range of substances. The use of chitosan, which has a very high adsorption capacity and is already produced from wastes, for heavy metal removal could be a solution that will both eliminate waste disposal and prevent pollution. The aim of the thesis is to determine the effects of different parameters on chitosan production and to test the success of the produced chitosan samples in the adsorption processes of selected heavy metals. For chitosan production, caridea (shrimp) and brachyura (crab) shells were reduced to different sieve sizes and subjected to chemical treatments at different deacetylation temperatures. In order to test

the success of chitosan production, FT-IR analyzes were applied to all samples from the raw material to the final product and the chemical structures of the samples were examined comparatively. In addition, color analyzes were carried out to examine the color changes of all samples. For each stage of the production, the production yield was calculated based on the weight loss. The produced chitosan samples were mixed in Antimony, Aluminium and Lead solutions for certain periods and adsorbed heavy metal ions. Then, the adsorption amounts were determined by ICP-OES analysis, and the obtained data were evaluated comparatively for all parameters.

Keywords: Adsorption, biopolymer, chitosan, heavy metal, seashell

ÖZET

Caridea ve Brachyura Kabuklarından Elde Edilen Kitosan ile Atık Sulardan Ağır Metal Giderimi

Zehra Özden ÖZYALÇIN

Kimya Mühendisliği Anabilim Dalı

Yüksek Lisans Tezi

Danışman: Doç. Dr. Azmi Seyhun KIPÇAK

Modern dünyanın temel sorunlarının başında atık problemi ve dolayısıyla kirlilik gelmektedir. Kirleticilerin başında gelen ağır metaller, kaynak suları ve toprakla karışarak canlı yaşama çoğu zaman geri dönüşü olmayan zararlar vermektedir. Bu nedenle, ağır metallerin uzaklaştırılması her geçen gün önemi artan bir konudur. Geridönüşümde kendine oldukça kısıtlı yer bulan balıkçılık ve su ürünleri yetiştiriciliği endüstrilerinde her yıl milyonlarca ton biyobozunumları uzun yıllar alan kitince zengin kabuklu deniz canlısı işlenmektedir. Önemli bir ekonomik değere sahip olan kitinin endüstriyel uygulanmaları fizikokimyasal özellikleri nedeniyle sınırlı kalmaktadır. Kitin moleküllerinin alkali ortamda deasetilasyonu ile elde edilen kitosan, kitinin sadece en ucuz ve basit türevi değil aynı zamanda çok çeşitli maddelerin adsorpsiyonu için kullanılan en yaygın biyopolimerlerdendir. Adsorpsiyon kapasitesi çok yüksek olan ve hali hazırda atıklardan üretilen kitosanın ağır metal gideriminde kullanılması hem atık bertarafını ortadan kaldıracak hem de kirlilik sorununu önleyecek bir çözüm olabilir.

Tezin amacı, farklı üretim parametrelerinin kitosan üretimi üzerine etkilerini tespit etmek ve üretilen kitosan numunelerinin seçili ağır metallerin adsorpsiyon işlemlerindeki başarısını test etmektir. Kitosan üretimi için, caridea (karides) ve brachyura (yengeç)

kabukları farklı elek boyutlarına indirilmiş ve farklı deasetilasyon sıcaklıklarında kimyasal işlemlere tabi tutulmuştur. Kitosan üretimindeki başarıyı test etmek amacıyla, hammaddeden son ürüne kadar tüm numunelere FT-IR analizleri uygulanmış ve numunelerin kimyasal yapıları karşılaştırmalı olarak incelenmiştir. Bunun yanında tüm numunelerin renk değişimlerini incelemek amacıyla renk analizleri gerçekleştirilmiştir. Her üretim safhası için numunelerin ağırlık kaybı baz alınarak üretim verimi hesaplanmıştır. Üretilen kitosan numuneleri Antimon, Alüminyum ve Kurşun çözeltilerinde belirli süreler boyunca karıştırılarak ağır metal iyonlarını adsorplaması sağlanmıştır. Adsorpsiyon miktarları ICP-OES analizleri ile ölçülmüş ve elde edilen veriler tüm parametreler için kıyaslamalı olarak değerlendirilmiştir.

Anahtar Kelimeler: Adsorpsiyon, ağır metal, biyopolimer, kabuklu deniz canlısı, kitin, kitosan

1
INTRODUCTION

1.1 Literature Review

Building healthy ecosystems is one of the main goals of societies. The concept of sustainability, good evaluation of resources, and recycling, are very important issues in order to create a healthy ecosystem and to ensure the continuity of natural resources and living life. However, the concept of sustainability also has limitations such as cost and efficiency.

In recent years, great efforts have been made to replace petrochemical products with renewable and sustainable ingredients. The importance of protecting the environment has also increased the work on the development of biodegradable and biocompatible polymers. Many polymers of natural origin are becoming attractive alternatives as they can reduce the need for fossil fuels. The most difficult part of this job is to obtain bio-sourced materials with equivalent properties to synthetic products.

Efforts to create a healthy ecosystem are progressing not only in the name of prevention of pollution but also in the compensation of pollution. The wastes emitted to the environment as a result of industrial and mining activities deeply affect the environment and human health. Among these wastes, it has been proven by many studies that especially heavy metals cause serious damage to living organisms, can be carcinogenic, and cause hereditary deterioration.

Considering all these contemporary problems, the use of biopolymers produced from waste in the removal of other pollutants is seen as a very bright solution. In this field, chitosan is an eye-catching biopolymer with superior adsorption abilities that can be obtained from shells of shellfish, insects, and fungi. In addition to its many industrial applications, chitosan is well-known for its excellent performance, especially in the removal of heavy metals.

While chitosan contributes to waste disposal and reduction of environmental pollution by being obtained from waste, it has been the focus of many scientific studies with its ability to remove the most dangerous pollutants. To summarize some of these studies for the production of chitosan from shellfish: Srinivasan et al. (2018) produced chitosan to measure the anticancer effects of chitosan in their study. In this study, ground shrimp shells were demineralized with 1/30 (w/v) 1 M hydrochloric acid (HCl) at room temperature for 75

minutes under continuous stirring. In the deproteinization stage, mixing was performed with 3 M sodium hydroxide (NaOH) at a ratio of 1/30 (w/v) and at room temperature for 75 minutes, and the color was removed with acetone and sodium hypochlorite. Deacetylation was carried out by mixing 50% NaOH with a 1/50 (w/v) ratio at 90 °C.

Charoenvuttitham et al. (2006) examined alternative extraction methods in the production of chitosan with black tiger shrimp shell waste and reported the general procedures for the chemical extraction of chitosan. In the study, they performed deproteinization with 1 M NaOH at a ratio of 1/15 (w/v) at 95°C for 6 hours. The demineralization step was completed in 30 minutes at ambient temperature with 0.25 M HCl at a ratio of 1/30 (w/v). In the study, it was also stated in the literature that when shellfish were used, deproteinization was performed using NaOH solution at 65-100°C and 1-10% (w/v) concentration. In addition, it has been stated that the material/solution ratio in the deproteinization stage causes a very low yield increase above 1/4 (w/v) and the reaction time is generally between 0.5 and 6 hours in literature studies. In addition, it has been stated that demineralization is usually performed with 1-8% HCl and 1-3 hour extractions.

Kucukgulmez et al. (2011) studied the physicochemical properties of by obtaining chitosan from the shells of a shrimp species Metapenaeus stebbingi. The deproteinization step was carried out with 2.5 N NaOH at 65 °C for 6 hours, while the demineralization step was carried out with 1.7 N HCl at 25 °C for 6 hours. Chitosan was also obtained by deacetylation with 50% (w/v) NaOH at 120 °C.

Teli & Sheikh (2012) examined the antibacterial applications of chitosan obtained from shrimp shells in their study. For this, the cleaned and ground peels were deproteinized with 1 M NaOH solution for 24 hours, demineralized with 1 M HCl solution, and then deacetylated using 50% NaOH solution.

In the studies of Kumari & Rath (2014), chitosan was obtained from fish scales. Fish scales were kept in 1% HCL and 2 N NaOH solutions for 36 hours in the demineralization and deproteinization stages, respectively. Then, color removal was done with potassium permanganate for 1 hour. In the deacetylation stage, chitin was converted to chitosan using a 50% NaOH solution.

Some studies for heavy metal adsorption studies of produced or commercially available chitosans can be summarized as follows: Chen et al. (2017) found that the modified chitosan-iron(III) composite showed high performance in the simultaneous removal of tetracycline,

an antibiotic, and the heavy metal cadmium(II), which is classified as a human carcinogen. In this way, it has been verified that both drug residues and heavy metals can be removed simultaneously.

Liu et al. (2015) investigated the adsorption of magnetic chitosan nanoparticle arsenic(III) and arsenic(V) in their study. In the study in which different initial metal concentrations were examined, it was determined that more than 95% of arsenic was adsorbed successfully. It has been determined that the removal of arsenic, which is considered the most dangerous metal, is achieved and chitosan nanoparticles can be used by regenerating repeatedly.

Eivazzadeh-Keihan et al. (2020) investigated the lead(II), copper(II), and chromium(VI) adsorption of modified chitosan composite. In this study, in which the carcinogenic effects of selected heavy metals were investigated, high adsorption rates were obtained especially with copper(II) and lead(II) ions.

According to Shahraki et al. (2020), lead(II) adsorption of modified chitosan was investigated. In the study examining the effects of the chemical properties of the adsorption medium on the adsorption mechanism, it was determined that chitosan supported by aromatic rings was quite successful in lead(II) adsorption.

Liu et al. (2012) investigated the adsorption of gold(III) and lead(II) using chitosan-based composite material. In order to test the suitability of the produced composite material for adsorption studies, chemical content and surface analyzes were performed and it was determined that optimum adsorption performance was obtained in acidic environments (pH 3.0-5.0) and the adsorption processes were spontaneous and endothermic.

Yan et al. (2011) studied the adsorption of copper(II) using modified chitosan hydrogel beads and found that the adsorbent could be easily desorbed and reused at low pH values.

Wang et al. (2012) investigated the recovery of gold(III) by carboxymethylation and sulfur cross-linked chitosan. In the study, in which the changes in the adsorption environment and process parameters were also examined, it was determined that the cross-linked chitosan samples produced under pH 4.0 and room temperature conditions showed high performance for gold(III) adsorption.

Gedam and Rajendra (2015) investigated lead(II) removal with iodate-doped chitosan composite in their study. Chitosan samples, which were subjected to surface examinations to determine their suitability for adsorption processes, were subjected to adsorption processes including different acidity, adsorbent concentration, and metal concentration. In

experiments that resulted in high yields, it was observed that iodate additive caused a decrease in chitosan pores.

Igberase et al. (2014) investigated the use of polyaniline grafted chitosan beads in the removal of copper(II) metal ions. In their study, in which process parameters and ambient acidity were also examined, adsorption isotherms, mechanism, and thermodynamics were investigated and they determined that copper(II) adsorption occurs spontaneously and endothermically in nature with chitosan samples produced.

Kyzas and Eleni (2013) investigated mercury(II) removal with modified chitosan samples in their study. In the study, which also included various characterization analyzes, it was determined that pH 5 for adsorption studies and pH 2 for desorption for cross-linked chitosan samples constituted the optimum working environment.

1.2 Objective of the Thesis

This study includes multiple interrelated objectives. Sustainability of resources and waste problems are among the biggest agendas of our world. The seafood processing industry, which is notorious for its failure in waste disposal, discharges its wastes rich in valuable components into the seas, causing both wastages of resources and pollution of the seas. The chitin in the content of these wastes, and the most known variation, chitosan, are natural, non-toxic, and biodegradable polysaccharide polymers whose effective application is known in many industries. Chitosan, which is formed by changing the chemical structure that limits the activity of chitin biopolymer, widely functions as an adsorbent with its low cost and easy production. The adsorption process is one of the most common methods preferred for the removal of pollutants such as heavy metals, dyes, and drug residues from wastewater and natural water sources with its low cost and ease of processing. Among these pollutants, especially heavy metals can cause hereditary disorders and even death, and threaten the continuity of all living things, especially humans, due to their bioaccumulation.

The first aim of this study is to convert the wastes of shellfish, which consists largely of chitin, into the high value-added biopolymer chitosan. In this way, both the reduction of waste disposal requirements and the need for raw materials to be used in different functions will be met from these wastes. In addition, the secondary aim of the study is to reduce the adverse effects of wastewater on living organisms by providing the use of chitosan, which is produced by using these wastes, for the removal of heavy metals, which is one of the most dangerous substances known, from aqueous environments. In line with these two purposes,

it aims to eliminate wastes with a valuable biopolymer material to be produced from animal wastes and contribute to the sustainability of both the seafood used as raw material and the sustainability of water resources.

Finally, another aim of the study is to examine the effects of the use of different raw materials and production parameters on chitosan production and to examine the effects of these parameters on adsorption amounts. It can be summarized what is mainly aimed in the study is to determine the chitosan production parameters that should be used for the adsorption study of specific heavy metals and to perform the adsorption more effectively.

1.3 Hypothesis

Food sustainability and waste problems, which develop with the rapid increase in the world population and consumption diversity, meet on a common denominator. The answer to these problems can be chitosan, again the common denominator of both problems. Chitosan, the most well-known derivative of chitin, which makes up the majority of the shell percentages of shellfish, is a polysaccharide biopolymer produced from waste and attracts attention with its wide application areas. Recovery of chitin, hence chitosan, from waste can be presented as a solution to the waste problems of the seafood processing industry. The conversion of chitin to chitosan through various chemical processes reduces the restrictions on its physical and chemical properties. Due to the reduction of these restrictions, chitosan shows a very active adsorbent activity. Chitosan, which is currently obtained from wastes, stands out with its high adsorbent properties, especially in water and wastewater treatment processes. Metal and metal oxides, which are the cornerstones of many industries, are referred to as heavy metals due to their destructive effect on life and their bioaccumulation. These substances, which are among the leading water pollutants, must be removed from water resources for the sustainability of vitality and resources. In this arena, chitosan can be employed in heavy metal adsorption processes to solve the aforementioned food sustainability and waste issues. Chitosan's performance in these adsorption procedures is directly influenced by its physical and chemical structure. As a result, characteristics employed in the production stages of chitosan, such as raw material source, particle size, and processing temperature, have a direct impact on the quality of the final product and, as a result, the adsorption trial results obtained with these chitosan samples. Aside from that, each heavy metal has a different interaction with different adsorbents. Accordingly, different adsorption processes can be observed in the use of the same sample for the removal of different heavy metal ions.

2
SHELLFISH

Consumers today tend to diversify their diets among healthy alternatives (Harnedy & FitzGerald, 2012). In this perspective, with the triggering effect of population growth and increasing market opportunities, seafood has become a rapidly increasing food stock with its unique taste and texture (Venugopal & Gopakumar, 2017). Sea creatures, which make up about half of the total global biodiversity, are seen as an alternative to many food sources with the protein, peptide and amino acids they contain, and their consumption rates are increasing rapidly (Harnedy & FitzGerald, 2012). In 2014, while 146.3 million metric tons of seafood was used as human food, it was determined that seafood contributed approximately 20% of animal protein intake (Venugopal & Gopakumar, 2017). Seafood includes edible sea creatures such as bony and cartilaginous fish, shellfish, and mollusks. Shellfish is a common colloquial and fishing term for chitin-based exoskeleton-bearing seafood such as bivalve molluscs such as scallops, oysters, and mussels, crustaceans such as shrimp, crabs, and lobsters, and some echinoderms (Ruethers et al., 2018; Shellfish, 2022)

Crustaceans are a large group that includes crabs, lobsters, copepods, ostracods, crayfish, shrimps, mussels, and tiny water fleas (Ripley & Dana, 1859). Crustaceans are one of the world's oldest and most diverse arthropods, as well as one of the most successful groups of invertebrates, with 150,000 described species. In addition to being extremely successful in aquatic environments, some species have also evolved to adapt to land. Although approximately 90% of currently identified species are found in marine systems, the remaining 10% are found in various inland waterways and play a key role in numerous surface and subsurface lotic and lentic ecological processes (Hobbs et al., 2012). Crustaceans are anatomically diverse. They have developed a variety of body morphologies through the fusion of multiple parts as well as the development of very specific body parts and appendages. Crustaceans have a hard exoskeleton and this exoskeleton is incapable of growth. Therefore, as the creature grows, it leaves its old skeleton and creates a new one. This skeleton helps protect them from predators and reduces water loss (Diarte-Plata & Escamilla-Montes, 2020). Among seafood products, crustaceans have high commercial value. The number of crustaceans produced in 2018 was 9.4 million tons (FAO, 2021).

Molluscs are one of the richest and most popular subgroups of crustaceans in terms of species. Their bodies are soft and often have a crusty exterior. These creatures can live on land, in freshwater, or in seawater. Most of the invertebrate mollusks are cephalopods, gastropods, and bivalves. With over 100,000 species, gastropods make up over 80% of all mollusks and are by far the most diverse group in the phylum. While oysters, scallops, mussels, octopus, cuttlefish, and some snails contain high protein, gastropods, bivalves and scaphopod shells have been used for ornamental and monetary purposes throughout the ages. The total number of mollusks produced in 2018 is over 17.5 million tons (FAO, 2021).

There are more than 1000 species of crustaceans, 50000 species of mollusks and 13000 fish species that are estimated to exist in the oceans (Venugopal & Gopakumar, 2017). The main crustaceans with high commercial value are shrimp, mussel, lobster, and crab species, and their consumption has been increasing steadily (Rebouças et al., 2021).

2.1 Brachyura

Crabs are decapod crustaceans belonging to the Brachyura infraorder that can live in both fresh and salt water, as well as on land, and have a characteristic projecting belly, hard skeleton, and claws. Their shells are mostly composed of chitin. There are 7000 known species of crabs with sizes (leg spans) ranging from a few millimeters to 4 m (Chen et al., 2008; Davie et al., 2015). Some of the most commercially valuable species are *Portunus trituberculatus, Callinectes sapidus, Scylla serrata* and *Cancer pagurus* (Figure 2.1). Crabs usually shows sexual dimorphism. Males have a long triangular protrusion of the abdomen, while females have a wider, rounded abdomen that is used to carry fertilized eggs (Guerao & Rotllant, 2009).

Figure 2.1 Brown crab (*Cancer pagurus*) (Whole Cooked Male Crab, n.d.)

Crabs are an essential part of the world's aquaculture industry, accounting for 20% of all shellfish consumption. While the capture was 1.5 million tons, the financial value reached 4.6 billion dollars in 2019, with over 5.8 thousand tons exported (FAO, 2021). Crabs are rich in protein, minerals, precious oil, enzymes, and chitin. Because of the high percentage of shell in crab processing, biowaste is produced, principally chitin, which can pose sustainability issues in fisheries and seafood farms (Nguyen et al., 2020).

2.2 Caridea

Shrimps are swimming decapod crustaceans with elongated bodies, a narrow muscular abdomen, long antennae, and slender legs, including the suborders Caridea (true shrimp) and Dendrobranchiata (prawns). The definition of shrimp can be used to name any small crustacean resembling a shrimp. However, according to the definition of FAO (Food and Agriculture Organization of the United Nations), species living in freshwater are defined as prawns, and species living in marine and brackishwater are defined as shrimp (Fast & Lester, 2013). There are thousands of shrimp living in different habitats. The most commercially advanced shrimp group is the Caridea (Shrimp, 2022), known as the caridean shrimp or true shrimp. *Pandalus borealis*, which is given in Figure 2.2, commonly known as pink shrimp, is the most widely consumed and commercially important caridea species. Caridea can have a body length of between 1.2 cm and 30 cm and a lifespan of 1 to 6.5 years (Caridea, 2022).

Figure 2.2 Pink shrimp (*Pandalus borealis*) (Fulcher's Brand Royal Red Shrimp, n.d.)

Shrimp, whose production has increased by 76.6% in the last decade, is one of the products with the highest commercial value among seafood with its contribution to global aquaculture production (El-Sayed, 2021). While shrimp reached a financial value of 25.6 billion US dollars with an export of over 4.7 million tons in 2019, it is estimated that the export amount will reach 7.28 million tons and the financial value will reach 67.6 billion US dollars by 2025. Asian countries (Thailand, Japan, and South Korea) constitute 80% of the world's market in shrimp farming (Nirmal et al., 2020; FAO, 2021). About 25% of exported shrimps

undergo cooking or shell removing processes (Pohling et al., 2022). During these processing activities, more than half of the biomass of the shrimps, including the head, internal organs, and shells, is discharged into the sea as waste or buried in the ground. These organs, which are classified as waste, are products of financial value rich in protein, minerals, valuable oil, and chitin. Considering their high tonnage production, it is essential to compensate for the loss of bioactive material during processing both economically and in terms of the sustainability of shrimp production (Nirmal et al., 2020; Dave et al., 2020).

2.3 Sustainability and Waste Treatment Requirements

As the shellfish is one of the world's most important aquaculture categories, sustainability studies in its production and processing are essential for food supply and safety (Azra et al., 2021). A large amount of seafood waste is released each year as marine processing by-products, consisting of viscera, heads, skins, fins, and shellfish. These by-products are usually either dumped into the sea as waste or buried in the ground or used as animal feed or fertilizer (Harnedy & FitzGerald, 2012). It is estimated that 6 to 9 million tons of waste is generated annually worldwide, especially in the production of crustaceans such as shrimp, crabs and lobsters (Kaisler et al., 2019). While the value of these wastes, mostly consisting of shells, is 100 - 120 USD/ton, the disposal cost is estimated to reach 150 USD/ton (Yan & Chen, 2015). The recovery of high-value functional components contained in these by-products can offer a solution to deal with the associated legal restrictions, high cost, and environmental problems experienced during waste disposal (Harnedy & FitzGerald, 2012).

The scarcity of environmental resources has led many countries around the world to sustainable production and consumption regimes. In this sense, many studies are being conducted on the recovery of useful bioactive compounds in wastes and making the recovered products useful again. It is known that large volumes of biomass waste occur, especially in the production of shellfish. However, the number of studies on the recovery of these products is very few compared to terrestrial biomass (Moovendhan et al., 2019; Rebouças et al., 2021). According to the data published by FAO, a total of 10 million tons of crustaceans and 18 million tons of mollusks were produced in 2018 (FAO, 2021). During the processing of these products, 20% to 70% of the biomass is assorted as waste. Since this biomass, which is separated as waste, contains highly degradable biological factors, it should be disposed of shortly after production or processing. Shellfish wastes, which are disposed of in erroneous ways, cause many negative effects on the environment, especially on aquatic resources, as it creates a suitable environment for microbial proliferation. Bioactive

compounds in the composition of crustacean wastes create great potential areas for the recovery of these wastes. Crustacean and mollusc wastes have high financial value with essential amino acids, valuable fatty acids, minerals, carotenoids, and chitin and its derivatives (Sowmya et al., 2011; Routray et al., 2019; Rebouças et al., 2021). Depending on the type of these wastes, they may contain 30-40% protein, 30-50% minerals, 15-40% chitin, 10-60% fatty acids, and important bioactive compounds such as polyunsaturated fatty acids, collagen, and vitamins. These valuable bioactive compounds can be recovered by various methods and their activity can be increased. Recovered compounds can find applications in many industries such as agriculture, livestock, pharmaceuticals, food, cosmetics, nutricosmetics, and textiles (Andonegi et al., 2020; Sah et al., 2019).

3
CHITOSAN

Chitin is the most abundant structural linear polysaccharide after cellulose. Chitin, whose chemical formula is given in Figure 3.1, acts as a protective and supporting material in the cell walls of fungi, exoskeletons of arthropods, cuticles of insects, and shells of crustaceans. It is known that the shells of some shellfish contain up to 75% chitin (Kou et al., 2021). Chitin is generally produced from crab, shrimp, krill shells, and mushrooms, which have high biomass, low cost and require waste disposal (Yan & Chen, 2015; Bakshi et al., 2020). Chitin is a biodegradable material with bioactive and non-toxic properties, but chitin derivatives with high solubility are compounds of high commercial interest because they are insoluble in water and almost all organic solvents (Rebouças et al., 2021; Aranaz et al., 2021).

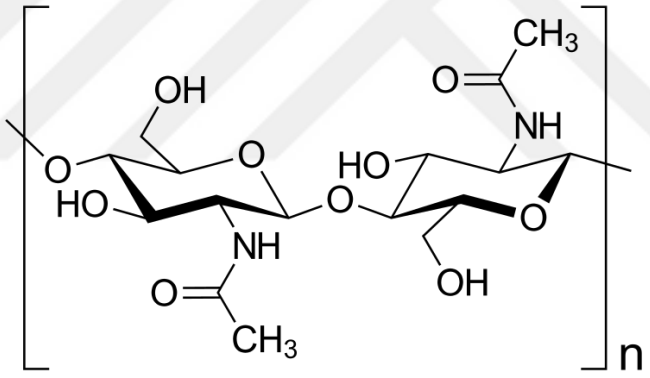

Figure 3.1 Chemical structure of chitin (part of the polymer chain) (Chitin, 2022)

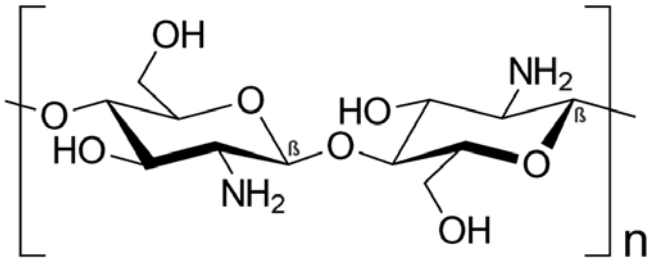

Figure 3.2 Chemical structure of chitosan (part of the polymer chain) (Chitosan, 2022)

Chitosan, whose chemical formula is given in Figure 3.2, is the cheapest and most common functional derivative of chitin, obtained by partial deacetylation of chitin. Depending on the source of chitin, it becomes soluble in aqueous acidic environments when the degree of deacetylation reaches about 50%. The degree of deacetylation is the main parameter that

directly affects the solubility and distinguishes chitin from chitosan. Chitosan, which is insoluble in basic environments, has high solubility, especially in media with a below pH 6 (Rebouças et al., 2021; Gzyra-Jagieła et al., 2019; El Knidri et al., 2018). Thanks to the fact that each D-glucosamine unit in the structure of chitosan contains a free amino group, it undergoes protonation in acidic environments and shows antimicrobial and bioactive properties such as antibacterial, antifungal, antiviral, antioxidant, metal chelator (El Knidri et al., 2018).

Chitosan is the only pseudo-natural polycationic polymer. Thanks to its high biocompatibility, biodegradability, and adsorption properties, it can find its place in many industries such as biotechnology, cosmetics, textiles, paper, water treatment, and pharmaceuticals in different forms such as gel, film, and fiber (Yan & Chen, 2015; Gzyra-Jagieła et al., 2019; Saheed et al., 2021).

3.1 Physicochemical Properties of Chitosan

3.1.1 Degree of Deacetylation and Solubility

Many physicochemical and biological properties of chitosan such as solubility, hydrophilicity and crystallinity depend on the degree of deacetylation. For example, the viscosity of the chitosan solution is directly proportional to the concentration and degree of deacetylation and inversely proportional to the temperature (Bakshi et al., 2020; Aranaz et al., 2021; El Knidri et al., 2018). Deacetylation at a high level indicates a high concentration of amino groups in the molecular chain. As a result, molecules with a higher degree of protonation have higher water solubility. The molecular weight of chitosan is another important factor that influences its bioactivity. The free amino group in chitosan's molecular chain is protonated by the hydrogens in the aqueous solution, transforming it into a positively charged polyelectrolyte. The presence of protons in an acidic environment has an influence on the hydrogen bond structure, causing chitosan to dissolve in water (Wang et al., 2020). Since the number of intermolecular hydrogen bonds will be less in low molecular weight chitosan, the entanglement of the chains and the solubility reducing conditions are reduced. Accordingly, the lower the molecular weight, the more the solubility of chitosan tends to increase. For example, chitosan with a molecular weight below 20 kDa shows higher biological activity than chitosan with a molecular weight above 120 kDa and has higher solubility in aqueous media. In addition, chitosan with molecular weights below 30 kDa can be dissolved in water in the form of free amine without acidification of the environment.

However, protonation of amino groups is required by adjusting the pH of the medium above 30 kDa (Wang et al., 2020; Kou et al., 2021).

Chitosan molecules have high solubility in weak acid environments and are insoluble in basic media without interference. Another factor affecting the solubility of chitosan is the strength of the acid in the medium. While the type of acid used can directly affect the solubility, some inorganic and organic acids such as hydrochloric acid, phosphoric acid, lactic acid, propionic acid, acetic acid, and citric acid can dissolve after prolonged mixing processes. Besides, formic acid and ethanoic acid are the most common acids used for the dissolution of chitosan. When the solution pH is below 4, the protonation of the amino groups increases, and many cationic sites are formed on the chitosan. As the polarity increases, electrostatic repulsion develops between the charged groups, and the polymer swells, increasing its solubility (Saheed et al., 2021; Bakshi et al., 2020).

The chemical properties of chitosan are related to its functional properties. The acetylated part combined with hydrogen bonds provides the improvement of molecular stability and structural properties. The amino and hydroxyl groups in the chitosan structure can be easily affected by modifications. This allows for many chemical treatments and modifications that can be applied to improve chitosan's physical and chemical properties. In addition, the characteristic chemical properties of chitosan are associated with biological properties such as biocompatibility and biodegradability (Saheed et al., 2021).

3.1.2 Antimicrobial and Bioactive Properties

Chitosan exhibits antimicrobial properties, especially in acidic environments, thanks to its cationic structure. It has been proven many times by literature studies that these properties are effective against bacteria, algae and fungi. The antimicrobial effects of chitosan may vary depending on its molecular weight, deacetylation degree, ambient pH, protonation amount, and the microorganism it will affect. Molecular weight affects the communication of chitosan with microorganism cells, the degree of deacetylation affects the solubility and bioactivity, and the pH of the environment affects the amount of protonation (Cheung et al., 2015; Oladzadabbasabadi et al., 2022).

Thanks to its high protonation in acidic environments, chitosan can penetrate the anionic cell walls of microorganisms with its high affinity amino groups. High molecular weight chitosan cannot pass through the cell membrane of the microorganism. Chitosan, which binds to negatively charged components on the cell surface, changes cell permeability and restricts

the cells' access to nutrients, causing cell attachment and disruption of cell integrity. In addition, low molecular weight chitosan (<5000 kDa) can leak into the cell, bind with DNA and inhibit mRNA synthesis. Thus, the enzymatic reactions of the cell are interrupted and cell death may occur. Gram-negative bacteria, most of which are pathological, have more negative charges on their surfaces than gram-positive bacteria. Therefore, they interact more easily with the cationic chitosan, and the antimicrobial effects of chitosan appear (Cheung et al., 2015; Oladzadabbasabadi et al., 2022).

Various studies have discovered that chitosan has antifungal capabilities through interfering with fungi's enzymatic processes. In this way, positive effects have been observed on the growth of many plants. The antifungal activity of chitosan may differ according to its molecular weight, degree of deacetylation and fungal species. The activity of the cationic structure of chitosan with the anionic phospholipids of the fungal cell membrane and the effects of chitinase accumulation and proteinase inhibitor synthesis disrupting the enzymatic processes of fungi can be given as the reasons for its antifungal activity (Cheung et al., 2015; Oladzadabbasabadi et al., 2022).

Chitosan is a biopolymer known for its antioxidant properties. Thanks to the functional amino and hydroxyl groups in its structure, it plays a role in the removal of excessive free radicals. In this way, it takes an active role in food film coatings and food packaging. In comparison to high molecular weight chitosan, low molecular weight chitosan has more active antioxidant capabilities. Chitosan has been shown to have inhibitory effects on lipid oxidation and to play a role in the elimination of reactive oxygen species in numerous studies. Chitosan is well known for its antioxidant activities as well as chelating and adsorption properties of metal ions in biological systems (Oladzadabbasabadi et al., 2022).

3.2 Chitosan Extraction

Chitosan extraction uses two fundamental extraction processes biological and chemical. The chemical process involves using various acid and base solutions to remove calcium carbonate, protein, mineral, and color pigments from the raw material. Chemical extraction is preferred in industrial applications due to the low process time. Furthermore, chitosan can be extracted biologically using enzymatic and fermentation processes (Kou et al., 2021; El Knidri et al., 2018).

3.2.1 Chemical Extraction

Chemical extraction of chitosan mainly consists of demineralization, deproteinization, and deacetylation processes. In addition to these processes, decolorization, deodorization and depolymerization processes can be included in the process according to the desired end product (El Knidri et al., 2018; Rebouças et al., 2021).

3.2.1.1 Demineralization

Demineralization is applied to remove calcium carbonate and calcium chloride, which are the main inorganic compounds of the exoskeleton, in processes using crustaceans as a source. While different acids can be used in this step, it has been determined by literature studies that the highest decalcification performance is provided by hydrochloric acid and secondarily acetic acid. In addition, it has been determined that some acids, such as citric acid and phosphoric acid, have high decalcification performance but are not suitable for industrial applications because they form insoluble by-products. In the demineralization stage, which is usually carried out with a dilute hydrochloric acid solution at a certain time and temperature, the process efficiency can be increased by using high acid concentrations and low crust-acid ratios (Kou et al., 2021; El Knidri et al., 2018).

3.2.1.2 Deproteinization

Deproteinization is applied to remove the proteins in the raw material by treating them with a base solution. In this process, base solutions such as sodium hydroxide, sodium hypochlorite, potassium hydroxide, sodium carbonate, and sodium bicarbonate can be used. In addition, the most successful bases in terms of protein removal were determined as sodium hydroxide and potassium hydroxide. In the deproteinization stage, which is usually carried out with dilute sodium hydroxide solution at a certain time and temperature, organic components other than chitin are removed as well as proteins. Minerals and proteins separated after demineralization and deproteinization stages can be evaluated as animal feed and fertilizer. In addition, the product obtained as demineralized and deproteinized is called chitin (Kou et al., 2021; El Knidri et al., 2018).

3.2.1.3 Deacetylation

Deacetylation is applied to transform chitin into chitosan by removing the acetyl groups in the chitin structure. This process, in which the acetamide group in the chitin structure is replaced by hydroxyl groups, is usually carried out by using a highly concentrated sodium or potassium hydroxide solution by mixing at certain temperatures. The degree of acetylation

or degree of deacetylation is the determining factor in polymer solubility. Deacetylation of chitin, which has very low solubility properties, is a critical step for this biopolymer to function by providing solubility (El Knidri et al., 2018; Rebouças et al., 2021). The degree of deacetylation and the efficiency of the reaction are related to the reaction temperature, base solution concentration, and reaction time. Although the use of high reaction temperature and base concentration may increase the degree of deacetylation, it may cause a decrease in the molecular weight of chitosan. The process of deacetylation progresses rapidly when the chemical treatment of chitin begins and slows down over time. Increasing the processing time increases the amount of deacetylation, as well as causes the degradation of the chitin molecular chain in long-term processes (over 2 hours), which may cause a decrease in the reaction efficiency of deacetylation. This may be due to the increase in the viscosity of the solution used over time (Kou et al., 2021).

3.2.2 Biological Extraction

Chitosan can also be extracted using specific enzymes or fermentation methods, in addition to chemical processes. The degree of polymerization and deacetylation of chitosan obtained by biological methods may differ from those obtained by chemical methods (Rebouças et al., 2021).

3.2.2.1 Enzymatic methods

Enzymatic methods involve a demineralization step using acids for mineral removal. With the various enzymes that come into play during the deproteinization stage, it is ensured that the samples are purified from their proteins. The proteinases used in this step are usually obtained from various microbes or fish guts. In addition, genetically modified microorganisms can be used for both deproteinization and deacetylation. Contrary to the chemical method, deproteinization and deacetylation stages can be studied at much lower temperatures (Kou et al., 2021).

The fact that the enzymes used in the deproteinization and deacetylation stages are more costly than the acid and base solutions used in chemical methods and the process efficiency is lower than chemical methods creates an unfavorable environment for industrial applications. In addition, the deacetylation degree of chitosan samples obtained by enzymatic methods is lower than those obtained by chemical methods. In order to increase the process efficiency, deacetylation can be applied by chemical methods after enzymatic deproteinization. In this way, a combined biological and chemical system can be established.

In this way, the problems of unreacted residual protein and a low degree of deacetylation can be resolved to some extent (Kou et al., 2021).

3.2.2.2 Fermentation methods

Fermentation methods have been developed to solve the problems created by enzymatic methods. The cost problem can be optimized in enzymatic methods with fermentations carried out with microorganisms that can multiply quite rapidly (Kou et al., 2021).

The demineralization process takes place when microbial strains used in fermentation methods secrete lactic acid or other organic acids. Compared to chemical methods, biological methods, which are more advantageous because they do not involve the use of additional acids and bases for reactions, are also disadvantaged by more complicated production processes. The fermentation process takes quite a long time compared to chemical methods. In addition, by-product calcium lactate may be formed in fermentations containing lactic acid. Chitosan extracted by fermentation has a higher molecular weight and therefore strong mechanical properties, compared to chemically extracted chitosan samples, which have low molecular weight (high solubility) and a high degree of deacetylation (strong biological properties). In addition, this method, which includes specific microbial strains, also brings biosecurity problems. The risk of contamination, the use of high-risk strains, and the high cost of equipment required for the entire system are among the disadvantages of this method (Kou et al., 2021).

3.3 Industrial Application of Chitosan

3.3.1 Agriculture Applications

Numerous studies and findings have been documented on the plant growth-promoting in vitro, in vivo, soil, pot, and bio-fertilization applications of chitosan (Chakraborty et al., 2020). Metals and metal oxides found in soil and irrigation water, such as iron, copper, silver, silicon, zinc, zinc oxide, and titanium dioxide, are known to restrict plant growth above certain concentrations. Chitosan contributes to plant growth by adsorbing these heavy metals with its high adsorption abilities (Kumaraswamy et al., 2018; Wang et al., 2020). In addition, the seeds covered with chitosan film prevent the growth of pathogenic organisms such as bacteria and fungi, hence supporting plant growth and increasing the resistance of plants to disease-causing agents. The natural selective properties of chitosan support a variety of physiological and biochemical responses necessary to sustain plant growth and prevent disease. With increasing the intake of phenolic compounds necessary for plant growth,

thickens the cell wall and thus strengthens the natural defense mechanisms. Chitosan can be used for the encapsulation of necessary macro and micronutrients, and it can also serve as a nitrogen source for plants thanks to the amino group it contains (Kumaraswamy et al., 2018). Since the growth and number of shoots, roots, and flowers depend on the growth rate of the plant, it has a great effect on organ development. These advantages of chitosan, not only reduce the use of fertilizers and pesticides but also increase the harvest yield (Wang et al., 2020; Chakraborty et al., 2020). Similar to its use in the pharmaceutical industry, it contributes to the regulation of the development process of plants by regulating the release of supportive drugs and pesticides used in plant development (Wang et al., 2020). In addition, since chitosan molecules are highly hydrophilic, they reduce the osmotic pressure in the cells and reduce the stress in the tissues, supporting the uptake and availability of important nutrients. It facilitates nutrient uptake by accelerating the work and breakdown of macromolecules such as starch and protein and can support the division of stem cells by activating plant hormones (Chakraborty et al., 2020).

3.3.2 Cosmetic Applications

Chitosan can be effectively used in many skin, hair, make-up and oral care products with its antimicrobial properties and high moisture retention. While chitosan-fortified skin products reduce moisture loss, their chelating properties prevent the absorption of metals that may be contaminated with cosmetic products by the skin. They are added to hair care products, hair sprays, shampoos, fixing lotions, hair moisturizers and softeners, and play a role in preserving the moisture of the hair, increasing its strength and preventing damage. Chitosan is also used in lotions, creams, face masks, facial cleansing milks and shower products with their antimicrobial and moisture-retaining effects. They are found in mouthwashes and toothpastes because they reduce bad breath and prevent plaque formation. In addition, they can be included in many makeup products such as nail polish, eyeshadow and lipstick (Kumaraswamy et al., 2018; Morin-Crini et al., 2019; Abd El-Hack et al., 2020).

3.3.3 Food Applications

Chitosan and its derivatives are used to preserve foods and extend their shelf life since they contain several protective qualities such as antibacterial, antioxidant, antifungal, and antiviral effects. Many food products, such as meat, fish, vegetables, and fruits, can benefit from chitosan coating and chitosan-based packaging solutions. Chitosan films are an ideal alternative to plastic packaging for food products since they are non-toxic, edible, water-insoluble, and biodegradable. Chitosan film treatments have been shown to minimize

moisture loss in foods and balance moisture distribution, as well as successfully extend shelf life (Kumaraswamy et al., 2018; Tian & Liu, 2020; Kritchenkov et al., 2019). Chitosan films have been shown to delay the ripening and dehydration of fruits and vegetables, prevent the degradation of meat, and reduce lipid oxidation when applied directly to food. Reduced lipid oxidation has benefits such as color and nutritional value preservation, freshness preservation, and sensory attributes preservation. The addition of several active chemicals to chitosan's packaging capabilities has the potential to improve its capabilities. Bioactive compounds such as polyphenols and essential oils can be used to support chitosan films, improving their antibacterial and antioxidant capabilities and thereby extending the shelf life of food (Tian & Liu, 2020; Hu & Gänzle, 2019).

Chitosan and its derivatives are also used as additives in food applications, as thickening agents, decolorizing, and stabilizing agents. Thanks to the adsorption abilities of chitosan, harmful pigments in foods can be adsorbed and pigment toxicity can be reduced. Likewise, it can collect heavy metal ions contaminated with foods in various ways and help them to be removed from the body (Kumaraswamy et al., 2018).

Studies have shown that with foods to which chitosan is added as dietary fiber, fat absorption is reduced and it contributes to lowering cholesterol. Thus, it has been determined that it facilitates body fat loss, reduces blood pressure and increases the excretion of atherogenic saturated fatty acids. In addition, chitosan-added animal feed and supplements are a growing market (Morin-Crini et al., 2019).

3.3.4 Pharmaceuticals and Medical Applications

Since chitosan is a natural, safe and non-toxic polysaccharide, it is compatible with human tissues. It supports tissue repair with antibacterial, hemostatic and analgesic effects and is widely used in skin, cartilage, cornea, blood vessel and liver tissue repairs. Chitosan film has great application potential in skin and corneal repair and regeneration with its excellent moisture retention, air permeability and strength. The repeating subunit N - acetylglucosamine in the chemical structure of chitosan is an important part of skin tissue. In this way, chitosan-based dressings can prevent wound infection and improve the wound healing process (Kumaraswamy et al., 2018). Chitosan also offered effective solutions for drug release regulation like other polysaccharides. Chitosan-based drug delivery systems are applied in the form of solutions, gels, tablets, capsules, fibers, films and sponges, in different regions and in different ways of intake (Shariatinia, 2019; Morin-Crini et al., 2019). Chitosan nanocomposites provide special systems that allow the release of targeted drugs at the

desired rate. Thus, it increases the solubility of drugs that form stable complexes and insoluble, and their delivery to the relevant region. Other medical applications of chitosan include drug encapsulation, enzyme and cell immobilization, gene delivery, bioimaging, and biosensing. It is known that chitosan is a common research area in anti-cancer studies and successful results have been obtained in studies on mice. (Shariatinia, 2019; Morin-Crini et al., 2019; Ali & Ahmed, 2018).

3.3.5 Textile Applications

Because of its compatibility with human tissues, chitosan is employed in various of textile products, particularly cosmetic textiles. It is a preferred biopolymer due to its antimicrobial properties, high biocompatibility and biodegradability, chelating properties, deodorization properties, wound healing activity and low cost. Chitosan fibers, with their high antibacterial and antifungal properties, can be included in a wide variety of textile products, especially in products for babies and people with special needs. Especially modified chitosan, provide many properties such as excellent anti-wrinkle, ultraviolet blocking, water repellency, self-cleaning to the textile products (Kumaraswamy et al., 2018; Morin-Crini et al., 2019).

3.3.6 Wastewater Treatment

Chitosan and its derivatives are widely used as adsorbents for various pollutants such as dyes and metal ions. Chitosan, which is biodegradable and non-toxic, low cost, and of natural origin, has been the focus of many studies with its adsorption capabilities (Nasrollahzadeh et al., 2021; Keshvardoostchokami et al., 2021). Chitosan is an effective bio-adsorbent, thanks to its large number of reactive amino (-NH_2) and hydroxyl (-OH) groups in its structure, especially in aqueous wastes containing pollutants such as heavy metals, dyes, fluoride, which can be found at high rates in industrial wastes. Many industries use a wide variety of synthetic dyes. Wastewaters containing dyes that are not properly discharged pose a life-threatening threat to many aquatic organisms and cause environmental problems that are difficult to recover from. It is known that more than 10,000 different colorants are used in textile industries alone (Keshvardoostchokami et al., 2021; Kumar et al., 2019; Piccin et al., 2009). Heavy metals, another dangerous pollutant, are known to both cause bioaccumulation and restrict the vital functions of living things. It has been determined that water contaminated with heavy metals causes growth disorders in plants and cancer, cardiovascular diseases, developmental disorders, and fetal death in animals. It is therefore vital to remove heavy metals, which have become a global problem, from wastewater. It has been proven by numerous studies that chitosan adsorbs many heavy metals such as cadmium,

mercury, arsenic, iron, copper, cobalt, zinc, lead, titanium, and aluminium. Besides, chitosan is known to be effective in the adsorption of radioactive elements (Wang et al., 2009; Liu, 2012). The use of chitosan and its derivatives in water treatment has been reported as “greener” and safe alternatives to other treatment methods (Kumaraswamy et al., 2018; Abd El-Hack et al., 2020).

4
HEAVY METALS

Heavy metal pollution is one of the main environmental problems that humanity is struggling to cope with, growing as technology develops. It has become a source of great concern due to the negative effects it causes on living life around the world. The concept of heavy metal is a controversial definition, often used for toxic metals and metalloids. Although some researchers define "heavy metals" as a group of elements with a density greater than 4 g/cm^3, some metals with a density less than 4 g/cm^3 such as aluminium are toxic, while some heavier metals such as gold are typically not toxic (Vareda et al., 2019; Mazhar & Ilyas, 2019; Vardhan et al., 2019). The toxicity of metals depends on parameters such as their effect on living organisms, the problems to be experienced in its bioaccumulation, and the nature of the metal (Briffa et al., 2020).

Heavy metals are naturally prevalent in the earth's crust, and they can pollute soil and water as a result of volcanic eruptions, earthquakes, soil erosion, metal corrosion, and rock fragmentation. In addition, the biggest problem threatening the environment is the high use of these heavy metals and uncontrolled waste disposal policies with the increase in industrialization. Heavy metals can find their place in almost every industry such as the mining and metal processing industry, automotive, medicine, pesticide, wood processing, chemistry, paint, tannery, food, textile, petrochemistry, and electronics. In addition, sewers and fertilizers are also intense sources of heavy metals (Briffa et al., 2020). The main reason for this is that these metals are not biodegradable and cause bioaccumulation in living things. Accumulation rates in living organisms change with the effect of the food chain. People in the last link of the food chain are the group most affected by this bioaccumulation.

Some heavy metals are eliminated as a result of metabolic activity when inhaled or eaten, whereas others might be retained by various organs in the body. While some metals, such as zinc, copper, iron, and chromium, are required for life at low concentrations, others, such as lead, arsenic, aluminium, and mercury, are not required and may have hazardous consequences even at low concentrations. The toxicity of metal is closely linked to its oxidation and the pH of the surrounding environment. Most heavy metals are known to have more active effects in acidic conditions (Vardhan et al., 2019; Vareda et al., 2019; Kapahi & Sachdeva, 2019).

4.1 Environmental and Health Effects of Heavy Metals

4.1.1 Water Pollution

Water pollution is a global issue that must be addressed swiftly because water is essential for all living organisms. Heavy metal contamination in underground or surface water resources may result in problems with various physical, chemical, and biological processes. While heavy metals can contaminate water resources by natural means such as volcanic activities, fires, acid rains, and earthquakes, the main cause of pollution is human activities. A wide variety of heavy metals are used in many industries such as petrochemical, pharmaceutical, chemical, food, paint, mining, polymer, textile, paper, automotive, glass, and medical (Briffa et al., 2020; Vardhan et al, 2019). The discharge of industrial wastes and sewage into water resources without being subjected to appropriate treatment processes, crude oil spills in the seas, and soil pollution created during mineral exploration and extraction activities cause the heavy metal concentrations of water resources to rise to a level much higher than they should be. This pollution, especially in freshwater resources, threatens the health of living things (Briffa et al., 2020; Kapahi & Sachdeva, 2019). Heavy metals can create changes in the physical conditions of the aquatic environment such as pH, amount of substrate, and density. While this situation makes the living conditions of aquatic creatures difficult, it poses a great danger in terms of the continuity of the species as it may cause serious problems such as reproductive problems (Vardhan et al., 2019).

4.1.2 Soil Pollution

Soil pollution is caused by the uncontrolled release or burying of wastes containing heavy metals, such as industrial wastes, mining wastes, pesticides, non-standard paints, and fertilizers. Soil pollution is indirectly caused by water pollution. Irrigation waters of unknown origin, especially used in agricultural lands, pose a great threat to environmental health and safety. Soil pollution is indirectly caused by water pollution. Irrigation waters of unknown origin, especially used in agricultural lands, pose a great threat to environmental health and safety. These waters, which may have been contaminated with heavy metals as a result of the mixing of industrial wastes or sewage waters or the accidents experienced during the transportation of toxic chemicals, may cause bioaccumulation in agricultural lands, the products grown in these lands, crops, and related food chains. Heavy metals are non-biodegradable and have negative impacts on the biodegradability of the items that they

contaminate. This situation causes the soil quality to decrease and the natural balance to deteriorate (Briffa et al., 2020; Kapahi & Sachdeva, 2019). In addition, heavy metals are toxic to plants and adversely affect plant growth by preventing the absorption of beneficial minerals. In order to ensure sustainability in agriculture, heavy metal ratios of soil and irrigation water should be kept under certain concentrations (Kumaraswamy et al., 2018; Wang et al., 2020)

4.1.3 Effects on Human Health

All metals, including essential ones, may cause problems in living organisms above certain concentrations. Essential metals are the elements needed for the continuity of life and the functioning of various organs as they should. In the case of their deficiency, various organ dysfunctions can be experienced. In addition, non-essential metals have no biological function for living organisms, and in the case of bioaccumulation, they can create toxic effects and limit vital activities. The toxic effects of metals may vary with factors such as their concentration, metal uptake and excretion rate, and tissue distribution. Ingestion is the most common way for metals to enter the body. In addition, skin exposure and inhalation are possible. While the majority of metals taken by the body are excreted through metabolic processes, some may accumulate in certain organs. These metals, which can be stored in proteins, interact with DNA and cause cellular malfunction by disrupting DNA structure (Briffa et al., 2020). It can also cause problems with the digestive, renal, reproductive, endocrine, immunological, cardiovascular, neurological, and skeletal systems. Many serious medical occurrences are linked to excessive heavy metal concentrations, including mental retardation, bone curvature, fetal mortality during pregnancy, cancer, visual impairment, kidney failure, Parkinson's disease, and Alzheimer's disease (Vardhan et al., 2019; Klein, 2019; Jeong et al., 2020; Mani et al., 2019; Kumar et al., 2020).

As a result of heavy metal pollution of water and soil, heavy metal bioaccumulation develops in aquatic creatures and plants. This circumstance poses a hazard to all living creatures and has ramifications for the food chain. As you progress up the food pyramid, the rate of accumulation increases rapidly. As a result, omnivores, which include humans, are the group most at risk (Briffa et al., 2020). In this context, removing heavy metal contamination from water and wastewater, which is the primary cause of bioaccumulation, is critical. Despite the fact that many countries place restrictions on the use of heavy metals, the pollution burden continues to rise. In addition to the restriction of the use of this pollutant, which directly

threatens the world's resources and living life, it is necessary to control the bioaccumulation, especially by treating wastewater (Vardhan et al., 2019; Vareda et al., 2019).

4.2 Antimony

Antimony (Sb) is a silvery-white metal that occurs naturally in the earth's crust. Because of its relatively flexible structure, it is employed in a variety of hardened alloys. Table 4.1 and Figure 4.1 show the physical properties of antimony, which is a group V metalloid element (Sundar & Chakravarty, 2010; Boreiko & Rossman, 2020).

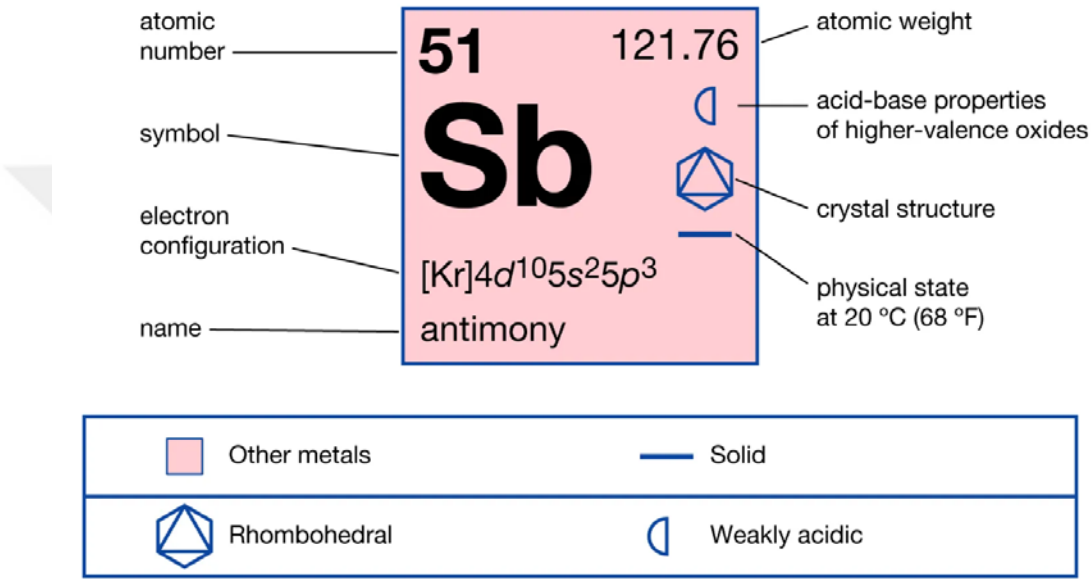

Figure 4.1 Element properties of antimony (Britannica, 2022)

Antimony can be found in nature for a range of factors, including volcanic activity, rock fragmentation, natural erosion of antimony ore, and fires. In addition, since lead acid is used in the content of many industrial products such as batteries, fire extinguishers, flame retardants, pipes, semiconductors, solder, plastics, and dyes, it is revealed during the production stages and waste disposal stages. Mining activities and mine sites, in particular, have been recognized as the sources of the most antimony contamination (Sundar & Chakravarty, 2010; Boreiko & Rossman, 2020; Li et al., 2018; He et al., 2012).

Antimony as a non-essential metal can be absorbed and stored by plants. The presence of antimony above certain concentrations can have effects that slow down the growth of plants and change the plant root morphology. In addition, the presence of antimony usually together with arsenic and lead indirectly causes higher toxic effects (Li et al., 2018; Sundar & Chakravarty, 2010; Xu et al., 2021; Feng et al., 2020).

Table 4.1 Element properties of antimony (Antimony, 2022; IARC, 2019)

Atomic Number	51
Atomic Weight	121.76
Phase at STP	Solid
Density (Near R.T.)	6.69 g/cm^3
Tolerable Daily Intake	6 μg / kg of body weight
Classification of International Agency for Research on Cancer (IARC) Monographs	Pentavalent antimony – 3 (Not classifiable as to its carcinogenicity to humans) Trivalent antimony – 2A (Probably carcinogenic to humans)

Antimony is generally taken into the body by inhalation. The amount of antimony in the air is formed as a result of fossil fuels, garbage incineration, and metalworking activities. Antimony can show various toxic effects, especially in people working or living in these areas. As metal toxicity depends on many parameters such as exposure route, duration, and presence of other contaminants the toxic effects of antimony cannot be fully measured for humans. Besides many diseases that are estimated to be induced, no directly determined the toxic effect of antimony has been detected under certain doses. Inhalation of antimony in high doses or during long exposure times may cause respiratory system diseases such as bronchitis, emphysema, inactive tuberculosis, respiratory tract irritation, and pneumoconiosis (Nishad & Bhaskarapillai, 2021; Filella, 2009; Xu et al., 2021). In addition, antimony toxicity is thought to be associated with cardiovascular problems such as variable blood pressure and varying electrocardiographic values, and gastrointestinal problems such as abdominal pain, diarrhea, vomiting, and ulcers. It is known that skin exposure at high concentrations at high temperatures also causes skin rashes, which are defined as "antimony spots". In some studies, it has been reported that it may cause spontaneous abortions and menstrual disorders after long-term exposure (Sundar & Chakravarty, 2010).

In animal trials, acute poisoning with antimony trioxide resulted in cancer and death in rats. Despite this, the IARC has classed antimony trioxide as a potential human carcinogen since

there is insufficient data to indicate that it is carcinogenic in people (Nishad & Bhaskarapillai, 2021; Li et al., 2018; Sundar & Chakravarty, 2010).

The World Health Organization Drinking Water Quality guidelines set a tolerable daily intake for antimony of 6 µg/kg body weight/day. The Joint FAO/WHO Expert Committee on Food Additives (JECFA) has specified a limit of 0.04 mg/kg body weight in food additives. It is also listed as hazardous waste in the Basel Convention on the cross-border migration of wastes containing antimony (Sundar & Chakravarty, 2010; Li et al., 2018; Bagherifam et al., 2019).

4.3 Aluminium

Aluminium (Al) is the most abundant metal in the earth's crust, yet it is not required for living organizms. Aluminium is a versatile metal that can be combined with other metals to make alloys, has a thermal conductivity sixteen times that of stainless steel, and can lower suspended particles and bacteria levels. This metal, which is extremely soft in its pure form, accounts for 8.8% of the mass of the earth's crust. Many research are conducted, particularly on the hazardous effects of orally ingested aluminium (Alabi & Adeoluwa, 2020; Alasfar & Isaifan, 2021; Jeong et al., 2020; Sieg et al., 2018). Figure 4.2 and Table 4.2 show the elemental characteristics of aluminium.

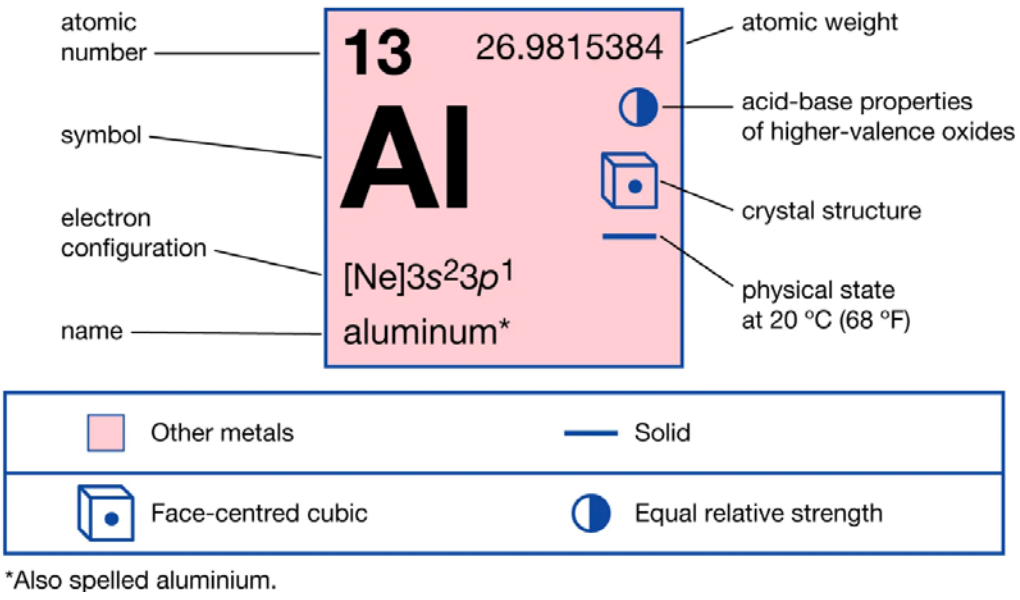

Figure 4.2 Element properties of lead (Britannica, 2020)

Table 4.2 Element properties of aluminium (Aluminium, 2022; IARC, 2019; Lyons-Weiler & Ricketson, 2018)

Atomic Number	13
Atomic Weight	26.98
Phase at STP	Solid
Density (Near R.T.)	2.70 g/cm^3
Daily Intake Limit	1 mg/kg body weight
Classification of IARC Monographs	Aluminium production – 1 (Carcinogenic to humans)

Since aluminium has a high solubility in an acidic environment, it can spread to the environment due to natural causes such as contact of aluminium-rich rocks with water, volcanic activities, and acid rains. In addition, aluminium is used in a wide range of sectors such as cosmetics as toothpaste and antiperspirants, pharmaceuticals as antacids, buffered aspirin and anti-diarrheal drugs, vaccines, kitchenware as cookware, cooking utensils, storage containers, and foil, construction products as the exterior, roof, doors, and windows, automobile and aircraft parts, beverage cans, jewelry, and ornaments. Aluminium is released into nature at the production, processing, consumption, and waste disposal stages of these products. Aluminium is a metal with high recyclability. Since the contents of scrap metal used as a source during recycling vary, highly toxic metals such as lead and arsenic can contaminate recycled products. This is a dangerous result indirectly brought about by the use of aluminium (Alabi & Adeoluwa, 2020; Alasfar & Isaifan, 2021).

Around half of the world's arable land is acidic. As aluminium is very soluble in acidic media, it results a water and soil pollution. The roots of many plants absorb and store aluminium and its derivatives. Aluminium can build up in the roots, leaves, and fruits of plants. Because its solubility varies with pH, the amount of aluminium in plants varies with the acidity of the soil or irrigation water. Plants do not benefit from stored aluminium in terms of metabolism, and it also reduces the absorption of key elements like potassium,

calcium, and phosphorus, which are required for plant growth, by reducing root development (Alabi & Adeoluwa, 2020; Shetty et al., 2021; Chauhan et al., 2021; Zhu et al., 2018).

Aluminium is ingested mostly through food, drink, and pharmaceuticals. Although plants store this metal naturally, aluminium compounds can be chemically added to some foodstuffs. Furthermore, aluminium-based cooking equipment, foil, and storage containers can contaminate the foodstuffs. Because of its inexpensive cost, aluminium cookware is widely utilized in many countries. The amount of aluminium in food is affected by a number of parameters, including pH, contact time, and contact temperature. Aluminium can also be ingested through breathing, smoking, drugs, pharmaceuticals, and vaccines (Alabi & Adeoluwa, 2020). Aluminium is absorbed extremely slowly through the intestines. Subcutaneously injected aluminium, on the other hand, does not enter the circulation since it remains beneath the skin. Aluminium is absorbed mostly from the acidic stomach environment and then goes into the bloodstream. If kidneys are working properly, aluminium that enters the blood is substantially (95%) removed from the body via the kidneys. Bile removes a little percentage of ingested aluminium (2%) from the body. The rest can be stored in organs such as the liver, spleen, parathyroid glands, and kidneys, particularly the bones. Aluminium bioaccumulation can induce toxicity in a variety of tissues, including the brain, kidneys, bones, and nervous system (Klein, 2019; Jeong et al., 2020; Sieg et al., 2018).

The difficulty of determining the amount of exposure to aluminium makes it difficult to detect the health problems it causes, and it has also led to different opinions in determining the limitations of food products. Various compounds of aluminium are used as food additives under certain limits (Jeong et al., 2020). JECFA reported the provisional tolerable weekly intake for aluminium as 7 mg/kg body weight in 1989. This value was updated as 2 mg/kg body weight per week in 2011. Agency for Toxic Substances and Disease Registry (ATSDR) reported Aluminium daily intake as 1 mg/kg body weight (7 mg/kg body weight per week), while European Food Safety Authority (EFSA) reported 1 mg/kg body weight per week (Lyons-Weiler & Ricketson, 2018; Tietz et al., 2019; Stahl et al., 2011; Alasfar & Isaifan, 2021).

Aluminium intake over the specified limits can pose a serious threat to health. The placement of aluminium in the bones instead of calcium brings with it diseases such as osteomalacia, and hypercalciuria. If aluminium is released from the bones, the calcium in the blood rapidly attacks the bones and indirectly causes hypocalcemia. There are many studies and findings claiming that aluminium bioaccumulation also causes kidney failure, Parkinsonism

dementia, breast cancer, neurodegenerative disorders, and Alzheimer's disease (Shetty et al., 2021; Klein, 2019; Sieg et al., 2018; Jeong et al., 2020).

4.4 Lead

Lead (Pb) is a bluish-gray, highly toxic, non-biodegradable metal. It is used in many industries because of its physical properties that can be easily formed, resistant to corrosion, low cost, and high compatibility for alloys. Lead exhibits toxic properties in its inorganic and organic forms, even at low concentrations. It is the second most toxic metal in the world after arsenic and makes up 0.002% of the earth's crust (Soltaninejad & Shadnia, 2018; Njati & Maguta, 2019; Mani et al., 2019; Kumar et al., 2020). Elemental properties of lead are given in Figure 4.3 and Table 4.3.

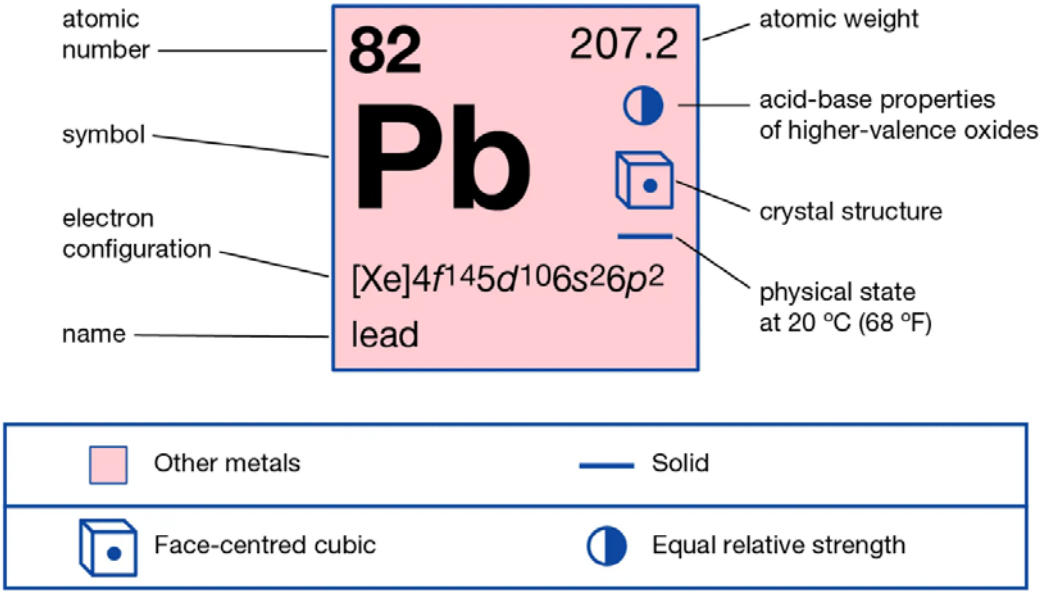

Figure 4.3 Element properties of lead (Britannica, 2021)

Lead has contributed to the development of many industries with its physical and chemical properties. Various metal alloys, automotive battery manufacturing, petrochemicals, batteries, pesticides and fertilizers, mining, ammunition production, construction materials such as plates, pipes, and paints, and nuclear and marine industries are the main applications of lead use (de Souza et al., 2018; Mani et al., 2019). With the widespread use of lead, the environmental effects of this toxic heavy metal are increasing. Lead pollution may occur due to natural causes such as geochemical weathering, volcanic activity, and surface movements in mining areas. But the main cause of pollution is industrial activities. Lead and its oxides threaten life through exhaust gases, and contaminated food, and water (Kumar et al., 2020).

Lead is one of the most dangerous soil pollutants that inhibit plant growth. The main sources of lead in the soil are fertilizers, pesticides, and exhaust gases. Lead metal, which is not essential for living things, is absorbed by plant roots and accumulates in the roots without dissolving. Absorbed lead can induce growth retardation, genetic mutation, and oxidative reactions in plants while reducing seed germination rate, photosynthetic pigment biosynthesis, carotenoid and chlorophyll content (Zafar-ul-Hye et al., 2020; Shahid et al., 2021; Aouini et al., 2018).

Table 4.3 Element properties of lead (Lead, 2022; IARC, 2019)

Atomic Number	82
Atomic Weight	207.19
Phase at STP	Solid
Density (Near R.T.)	11.34 g/cm^3
Blood Lead Level Limit	5 μg / 100 g of blood
Classification of IARC Monographs	Lead compounds, inorganic – 2A (Probably carcinogenic to humans) Lead compounds, organic – 3 (Not classifiable as to its carcinogenicity to humans)

As a result of lead pollution and the effect on the food chain, lead bioaccumulation may occur in animals and humans. Lead metal, which has no function for vital activities, can cause cancer by causing various diseases and disorders in most organ systems of humans and animals (Soltaninejad & Shadnia, 2018; Bhattacharya, 2019; Shahid et al., 2021).

Although lead poisoning accounts for 0.6% of the worldwide burden of disease and is recognized as a human carcinogen by IARC, restrictions on lead use have not reached sufficient levels. Lead exposure in humans can cause neurological problems such as behavioral and cognitive problems, chronic problems such as disruption and dysfunction in the cardiovascular, musculoskeletal, renal, and reproductive systems, and health problems such as growth retardation, late puberty, and hearing loss in infants and children (Mani et

al., 2019; Bhattacharya, 2019; Kumar et al., 2020). The main problem caused by lead in the human body is that it accumulates in the body by imitating essential metal ions and prevents metabolic activities due to metal ions that cannot be taken into the body (Mani et al., 2019).

The US Centers for Disease Control and Prevention has determined the reference limit for lead in blood as 5 µg/dL in children and 10 µg/dL in adults (Mani et al., 2019; de Souza et al., 2018; Kumar et al., 2020). In addition, the occupational exposure level was determined as 5 µg/dL. Every individual is exposed to lead in a variety of ways, primarily by inhalation and ingestion. Since the toxic effect of lead in the human body varies with factors such as age, gender, ethnicity, exposure time, and amount, a phenotype could not be determined for diseases caused by lead exposure. This situation causes insufficient steps to be taken to limit the use of lead (Mani et al., 2019).

Lead is a cytotoxic metal that slowly poisons living things and restricts vital functions. It may take years for the effects to be observed. More than 90% of inhaled and ingested lead interacts with red blood cells. In addition, absorbed lead affects the mineral metabolism of calcium and phosphorus by inhibiting kidney enzymes and reducing their absorption, and is stored in bones and teeth by binding to the place of calcium and phosphorus that cannot be taken into the body. Thus, it causes developmental disorders in bones, delayed healing, and osteoporosis (de Souza et al., 2018; Mani et al., 2019; Ciosek et al., 2021).

The largest group at risk for lead absorption in children and infants. While it is estimated that adults can absorb 3-10% of ingested lead, it is estimated that this rate can increase up to 40-50% in children. For this reason, lead absorption may increase during pregnancy. Lead poisoning in children can result in significant consequences such as mental retardation, cognitive-developmental delay, anemia, fatigue, hyperactivity, decreased nerve conduction, and impaired motor functions. Especially the problems in the brain can reach irreversible and incurable points (Kumar et al., 2020).

5
WASTE WATER TREATMENT

Water is the most vital ingredient for life. This vital component is threatened by many organic and inorganic pollutants due to the rapidly developing industries and increasing population. Global water reserves are polluted due to unsustainable practices and freshwater scarcity is becoming the most basic and common problem for all living things (Singh et al., 2020). In our world, where only 0.036% of the water resources are suitable for consumption, approximately 80% of the population is currently trying to cope with the problems related to water supply and safety (Jayaswal et al., 2018). If adequate and sustainable methods are not developed, it is predicted that many Asian, European, and African countries will experience water shortages until 2025 (Vasudevan & Oturan; 2014).

Water pollution is the main cause of vital problems that are very difficult to recover, such as the decrease in usable water resources, the infertility of agricultural lands, and bioaccumulation in living things. Besides natural resources such as volcanic activities, earthquakes, floods, soil erosion, erosion of rocks by water, and animal manure, the main source of water pollution is human activities (Singh et al., 2020; Mitiku, 2020). Uncontrolled discharge of water used in industries, wrong waste policies, pesticides, fertilizers produced in animal farms, sewage, and domestic wastes, in short, almost all production and consumption activities of people can cause pollution. Due to the water cycle, air and soil pollution also induces water pollution and causes pollution to be transported around the world.

About 30% of the world's freshwater reserves are used by industries that produce wastewater that may contain many different pollutants. Most of these wastewaters are discharged without treatment (Jayaswal et al., 2018). These wastewaters may contain pollutants such as heavy metals, radioactive substances, dyes, pesticides, drugs, and chemicals at legally acceptable rates. Many of these pollutants can cause bioaccumulation. Therefore, they threaten life even at low concentrations (Akpomie & Conradie, 2020). There are around 1500 known pollutants in freshwater ecosystems. Most of these pollutants are not biodegradable and cause bioaccumulation. The most common pollutants that threaten life in water resources can be listed as follows: agricultural pollutants (pesticides, fertilizers, phosphate, and nitrates), petrochemicals (microplastics, paints, fossil fuels), organic toxic

wastes (formaldehyde, phenols), household pollutants (detergents, surfactants, food waste), biological wastes (feces, pathogens, drugs), heavy metals (cadmium, aluminium, lead), radioactive pollutants (anthropogenic radioactive materials) (Mitiku, 2020). These types of waste are interconnected and induce each other. For example, heavy metals accumulated in plants through agricultural pollutants may be included in another waste group as manure or human feces after consumption of these plants. At this point, it can be said that many metals and metalloids, elements such as nitrogen, phosphorus, and their salts can create pollution and toxic effects with the effect of the water cycle or food chain (Singh et al., 2020).

Water pollution can change the properties of underground and surface water resources such as temperature, acidity, density, and chemical content, as well as cause changes in the biological structures of living things living in these water resources (Mitiku, 2020). In particular, drug residues and heavy metals that directly affect the biology of living things can cause serious health effects such as reproductive disorders, genetic, hormonal, and endocrine disorders, especially in aquatic organisms (Singh et al., 2020; Akpomie & Conradie, 2020). For the sustainability of water resources and living life, the treatment of polluting wastewater is of great importance. Conventional methods used for water purification include filtration, solvent extraction, precipitation, membrane separation, coagulation, reverse osmosis, electrocoagulation, precipitation, evaporation, advanced oxidation, chelation, reduction, photo-catalysis dispersion, ion exchange, solidifing, nanofiltration, irradiation, ozonation, electrophoresis, lime softening and also adsorption (Akpomie & Conradie, 2020; Mitiku, 2020).

5.1 Water Treatment Methods

5.1.1 Precipitation Methods

5.1.1.1 Chemical precipitation

It is a widely employed low-cost simple water treatment method. The process is carried out by adding the precipitating agent after the ambient acidity has been adjusted. This system, which works very well with high pollutant loads, is particularly efficient for metal and fluoride elimination. The precipitates and water obtained at the end of the process are separated by filtration. In most, the chemical precipitation processes, hydroxide compounds act as precipitators. Depending on the type of pollutant to be precipitated in hydroxide precipitation processes, the precipitation process can be supported by adding various chemical coagulants. Although the processing costs are low, a large amount of sludge is

formed at the end of the process, which requires disposal. Sludge formation is a limiting factor in the application of chemical precipitation. Another precipitant used in chemical precipitation is sulfur. Since some sulfide compounds have lower solubility than hydroxide compounds of the same pollutants, they are more easily involved in the precipitation process. The precipitation with sulfur is also suitable for operation in wider pH ranges. In addition, there is a danger that sulfur-containing compounds may release toxic gases such as hydrogen sulfide. As a result of the sulfur precipitation process, sludge is formed by containing high amounts of pollutants, and disposal is required. This method, which is not efficient at low pollutant concentrations, may also result in higher salt concentrations and pH than desired in treated wastewater. This may require secondary treatment (Vardhan et al., 2019; Vareda et al., 2019; Crini & Lichtfouse, 2019).

5.1.1.2 Flocculation

It is the process of precipitating colloids by clumping with various coagulants and auxiliary chemicals. The process is quite simple and low cost. With the flocculation method, colloidal particles are bound to large agglomerates and removed from the system by sedimentation or filtration (Vareda et al., 2019). This system, which is suitable for the use of a wide variety of coagulants, can also be used to reduce bacterial activity. It is a very efficient system for the removal of insoluble pollutants from wastewater, although the chemical and biological oxygen demand are quite low. In addition, the processes required to remove the sludge from the system can be costly. In addition, some physical properties such as the acidity of the treated water may need to be monitored (Crini & Lichtfouse, 2019).

5.1.2 Ion Exchange

It is the process of displacing ions of the same charge between the insoluble solid resin and the wastewater. This process can be used to remove unwanted ions from the system, as well as to separate valuable compounds, such as precious metals, from wastewater (Vareda et al., 2019). The ion exchange process is a very fast, simple, and high-capacity process. In these systems, which can be easily installed and operated, the desired flow regime can be applied, multiple pollutants can be removed and a high level of treatment can be achieved (Vardhan et al., 2019; Crini & Lichtfouse, 2019). In this process, the wastewater to be purified is advanced in a column filled with ion exchange resin, and ion exchange is ensured between the ions in the resin and the wastewater ions. While the unwanted ions in the wastewater are attached to the resin, the ions in the structure of the resin are separated from the column with the purified water. When the resin reaches its total capacity, it is washed with the appropriate

regeneration solution and it is ensured to leave the ions that it has separated from the wastewater. Thus, the resin can be used repeatedly (Levchuk et al., 2018). While ion exchangers are widely used especially in the softening of hard water, the use of cation exchange resins is common for the removal of heavy metals. Synthetic resins can be used for ion exchange, as well as natural materials such as zeolites and silicate minerals. Although natural materials are cost-effective, they are not very suitable for industrial applications. Although the ion exchange process has the advantage that it can be sustained with less equipment, the cost of resin can be high. Resins have limited regeneration capacity and in some cases have to be destroyed. In addition to the disposal costs of the waste resin, the costs of regeneration solutions are a disadvantage of the system. There is a pH limitation for ion exchange processes. Accordingly, for the ion exchange to proceed correctly, the acidity of the environment must be kept under control. In addition, some organic substances such as oils can cause clogging in the resins. The fact that resins are generally not selective creates a disadvantage when it is desired to remove a particular contaminant from the system (Vardhan et al., 2019).

5.1.3 Electrochemical Methods

5.1.3.1 Electrocoagulation

It is a much faster and more effective process than traditional coagulation method. It consists of electrodes where oxidation and reduction reactions take place, respectively. Suitable for industrial-scale applications, this method does not require pH control and is highly efficient in removing colloidal particles, metals, dyestuffs, drug residues, phenolic compounds, and oils. The electrocoagulation process, which is simply a combination of oxidation, reduction, coagulation, and adsorption processes, involves the production of in situ coagulants by the electrical dissolution of ions at the anode and cathodes used. Thanks to the metal ions separated from the anodes and the hydrogen gas provided by the cathodes, the pollutants in the wastewater are floated. In this method, there is no need for auxiliary chemicals since electrons are the necessary reactive material. At the end of the process, a more stable sludge is formed compared to conventional settling methods. The resulting sludge brings additional waste disposal costs (Vardhan et al., 2019; Crini & Lichtfouse, 2019).

5.1.3.2 Electrodeposition

It is used in the processes of recovering valuable pollutants, especially precious metals, by using suitable electrodes. During these processes, while the pollutants are obtained in pure form, there is no waste that requires disposal. Therefore, electrodeposition is called a clean

process. It has low operating cost and is the preferred method for cation recovery (Vardhan et al., 2019; Vareda et al., 2019).

5.1.3.3 Electroflotation

It is a purification process that allows gas bubbles and pollutants produced by water electrolysis to float on the water surface. This process starts when the oxygen and hydrogen gases formed at the electrodes collide with the suspended pollutants while passing through the wastewater, producing agglomerated particles. When these agglomerates come to the water surface, they are separated from the water by stripping and collected. Electroflotation was first applied in mining and is a method used as a water treatment system. It is an effective method used for the removal of oils, greases, color pigments and metal ions. The purification process is generally related to the size of the gas bubbles formed. In addition to the need for less help, sludge formation is also less (Vardhan et al., 2019; Mohtashami & Shang, 2019; Crini & Lichtfouse, 2019).

5.1.4 Membrane Filtration

5.1.4.1 Ultrafiltration

It is the process of purifying water from pollutants using membranes with relatively large pores. It is generally used in the removal of metal ions, surfactant micelles, various polymers and some microorganisms (Vareda et al., 2019). It is operated by creating a low pressure environment for the removal or recovery of dissolved and suspended pollutants. Since the membrane pores used are larger than most dissolved solids, they cannot generally be filtered by ultrafiltration. Therefore, ultrafiltration applications may require secondary purification or reinforcing reinforcements such as polymers or micelles can be added to membrane structures (Vardhan et al., 2019). Since it is a selective permeable system, it can be applied for the purification of pollutants of the desired size or characteristics. In addition, the cost is high. In case of clogging, cleaning also creates additional costs. Ultrafiltration employs in the water treatments for contaminants in the range of 0.15 μm to 5×10^{-2} μm (Crini & Lichtfouse, 2019; El-Dessouky & Ettouney, 2002).

5.1.4.2 Electrodialysis or (Nanofiltration)

It operates between reverse osmosis and ultrafiltration processes as a target particle size. With the effect of the electrical driving force, the ions in the aqueous medium are allowed to pass through the membranes and the wastewater is purified. The applied cell voltage is low to prevent oxygen formation at the anode and hydrogen formation at the cathode (Wang et al., 2021). This results in lower pressure and relatively low energy consumption compared

to reverse osmosis. It also has the advantages of higher flow rate, easier processing and higher efficiency compared to reverse osmosis. It is an alternative treatment method especially for some cations (for example, heavy metals such as nickel, chromium and arsenic) (Touir et al., 2021). In this method, a selective permeable separation process is applied using charged membranes. This method, which is used for the removal of many heavy metals from wastewater, is generally used for the treatment of industrial wastewater and for the recovery of useful substances and for the production of drinking and process water from seawater. Although the energy consumption is low, it has disadvantages such as clogging of the membranes, low processing capacity and having a complex process. Nanofiltration employs in the water treatments for contaminants in the range of 5×10^{-2} μm to 5×10^{-3} μm (Vardhan et al., 2019; El-Dessouky & Ettouney, 2002).

5.1.4.3 Reverse Osmosis

It is the process of separating organic or inorganic pollutants from wastewater in a reverse osmotic pressure environment with a highly selective permeable membrane. This process, which provides a high purity end product, is generally used in the production of drinking water from seawater (Vardhan et al., 2019). Although processing costs and cleaning requirements are higher than other membrane systems, it is an effective and reliable treatment system. It provides a high-quality product due to its high purification performance. Reverse osmosis is very effective in separating drug residues, metal ions, hormones, macro and micropollutants, volatile and non-volatile organics, various ions and salts, biological materials, and microorganisms from water (Umar et al., 2015). In addition, due to the very small pores of the membrane, it requires acid or alkaline solutions, which can cause additional waste in the frequent cleaning stages. High pollutant concentrations may require pretreatment of the wastewater to be treated, as the membrane pores become clogged very quickly. It is not a suitable system for small and medium-sized businesses due to its high installation and operating costs. Reverse osmosis employs in the water treatments for contaminants in the range of 5×10^{-3} μm to 10^{-4} μm (Wang, 2021; El-Dessouky & Ettouney, 2002).

5.1.5 Adsorption

While most water treatment methods can work successfully at high pollutant concentrations, they are very costly and inefficient at low pollutant concentrations. Plant capacity requirements and the use of aluminium and chlorinated compounds or synthetic polymers in some methods result in secondary treatment requirements and additional costs (Mitiku,

2020; Vareda et al., 2019). Adsorption is the only wastewater treatment method with high efficiency, low processing requirements, and no secondary water treatment requirement depending on the type of adsorbent employed (Akpomie & Conradie, 2020). Adsorption is a solid-liquid mass transfer process in which the substance (adsorbate) to be removed is bonded to a solid surface called adsorbent by chemical or physical interactions. This process takes place in three steps (i) transport of the adsorbate from the aqueous solution to the adsorbent surface, (ii) adsorption to the adsorbent surface, and (iii) transport within the adsorbent (Vardhan et al., 2019; Chai et al., 2021).

Adsorption basically takes place in two ways as physical and chemical adsorption. Physical adsorption generates weak Van der Waals attractive forces and is a reversible process. Physical adsorption is suitable for multiple uses of the same adsorbent, as it is suitable for desorption, that is, reverse adsorption by transferring the adsorbate from the adsorbent surface. Thus, process and resource sustainability and low-cost processes can be operated. Besides, physical adsorption is less specific. Chemical adsorption is a process in which strong ionic or covalent bonds are established between the adsorbent and the adsorbate. This one-way and irreversible system is more specific than physical adsorption (Vardhan et al., 2019; Chai et al., 2021).

Adsorption efficiency and process cost are closely related to the physical and chemical properties of the adsorbent, such as surface area, kinetic mechanism, electrostatic charge and selectivity. In addition, the pH and temperature of the adsorption medium, the processing time, and the adsorbate concentration are among the factors affecting the process efficiency (Vareda et al., 2019; Chai et al., 2021). Since adsorption is directly related to the characteristics of the adsorbent, recent studies have focused on increasing the functionality of the adsorbent (Dai et al., 2018). There are a wide variety of synthetic or natural sourced adsorbents utillized for adsorption processes. Artificial/synthetic adsorbents are designed specifically to the area and the adsorbate to be used with high selectivity, besides their high cost, laborious production processes and high environmental burden. Furthermore, natural adsorbents with lower selectivity are inexpensive, simple to manufacture and process, and have a low environmental impact (Demir & Yalçin, 2014). Biopolymers (such as cellulose, chitin, chitosan), zeolites, clays, biochars, carbon adsorbents, plant and plant wastes (tea and coffee pulp, cassava waste, wheat and rice peel, banana peel, potato skin, corn cob and leaf, cocoa husk, sugar cane pulp, coconut and nut shells, fruit shells, etc.), eggshells, worm excrement, fish bones, algae, bacteria, fungi, are some examples of naturally sourced

adsorbents (Vareda et al., 2019; Chai et al., 2021; Akpomie & Conradie, 2020; Dai et al., 2018; Demir & Yalçin, 2014). Naturally sourced adsorbents are biodegradable as well as being easy to obtain. Thus, employing a biosorbent is using a waste biomass for the removal of pollutants in water contributes that to the sustainability of natural resources (Dai et al., 2018).

5.1.5.1 Adsorption Mechanism and Isotherms

In order to proceed adsorption process well, it is necessary to have a good understanding of various systems such as the mechanism of operation, equilibrium data, and adsorbent characterization. The adsorption equilibrium data is the most essential of these systems. The adsorbate concentration and interface concentration in the bulk solution reach a dynamic equilibrium when the adsorbate and adsorbent come into contact for a sufficient time. The adsorption kinetics of single and multi-component systems can be studied using this equilibrium data. The most common method to explain the interaction mechanism between adsorbents and adsorbates at a constant temperature is to model equilibrium data with adsorption isotherms. Information regarding the maximum adsorption capacity can be acquired using adsorption isotherm models. Because adsorption data is influenced by factors such as adsorbent type, physical properties of the adsorption medium, ionic charge, and interaction time, the employed isotherms may change as well. Freundlich, Langmuir, Dubinin–Radushkevich, Redlich-Peterson, and Temkin are some of the isotherms that are commonly employed to explain adsorption mechanisms (Wang & Guo, 2020; Al-Ghouti & Da'ana, 2020; N'diaye & Kankou, 2020).

The Freundlich isotherm is the first model constructed to detect the adsorption mechanism. This isotherm is applied to adsorption processes occurring on multi-domain (heterogonous) surfaces, allowing the definition of surface heterogeneity and an exponential distribution of active sites and energies (N'diaye & Kankou, 2020; Ayawei et al., 2017). The Langmuir isotherm was also one of the first models to be used. In this model, it is assumed that the adsorbate and the adsorbent are an ideal structure and that homogeneous and single-layer adsorption takes place with equal energy distribution. Langmuir isotherm, which is based on many assumptions, is not idealized in real systems, many researchers are working on various modified versions of the model (Majd et al., 2021; Azizian & Eris, 2021). The Dubinin–Radushkevich isotherm is a model that can operate only in the range of intermediate adsorbate concentrations and assumes that adsorption is related to the adsorbent pore volume. This model, which is examined on the basis of the adsorbent pore structure, is

generally applied to express the adsorption mechanism with Gaussian energy distribution on heterogeneous surfaces. The Dubinin–Radushkevich isotherm, which assumes multilayer adsorption, is often used to distinguish between physical and chemical adsorption in metal ion adsorption processes (Majd et al., 2021; Ayawei et al., 2017). The Redlich-Peterson isotherm is a hybrid model combining Langmuir, a single-layer adsorption model, and Freundlich, a multi-layer adsorption model. This model, which is not suitable for application for single-layer systems, includes an exponential and linear concentration relationship in the denominator and denominator, respectively, which can be applied in both homogeneous and heterogeneous adsorption systems, showing the adsorption equilibrium at different concentrations (N'diaye & Kankou, 2020; Majd et al., 2021). The Temkin isotherm is a model in which the heat of adsorption is assumed to decrease linearly as a result of increasing surface coverage for multilayer adsorption processes. In this isotherm, only the range of intermediate ion concentrations is taken into account, ignoring very high and low concentrations. The Temkin isotherm can be applied to gas-phase adsorption as well as liquid phase adsorption, which is a complex adsorption system (N'diaye & Kankou, 2020; Majd et al., 2021; Ayawei et al., 2017).

6
MATERIALS AND METHOD

The experimental system, which is the subject of the thesis, consists of two stages. In the first stage, chitosan was produced from crab and shrimp shells. In the second stage, the produced chitosans were used in adsorption of aluminium, antimony and lead.

6.1 Production of Chitosan

6.1.1 Material Preparation and Experimental Equipments

Crab and shrimp were purchased as fresh from a fish market in Istanbul in October 2020 and as waste from a seafood restaurant in Istanbul in October 2020. Freshly supplied products were kept in the refrigerator at -18 °C (1050T model; Arçelik, Eskisehir, Turkey) and the shells obtained as waste was kept in the refrigerator at +4 °C. Before the experiment, the samples were brought to room temperature. Later, the shells were separated from the flesh and membrane structures, they were separated from their remains with forceps and spatula. The cleaned shells were then washed with distilled water and left to dry overnight in a KH-45 model hot air oven (Kenton, Guangzhou, China) at 40°C to prevent any tissue fragments remaining on the shells from deteriorating. The cleaned shells before and after drying are given in Figures 6.1 and 6.2 for crab and shrimp, respectively.

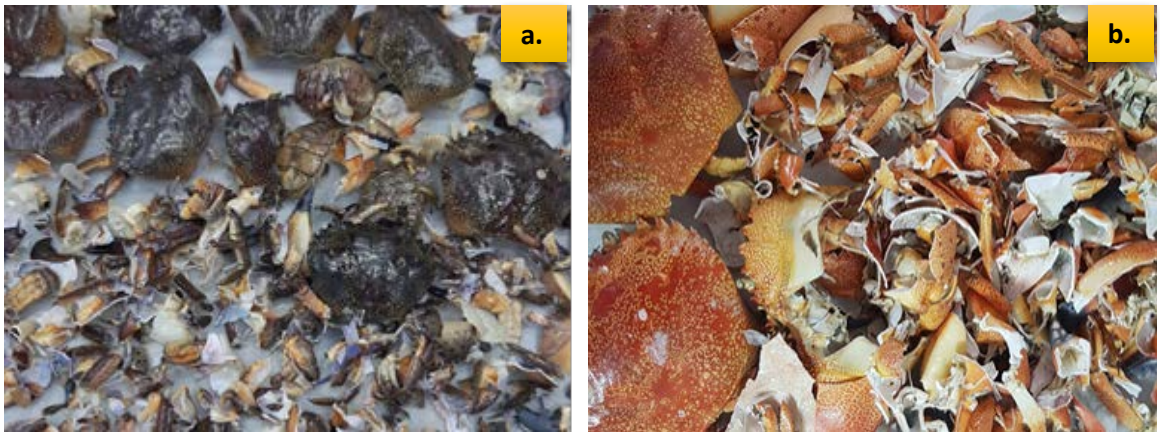

Figure 6.1 Crab shells a. cleaned and b. dried

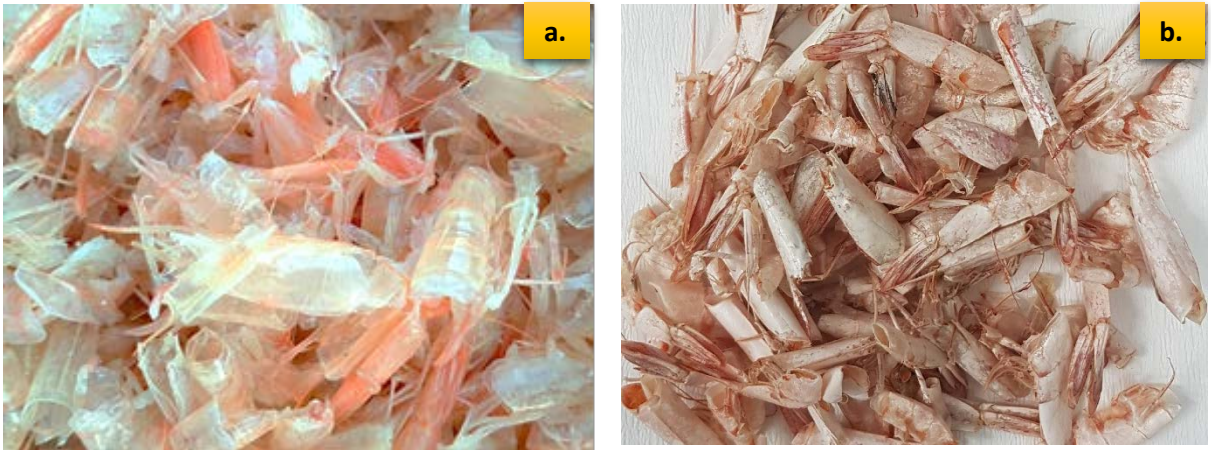

Figure 6.2 Shrimp shells a. cleaned and b. dried

Dried shells grounded in GRT-10BL model multi-function disintegrator until the desired sieve sizes were reached (Figure 6.3). The shells were classified into +60 mesh, -60, +40 mesh, and -40, +18 mesh sizes using stainless steel sieves as shown in Figure 6.4 and 6.5 for crab and shrimp shells, respectively.

Figure 6.3 Grinding of the shrimp shells

Figure 6.4 Crab shells divided into sieve meshes a. -40, +18 mesh, b. -60, +40 mesh, c. +60 mesh

Figure 6.5 Shrimp shells divided into sieve meshes a. -40, +18 mesh, b. -60, +40 mesh, c. +60 mesh

After the crab and shrimp shells have been prepared for processing, they were deproteinized and demineralized to remove protein, minerals, color pigments, and salts to transform shells

into chitin. The acetylamino groups (–NH–CH_3–(C=O)) in the structure of chitin were then transformed into amino groups using the deacetylation process, resulting in the conversion of chitin to chitosan. The chemicals used in these processes are hydrochloric acid fuming 37% (HCl, for analysis EMSURE® ACS, ISO, Reag. Ph Eur) and sodium hydroxide (NaOH, pellets EMPLURA®) from Merck Chemicals (Merck KGaA, Darmstadt, Germany). To prepare the 2% (v/w) NaOH solution used in the deproteinization step, 20 g of NaOH was dissolved with some distilled water and transferred to a 1 L flask and filled with distilled water. To prepare the 2% (v/v) HCl solution used in the deproteinization step, 54 mL of 37% HCl was transferred to a 1 L flask and filled with distilled water. In order to prepare the 30% (v/w) NaOH solution used in the deacetylation process, 300 g of NaOH was dissolved with some distilled water and transferred to a 1 L flask and filled with distilled water.

6.1.2 Deproteinization

The deproteinization step was done for the removal of the proteins, color pigments, and other organic materials. Firstly, 50 ± 0.04 grams of crab and shrimp shells were weighed with Radwag AS 220.R2 digital scale (Radwag, Radom, Poland) in beakers and 1:30 (w:v) 2% NaOH was added onto. The reaction was carried out on a magnetic stirrer with hotplate SMHS 3/6 (Witeg Labortechnik GmbH, Wertheim, Germany), under the agitation of 500 rpm at 80°C for 2 hours as shown in Figure 6.6 and 6.7 for crab and shrimp shells, respectively.

Figure 6.6 Deproteinization of crab shells

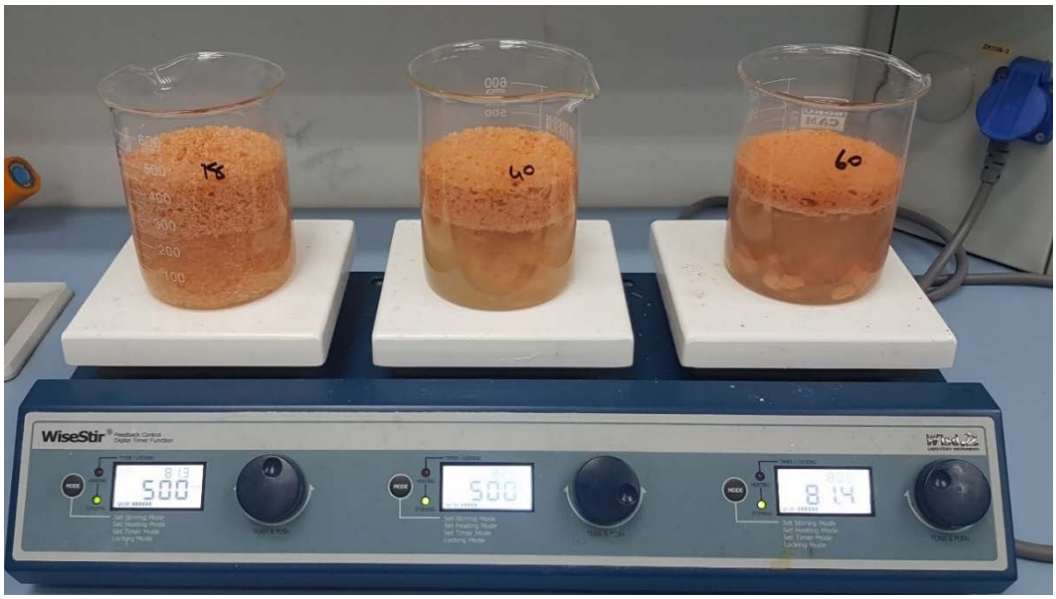

Figure 6.7 Deproteinization of shrimp shells

At the end of the process, the deproteinized shells were filtered under vacuum with the help of a vacuum pump. During the filtration process, the shells were washed with at least 2 L of distilled water until the filtrate color became transparent and the pH was neutral as shown in Figure 6.8 and 6.9 for crab and shrimp shells respectively. Then the shells were left on filter paper to dry in an oven at 40℃ overnight. To calculate the amount of protein and organic matter removed from the shells, the shells were weighed at the end of the process.

Figure 6.8 Filtration after deproteinization of crab shells

Figure 6.9 Filtration after deproteinization of shrimp shells

6.1.3 Demineralization

The demineralization was done to remove minerals from the deproteinized shells. The weighed deproteinized shells were treated with a 2% HCl solution at a ratio of 1:30 (w:v) on a magnetic stirrer at 500 rpm at 80°C for 2 hours. Then the demineralized shells were washed with at least 1 L of distilled water to pH adjustment and filtered under vacuum. The washed shells were then dried overnight in a 40°C oven on the filter papers as shown in Figure 6.10 and Figure 6.11 for crab and shrimp based samples respectively. The dried shell was weighed to calculate the amount of mineral loss.

After the deproteinization and demineralization stages, the shells are called chitin. Deacetylation of chitin in an alkaline environment provides chitin to transform into chitosan.

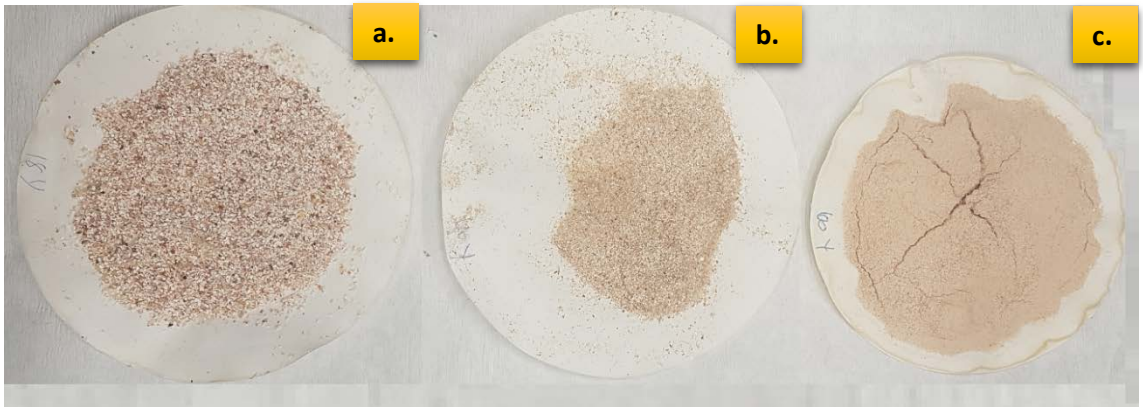

Figure 6.10 Dried chitin obtained from crab shells a. -40, +18 mesh, b. -60, +40 mesh, c. +60 mesh

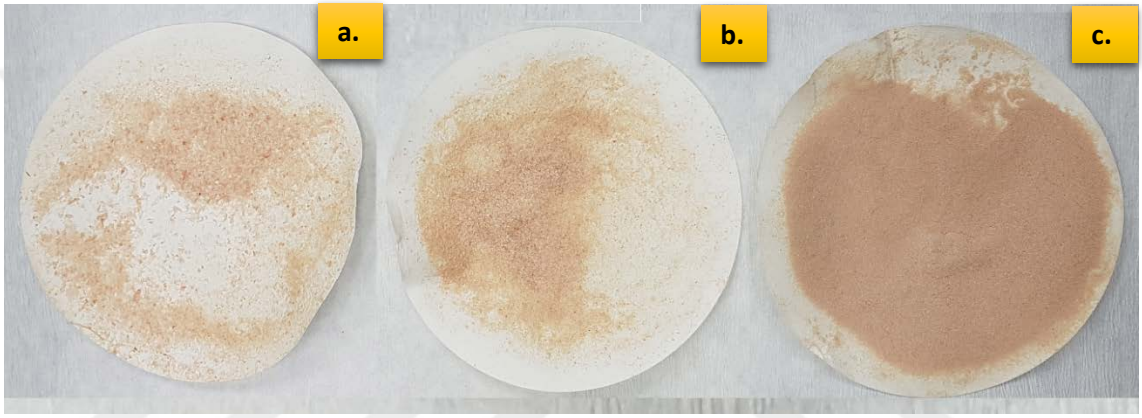

Figure 6.11 Dried chitin obtained from shrimp shells a. -40, +18 mesh, b. -60, +40 mesh, c. +60 mesh

6.1.4 Deacetylation

The deacetylation step is the conversion of chitin to chitosan by removing the acetyl group in chitin. For this process, the chitin samples obtained from the demineralization process were divided into 3 groups to be deacetylated at 60, 80 and 100 °C in order to observe the effect of temperature on the chitosan production efficiency. For each temperature, 7 ± 0.01 grams of sample was added with a 30% NaOH solution at a ratio of 1:30 w:v and mixed for 2 hours at 500 rpm in a magnetic stirrer. After the deacetylation step, which was completed by constantly controlling the solution level and temperature, it was washed with at least 1 L of distilled water until neutral pH was observed and filtered under vacuum. The product obtained after this step is called chitosan. Chitosan samples were weighed to determine yield after drying in an oven at 40°C overnight. Chitosan obtained from each production parameter have given in Figures 6.12 and 6.13 for crab and shrimp-based respectively.

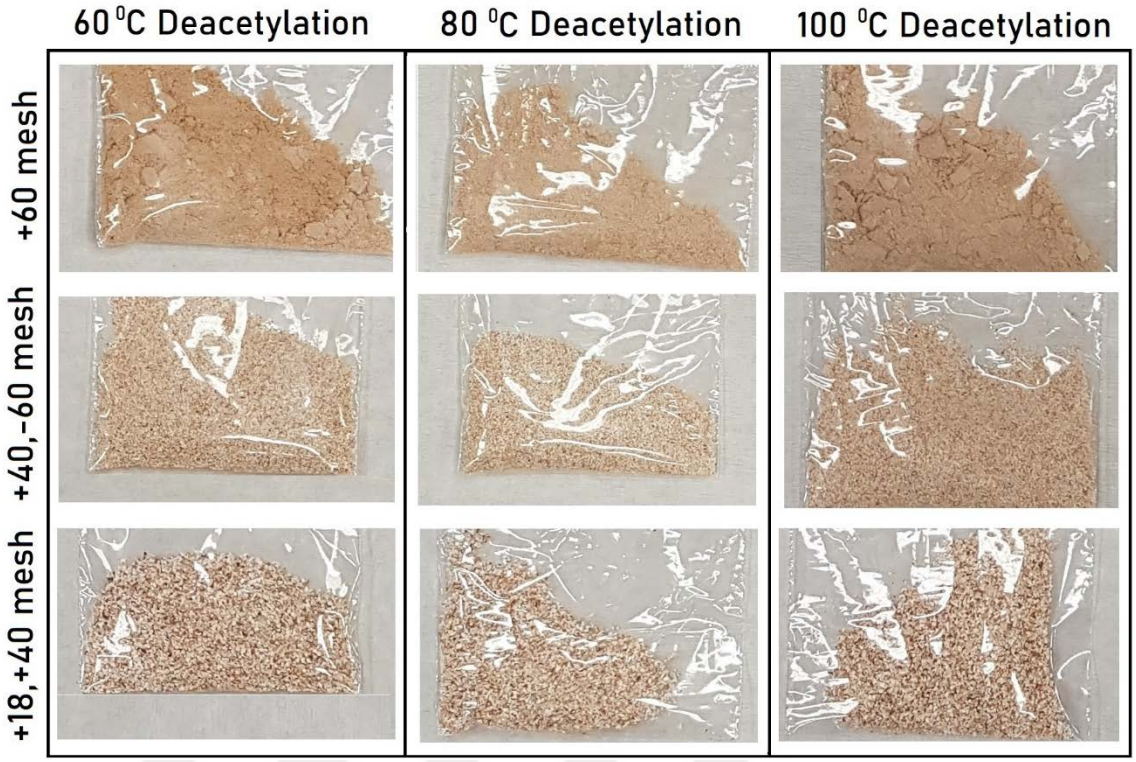

Figure 6.12 Crab-based chitosan samples a. -40, +18 mesh, b. -60, +40 mesh, c. +60 mesh

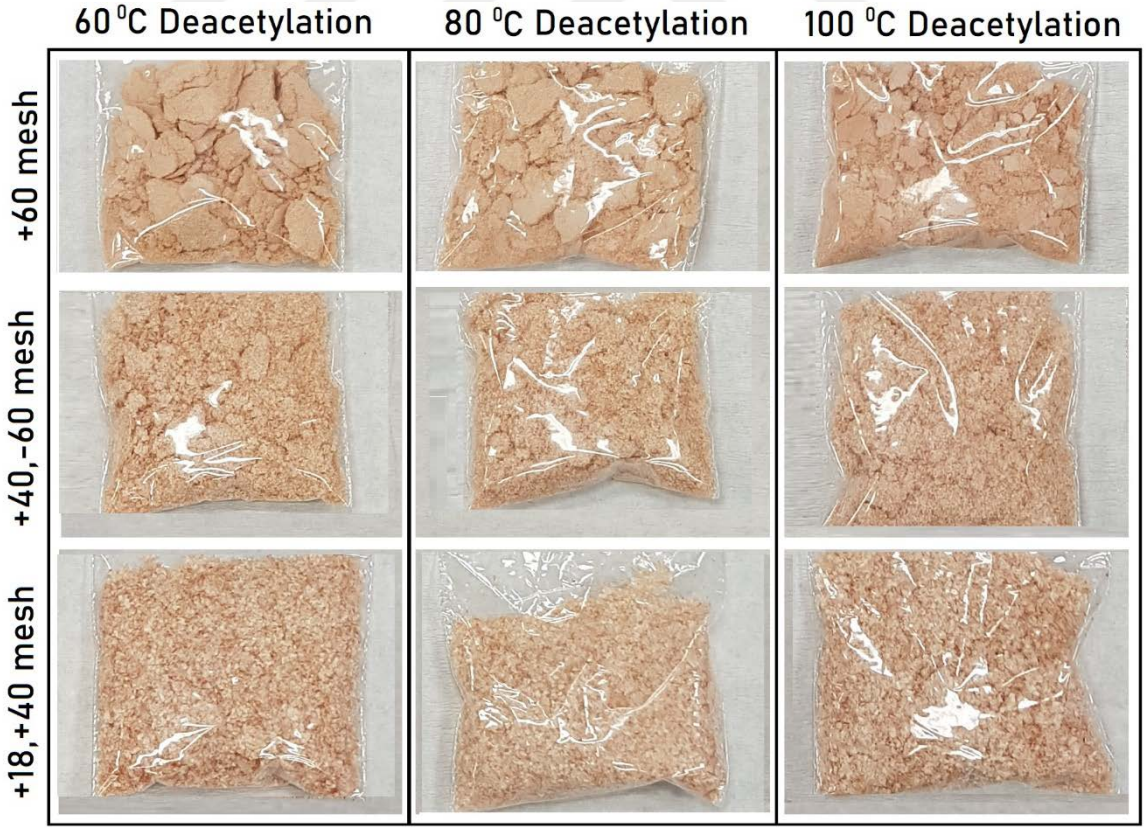

Figure 6.13 Shrimp-based chitosan samples a. -40, +18 mesh, b. -60, +40 mesh, c. +60 mesh

6.1.5 FT-IR Characterization

Fourier-transform infrared spectroscopy (FT-IR) is a vibrational spectroscopic technique used to detect the infrared (IR) absorption spectrum at the molecular level, based on dipole moments in the structure of a solid, liquid, or gas (Mohamed et al., 2017; Lopes et al., 2018). This method for identifying the molecular structure and functional groups based on atom vibration and rotation is based on the absorption of energy from a photon, which supports the transition from a low-energy state to a higher-energy state or an excited state. When continuous wavelength IR radiation passes through the analyzed sample, the light of a certain wavenumber is absorbed, resulting in the absorbance spectrum. This absorbance value is used to determine the physicochemical properties of molecular bonds. In this way, the fingerprint of a certain functional group of the molecule can be detected (Hou et al., 2018; Lopes et al., 2018).

From the FT-IR spectrometer, the transition energies corresponding to changes in the vibrational energy state for many functional groups are found in the IR middle region (4000 - 400 cm^{-1}). Therefore, the appearance of an absorption band in this region can be used to detect specific functional groups. Typically, four bond-type regions can be analyzed from the FTIR spectra. These bonds are single bonds (O–H, C–H, and N–H) that can be detected in the high wavenumber region of 2500 - 4000 cm^{-1}, triple and double bonds that can be detected in the medium wavenumber region of 2000 - 2500 cm^{-1}, and 1500 - 2000 cm^{-1}, respectively, and it can be detected as a complex vibrational pattern in which the molecule is read as a whole in the low wavelength region of 650 - 1500 cm^{-1} (Mohamed et al., 2017).

In the study, crab and shrimp shells that were used as raw material, chitin samples that were produced as an intermediate product, and final product chitosan samples were subjected to FT-IR analysis to confirm that the production stages have occurred successfully. FT–IR analyzes were performed with the Shimadzu IRPrestige-21 Fourier Transform Infrared Spectrophotometer (Shimadzu Corporation, Tokyo, Japan) at wavenumber 2000 - 650 cm^{-1}.

6.1.6 Production Yield

Percent yield calculations used for the deproteinization, demineralization and deacetylation steps were calculated as given in equations 6.1, 6.2 and 6.3, respectively. The yield value obtained after equation 6.2 also represents the production yield for the production of chitin from crab and shrimp shells. Accordingly, equation 6.3 represents the conversion efficiency from chitin to chitosan.

The point to be noted here is that the efficiency calculations were made based on weight. For the production of chitosan, it is necessary to remove protein, minerals, color pigments and other salts from the shells. The greater the removal rates of these substances, the greater the weight loss from the shell to the final product. Accordingly, the purity rate will be higher in the samples with higher weight loss, that is, with lower percent production yield.

$$\text{Deproteinization Yield } \% = \frac{\text{Dry deproteinized shells (g)}}{\text{Dry shells (g)}} \times 100 \qquad (6.1)$$

$$\text{Demineralization Yield (Chitin)}\% = \frac{\text{Dry demineralized shells (g)}}{\text{Dry deproteinized shells (g)}} \times 100 \qquad (6.2)$$

$$\text{Deacetylation Yield (Chitosan)}\% = \frac{\text{Dry deacetylated shells (g)}}{\text{Dry demineralized shells (g)}} \times 100 \qquad (6.3)$$

6.1.7 Color Analysis

Crab and shrimp shells, chitin and chitosan samples were subjected to color analysis and the color change that occurred during the processes was followed. Colorimeter device PCE-CSM 1 model (PCE Instruments UK Ltd., Southampton Hampshire, UK) was used for color analysis. Hunter color analysis is a method that shows the lightness value of the product with +L*, the redness value with +a*, the green value with -a*, the yellowness value with +b* and the blueness value with -b*, as shown in Figure 6.14. According to these results, how the production stages affect the color properties has been interpreted. ΔE (total color change) values were calculated by equation 6.4 (Malien-Aubert et al., 2001; Hunter & Harold, 1975; Ozyalcin & Kipcak, 2022).

Figure 6.14 Hunter color scale (Hunter L, a, b Color Space, n.d.)

$$\Delta E = \sqrt{(L_0 - L)^* + (a_0 - a)^* + (b_0 - b)^*} \quad (6.4)$$

where, L_0*, a_0* and b_0* values are the L*, a* and b* values of the shells, respectively.

6.2 Heavy Metal Adsorption

The chitosan samples were employed in adsorption experiments with heavy metals such as aluminium, antimony, and lead in solutions. It was determined to use chitosan samples produced by deacetylation at 80°C in adsorption experiments after assessing the production yield of chitosan samples produced by deacetylation at 60, 80, and 100 °C.

Furthermore, preliminary investigations revealed that the adsorption process stabilized about 3 hours. Products in contact with heavy metals were stored separately in accordance with laboratory safety rules during the processes.

6.2.1 Material Preparation

Standard solutions of Aluminium (119770, traceable to SRM from NIST $Al(NO_3)_3$ in HNO_3 0.5 mol/l 1000 mg/l Al Certipur®), antimony (170204, traceable to SRM from NIST Sb_2O_3 in HCl 2 mol/l 1000 mg/l Sb Certipur®), and lead (119776, traceable to SRM from NIST $Pb(NO_3)_2$ in HNO_3 0.5 mol/l 1000 mg/l Pb Certipur®) were provided from (Merck KGaA, Darmstadt, Germany) for the adsorption experiments. 20 ppm solutions were prepared from each heavy metal stock solution and employed in adsorption experiments with 0.1 grams of chitosan.

6.2.2 Adsorption Experiments

For the adsorption experiments, 50 mL of 20 ppm heavy metal solution was added to the 0.1 gram chitosan samples weighed into beakers. A total of 54 different adsorption systems were set up, in which crab and shrimp-based, +60 mesh, -60, +40 mesh, -40, +18 mesh chitosan samples were treated with aluminium, antimony and lead metal solutions for 1, 2 and 3 hours.

The adsorption process was carried out at room temperature (20 °C) on a magnetic stirrer with continuous stirring at 300 rpm. After the mixing times of 1, 2 and 3 hours, the solutions were filtered under vacuum. The filtrates were filled into amber bottles and labeled for analysis as shown in Figure 6.15. All glassware used between these processes was pre-washed, dried and brought to room temperature. Figure 6.16 depicts the steps of chitosan production and the adsorption stages.

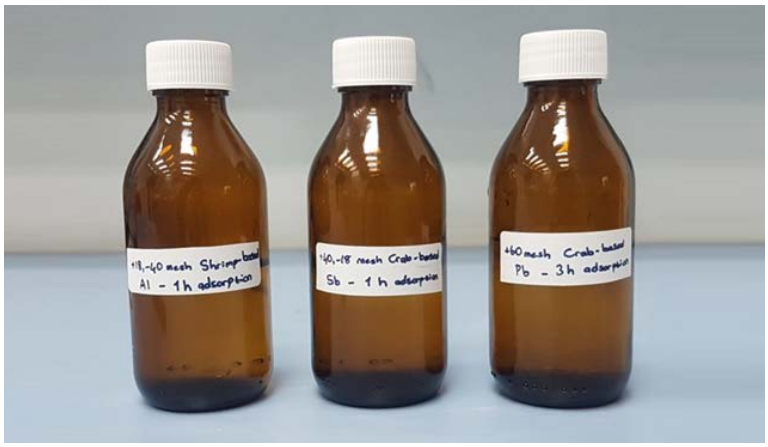

Figure 6.15 Adsorption filtrate solutions

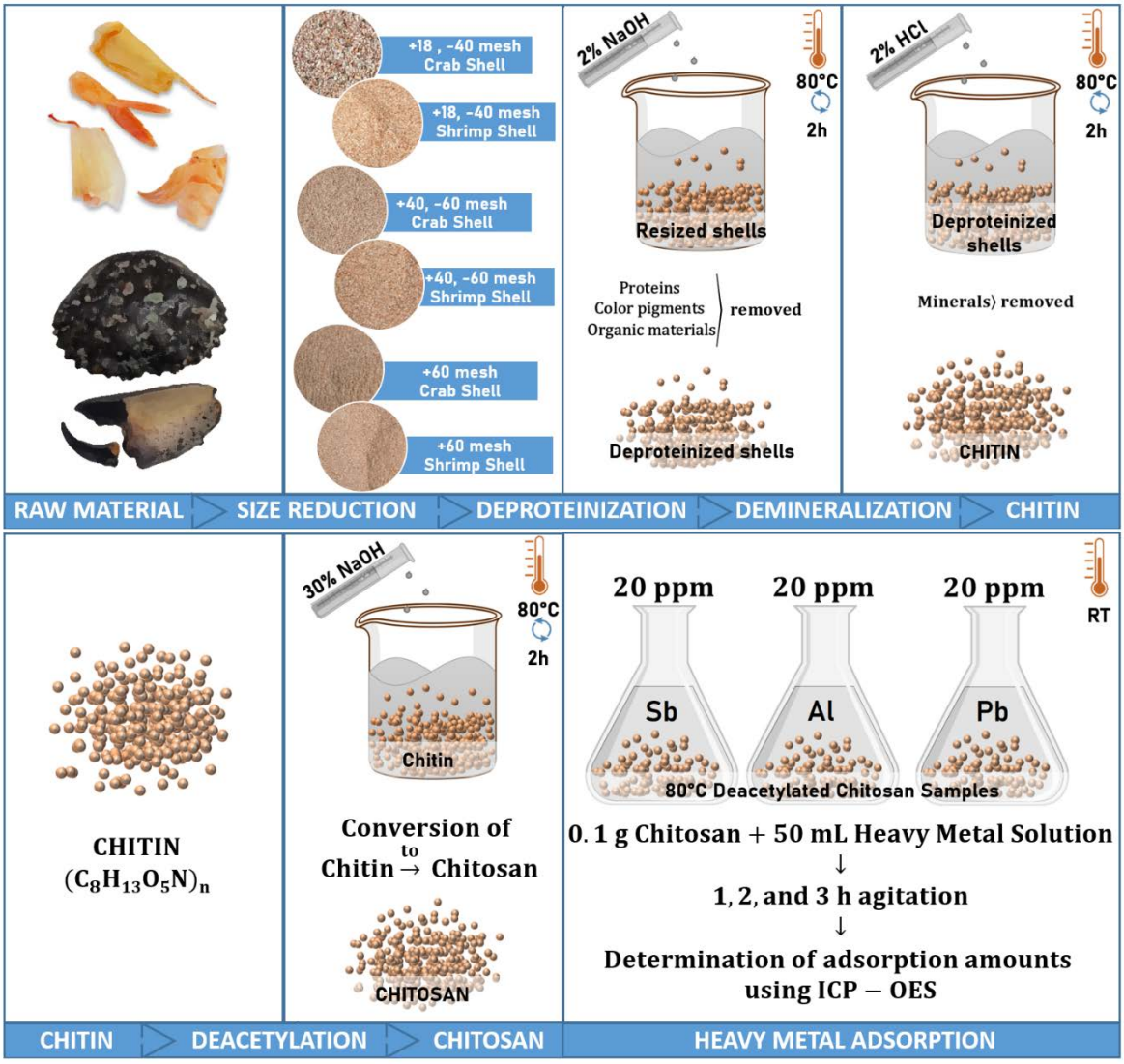

Figure 6.16 Summary diagram of chitosan production and heavy metal adsorption processes

6.2.3 ICP – OES Analysis

A Perkin Elmer Optima 2100 DV Inductively Coupled Plasma Atomic Emission Spectroscopy (ICP-OES) (PerkinElmer Inc., MA, USA) device equipped with an AS-93 autosampler, whose application parameters are given in Table 6.1, was used for elemental content analysis of the filtrates obtained at the end of the adsorption process.

Table 6.1 Perkin Elmer Optima 2100 DV atomic emission spectroscopy parameters

RF Power (W)	1300
Plasma gas flow rate (L min^{-1})	15
Auxiliary gas flow rate (L min^{-1})	0.2
Nebulizer gas flow rate (L min^{-1})	0.8
Sample flow rate (L min^{-1})	1.5
View mode (L min^{-1})	Axial
Read (L min^{-1})	Peak Area
Source equilibration time (s)	15
Read delay (s)	60
Replicates	3
Background correction	2-point (manuel point correction)
Spray chamber	Scott type spray chamber
Nebulizer	Cross-Flow GemTip Nebulizer
Detector	CCD
Purge gas	Nitrogen
Shear gas	Air
Gas	Argon

7
RESULTS AND DISCUSSION

In this section, yield calculations of chitosan production stages, FT-IR evaluations of produced chitosan samples, and adsorption results are evaluated comparatively.

7.1 Results of the Production of Chitosan

7.1.1 Deproteinization Results

The deproteinization process was carried out at 80 °C for 2 hours and it was observed the color pigments in the shrimp shells, in particular, were dissolved in the solution and removed from the shells. The amount of protein and organic matter lost during the reaction was calculated from the dry weights taken before and after the treatment. Yield values calculated based on the amount of substance lost in the process were given in Tables 7.1 and 7.2 for crab and shrimp shells, respectively.

Table 7.1 Yield percentage of deproteinization of crab shells

Mesh	Initial Weight (g)	Final Weight (g)	Weight Loss (g)	Yield (%)	Weight Loss (%)
-40, +18	50.0091	47.4065	2.6026	94.80	5.20
-60, +40	50.0387	46.8220	3.2167	93.57	6.43
+60	50.0092	47.0166	2.9926	94.02	5.98
Average	50.0190	47.0817	2.9373	94.13	5.87

When Table 7.1 is examined, the pre-deproteinization weights of crab shells were determined as 50.0091 g, 50.0387 g, and 50.0092 g for -40, +18, -60, +40 and +60 mesh sieve sizes, respectively, and the average weight was calculated as 50.0190 g. During the deproteinization, as a result of the dissolution of the protein, color pigment and organic substances in the shells, weight losses of 2.6026 g, 3.2167 g and 2.9926 g were observed in

-40, +18, -60, +40 and +60 sieve sizes and the average loss was calculated as 2.9373 g. The final weights of the samples after deproteinization were found to be 47.4065 g, 46.8220 g and 47.0166 g for the -40, +18, -60, +40 and +60 mesh sieve sizes, respectively, and the average final weight was calculated as 47.0817 g. Thus, the yield values calculated in deproteinized crab-based samples were found to be 94.80%, 93.57%, and 94.02% for -40, +18, -60, +40 and +60 mesh sieve sizes, respectively, and the average yield was calculated as 94.13%.

Table 7.2 Yield percentage of deproteinization of shrimp shells

Mesh	Initial Weight (g)	Final Weight (g)	Weight Loss (g)	Yield (%)	Weight Loss (%)
-40, +18	50.0067	34.9002	15.1065	69.79	30.21
-60, +40	50.0026	34.7881	15.2145	69.57	30.43
+60	50.0033	32.6712	17.3321	65.34	34.66
Average	50.0042	34.1198	15.8844	68.23	31.77

When Table 7.2 is examined, the pre-deproteinization weights of shrimp shells were determined as 50.0067 g, 50.0026 g, and 50.0033 g for -40, +18, -60, +40 and +60 mesh sieve sizes, respectively, and the average weight was calculated as 50.0042 g. During the deproteinization, as a result of the dissolution of the protein, color pigment and organic substances in the shells, weight losses of 15.1065 g, 15.2145 g and 17.3321 g were observed in -40, +18, -60, +40 and +60 sieve sizes and the average loss was calculated as 15.8844 g. The final weights of the samples after deproteinization were found to be 34.9002 g, 34.7881 g and 32.6712 g for the -40, +18, -60, +40 and +60 mesh sieve sizes, respectively, and the average final weight was calculated as 34.1198 g. Thus, the yield values calculated in deproteinized shrimp-based samples were found to be 69.79%, 69.57%, and 65.34% for -40, +18, -60, +40 and +60 mesh sieve sizes, respectively, and the average yield was calculated as 68.23%.

When the deproteinization yield of crab and shrimp shells is evaluated, it is clear that shrimp yields are significantly lower than crab samples. The fundamental explanation for this is that they contain more color pigments than crab shells and, as a result of their lower density and higher particle surface area, respond better to deproteinization. Since the amount of material removed from shrimp shells is higher than that of crab shells, the deproteinization yield was found to be lower.

Furthermore, when the mesh sizes are analyzed, it is discovered that the +60 mesh shells lose the greatest weight, while the -40 and +18 mesh shells lose the least. This is due to the increase in particle surface area per unit mass. The yield calculated here is inversely proportional to purity, as the purity of the final product improves as the amount of protein removed from the shells increases.

7.1.2 Demineralization Results

The demineralization process was carried out at 80 °C for 2 hours and it was observed the remained minerals were removed from the deproteinized shells. The amount of mineral lost during the reaction was calculated from the dry weights taken before and after the treatment. Yield values calculated based on the amount of substance lost in the process were given in Tables 7.3 and 7.4 for crab and shrimp shells, respectively.

Table 7.3 Yield percentage of demineralization of crab shells

Mesh	Initial Weight (g)	Final Weight (g)	Weight Loss (g)	Yield (%)	Weight Loss (%)
-40, +18	47.4065	33.8333	13.5732	71.3685	28.6315
-60, +40	46.8220	32.9591	13.8629	70.3923	29.6077
+60	47.0166	33.0455	13.9711	70.2848	29.7152
Average	47.0817	33.2793	13.8024	70.6819	29.3181

When comparing Tables 7.1 and 7.3, it can be seen that the pre-demineralization weights of the samples were the same as the post-deproteinization weights since all deproteinized shells

were processed. Accordingly, the pre-process weights were found to be 47.4065 g, 46.8220 g, and 47.0166 g for -40, +18, -60, +40, and +60 mesh sieve sizes, respectively, and the average weight was calculated as 47.0817 g. Due to mineral losses in demineralization samples, weight losses of 13.5732 g, 13.8629 g and 13.9711 g were observed in -40, +18, -60, +40 and +60 sieve sizes, respectively, and the average loss was calculated as 13.8024 g. The final weights of the samples after demineralization were found to be 33.8333 g, 32.9591 g and 33.0455 g for -40, +18, -60, +40 and +60 mesh sieve sizes, respectively, and the average final weight was calculated as 33.2793 g. Thus, the yield values calculated in demineralized crab-based samples were found to be 71.37%, 70.39% and 70.28% for -40, +18, -60, +40 and +60 mesh sieve sizes, respectively, and the average yield was calculated as 70.68%.

Table 7.4 Yield percentage of demineralization of shrimp shells

Mesh	**Initial Weight (g)**	**Final Weight (g)**	**Weight Loss (g)**	**Yield (%)**	**Weight Loss (%)**
-40, +18	34.9002	24.8971	10.0031	71.3380	28.6620
-60, +40	34.7881	23.3497	11.4384	67.1198	32.8802
+60	32.6712	23.5227	9.1485	71.9983	28.0017
Average	34.1198	23.9232	10.1967	70.1520	29.8480

When comparing Tables 7.2 and 7.4, it can be seen that the pre-demineralization weights of the samples were the same as the post-deproteinization weights since all deproteinized shells were processed. Accordingly, the pre-process weights were found to be 34.9002 g, 34.7881 g, and 32.6712 g for -40, +18, -60, +40, and +60 mesh sieve sizes, respectively, and the average weight was calculated as 34.1198 g. Due to mineral losses in demineralization samples, weight losses of 10.0031 g, 11.4384 g and 9.1485 g were observed in -40, +18, -60, +40 and +60 sieve sizes, respectively, and the average loss was calculated as 10.1967 g. The final weights of the samples after demineralization were found to be 24.8971 g, 23.3497 g and 23.5227 g for -40, +18, -60, +40 and +60 mesh sieve sizes, respectively, and the

average final weight was calculated as 23.9232 g. Thus, the yield values calculated in demineralized shrimp-based samples were found to be 71.34%, 67.12% and 72.00% for -40, +18, -60, +40 and +60 mesh sieve sizes, respectively, and the average yield was calculated as 70.15%.

When comparing the demineralization efficiency of crab and shrimp-based samples, it is clear that the yield percentages are extremely near. The mineral loss increased as the mesh size decreased in crab-based samples. This result supports the idea that lower shell sizes can be employed to get purer chitin and chitosan, which is in line with the deproteinization results. Unexpectedly, the maximum mineral loss in shrimp samples was seen in -40, +18 and -60, +40 mesh samples, rather than +60 mesh samples. This could be due to greater mineral concentration in the samples, or a filtration fault. The yield determined here should be inversely proportional to purity, just like the deproteinization phase.

7.1.3 Deacetylation Results

The deacetylation process was carried out at 60, 80, and 100 ℃ for 2 hours to observe the effect of temperature on the production yield. Deacetylation yield calculation was applied by comparing the dry weights taken before and after the reaction. The deacetylation yield data given in Tables 7.5, 7.6 and 7.7 for crab-based products for 60, 80 and 100 ℃ deacetylation temperatures respectively. Moreover, the deacetylation yield data given in Tables 7.8, 7.9 and 7.10 for shrimp-based products for 60, 80 and 100 ℃ deacetylation temperatures respectively.

Table 7.5 Yield percentage of 60 ℃ deacetylation of crab based chitin

Mesh	Initial Weight (g)	Final Weight (g)	Weight Loss (g)	Yield (%)	Weight Loss (%)
-40, +18	7.0044	5.6132	1.3912	80.1382	19.8618
-60, +40	7.0102	5.4430	1.5672	77.6440	22.3560
+60	7.0053	6.5430	0.4623	93.4007	6.5993
Average	7.0066	5.8664	1.1402	83.7276	16.2724

When Table 7.5 is examined, the pre-deacetylation weights of crab-based samples subjected to deacetylation at 60 ℃ were determined as 7.0044 g, 7.0102 g, and 7.0053 g for -40, +18, -60, +40 and +60 mesh sieve sizes, respectively, and the average weight was calculated as 7.0066 g. With the chemical changes occurring during the deacetylation process, 1.3912 g, 1.5672 g and 0.4623 g material losses were observed for the sieve sizes -40, +18, -60, +40 and +60 mesh, respectively, and the average material loss was calculated as 1.1402 g. The final weights of the samples after deacetylation were found to be 5.6132 g, 5.4430 g, and 6.5430 g for -40, +18, -60, +40, and +60 mesh sieve sizes, respectively, and the average final weight was calculated as 5.8664 g. Hence, the yield values calculated on the basis of material loss in 60 ℃ deacetylated crab-based samples for -40, +18, -60, +40, and +60 mesh sieve sizes, respectively, were found to be 80.14%, 77.64%, and 93.40% and the average yield was 83.73%.

Table 7.6 Yield percentage of 80 ℃ deacetylation of crab based chitin

Mesh	Initial Weight (g)	Final Weight (g)	Weight Loss (g)	Yield (%)	Weight Loss (%)
-40, +18	7.0023	5.4725	1.5298	78.1529	21.8471
-60, +40	7.0012	5.0703	1.9309	72.4204	27.5796
+60	7.0053	4.2227	2.7826	60.2786	39.7214
Average	7.0029	4.9218	2.0811	70.2840	29.7160

When Table 7.6 is examined, the pre-deacetylation weights of crab-based samples subjected to deacetylation at 80 ℃ were determined as 7.0023 g, 7.0012 g and 7.0053 g for -40, +18, -60, +40 and +60 mesh sieve sizes, respectively, and the average weight was calculated as 7.0029 g. With the chemical changes occurring during the deacetylation process, 1.5298 g, 1.9309 g, and 2.7826 g material losses were observed for the sieve sizes -40, +18, -60, +40 and +60 mesh, respectively, and the average material loss was calculated as 2.0811 g. The final weights of the samples after deacetylation were found to be 5.0703 g, 4.2227 g, and 5.6132 g for -40, +18, -60, +40, and +60 mesh sieve sizes, respectively, and the average final

weight was calculated as 4.9218 g. Hence, the yield values calculated on the basis of material loss in 80 ℃ deacetylated crab-based samples for -40, +18, -60, +40, and +60 mesh sieve sizes, respectively, were found to be 78.15%, 72.42%, and 60.28% and the average yield was 70.28%.

Table 7.7 Yield percentage of 100 ℃ deacetylation of crab based chitin

Mesh	Initial Weight (g)	Final Weight (g)	Weight Loss (g)	Yield (%)	Weight Loss (%)
-40, +18	7.0095	5.3590	1.6505	76.4534	23.5466
-60, +40	7.0288	5.1293	1.8995	72.9755	27.0245
+60	7.0088	5.1829	1.8259	73.9485	26.0515
Average	7.0157	5.2237	1.7920	74.4591	25.5409

When Table 7.7 is examined, the pre-deacetylation weights of crab-based samples subjected to deacetylation at 80 ℃ were determined as 7.0095 g, 7.0288 g and 7.0088 g for -40, +18, -60, +40 and +60 mesh sieve sizes, respectively, and the average weight was calculated as 7.0157 g. With the chemical changes occurring during the deacetylation process, 1.6505 g, 1.8995 g, and 1.8259 g material losses were observed for the sieve sizes -40, +18, -60, +40 and +60 mesh, respectively, and the average material loss was calculated as 1.7920 g. The final weights of the samples after deacetylation were found to be 5.3590 g, 5.1293 g, and 5.1829 g for -40, +18, -60, +40, and +60 mesh sieve sizes, respectively, and the average final weight was calculated as 5.2237 g. Hence, the yield values calculated on the basis of material loss in 100 ℃ deacetylated crab-based samples for -40, +18, -60, +40, and +60 mesh sieve sizes, respectively, were found to be 76.45%, 72.98%, and 73.95% and the average yield was 74.46%.

Table 7.8 Yield percentage of 60 ℃ deacetylation of shrimp based chitin

Mesh	Initial Weight (g)	Final Weight (g)	Weight Loss (g)	Yield (%)	Weight Loss (%)
-40, +18	7.0006	6.3424	0.6582	90.5982	9.4018
-60, +40	7.0075	5.6931	1.3144	81.2430	18.7570
+60	7.0098	4.4530	2.5568	63.5254	36.4746
Average	7.0060	5.4962	1.5098	78.4555	21.5445

When Table 7.8 is examined, the pre-deacetylation weights of shrimp-based samples subjected to deacetylation at 60 ℃ were determined as 7.0006 g, 7.0075 g, and 7.0098 g for -40, +18, -60, +40 and +60 mesh sieve sizes, respectively, and the average weight was calculated as 7.0060 g. With the chemical changes occurring during the deacetylation process, 0. 6582 g, 1.3144 g and 2.5568 g material losses were observed for the sieve sizes -40, +18, -60, +40 and +60 mesh, respectively, and the average material loss was calculated as 1.5098 g. The final weights of the samples after deacetylation were found to be 6.3424 g, 5.6931 g, and 4.4530 g for -40, +18, -60, +40, and +60 mesh sieve sizes, respectively, and the average final weight was calculated as 5.4962 g. Hence, the yield values calculated on the basis of material loss in 60 ℃ deacetylated shrimp-based samples for -40, +18, -60, +40, and +60 mesh sieve sizes, respectively, were found to be 90.60%, 81.24%, and 63.53% and the average yield was 78.46%.

When Table 7.9 is examined, the pre-deacetylation weights of shrimp-based samples subjected to deacetylation at 80 ℃ were determined as 7.0061 g, 7.0021 g and 7.0016 g for -40, +18, -60, +40 and +60 mesh sieve sizes, respectively, and the average weight was calculated as 7.0033 g. With the chemical changes occurring during the deacetylation process, 1.1562 g, 1.3609 g, and 2.7008 g material losses were observed for the sieve sizes -40, +18, -60, +40 and +60 mesh, respectively, and the average material loss was calculated as 1.7393 g. The final weights of the samples after deacetylation were found to be 5.8499 g, 5.6412 g, and 4.3008 g for -40, +18, -60, +40, and +60 mesh sieve sizes, respectively, and

the average final weight was calculated as 5.2640 g. Hence, the yield values calculated on the basis of material loss in 80 ℃ deacetylated shrimp-based samples for -40, +18, -60, +40, and +60 mesh sieve sizes, respectively, were found to be 83.50%, 80.56%, and 61.43% and the average yield was 75.16%.

Table 7.9 Yield percentage of 80 ℃ deacetylation of shrimp based chitin

Mesh	Initial Weight (g)	Final Weight (g)	Weight Loss (g)	Yield (%)	Weight Loss (%)
-40, +18	7.0061	5.8499	1.1562	83.4976	16.5024
-60, +40	7.0021	5.6412	1.3609	80.5644	19.4356
+60	7.0016	4.3008	2.7008	61.4260	38.5740
Average	7.0033	5.2640	1.7393	75.1626	24.8374

Table 7.10 Yield percentage of 100 ℃ deacetylation of shrimp based chitin

Mesh	Initial Weight (g)	Final Weight (g)	Weight Loss (g)	Yield (%)	Weight Loss (%)
-40, +18	7.0070	5.9248	1.0822	84.5560	15.4440
-60, +40	7.0078	5.6052	1.4026	79.9852	20.0148
+60	7.0078	4.8604	2.1474	69.3570	30.6430
Average	7.0075	5.4635	1.5441	77.9661	22.0339

When Table 7.10 is examined, the pre-deacetylation weights of shrimp-based samples subjected to deacetylation at 80 ℃ were determined as 7.0070 g, 7.0078 g and 7.0078 g for -40, +18, -60, +40 and +60 mesh sieve sizes, respectively, and the average weight was calculated as 7.0075 g. With the chemical changes occurring during the deacetylation

process, 1.0822 g, 1.4026 g, and 2.1474 g material losses were observed for the sieve sizes -40, +18, -60, +40 and +60 mesh, respectively, and the average material loss was calculated as 1.5441 g. The final weights of the samples after deacetylation were found to be 5.9248 g, 5.6052 g, and 4.8604 g for -40, +18, -60, +40, and +60 mesh sieve sizes, respectively, and the average final weight was calculated as 5.4635 g. Hence, the yield values calculated on the basis of material loss in 100 ℃ deacetylated shrimp-based samples for -40, +18, -60, +40, and +60 mesh sieve sizes, respectively, were found to be 84.56%, 79.99%, and 69.36% and the average yield was 77.97%.

When the deacetylation yields of crab and shrimp-based samples were examined, it was revealed that crab-based samples lost more material than shrimp-based samples during the deacetylation stage, which was in contrast to what was observed in deproteinization and demineralization stages. In terms of particle sizes, smaller particle sizes were shown to result in lower yields, which was consistent with the previous two stages. Finally, when the effect of temperature on production efficiency was evaluated, the lowest yield was found in deacetylated chitosan samples deacetylated at 80°C, followed by 100 and 60°C, respectively.

7.1.4 FT-IR Characterization Results

FTIR spectroscopic analysis was used to determine the chemical structure of the samples from shells to final product chitosan. FT-IR spectrum of the crab-based products from left to right for mesh sizes +18,-40, +40,-60, and +60 are given in Figures 7.1 to 7.5 respectively for crab shells, crab based chitin, 60 °C deacetylated crab-based chitosan, 80 °C deacetylated crab-based chitosan, 100 °C deacetylated crab-based chitosan. FT-IR spectrum of the shrimp-based products from left to right for mesh sizes +18,-40, +40,-60, and +60 are given in Figures 7.6 to 7.10 respectively for shrimp shells, shrimp based chitin, 60 °C deacetylated shrimp-based chitosan, 80 °C deacetylated shrimp-based chitosan, 100 °C deacetylated shrimp-based chitosan.

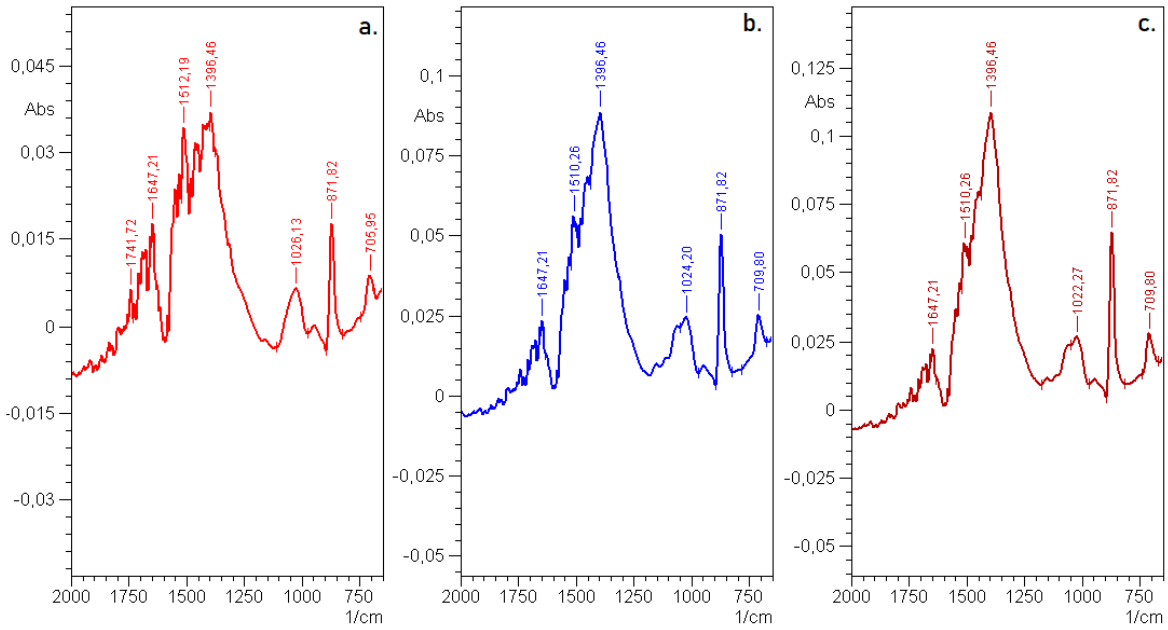

Figure 7.1 FT-IR spectra of crab shells a. -40, +18 mesh, b. -60, +40 mesh, c. +60 mesh

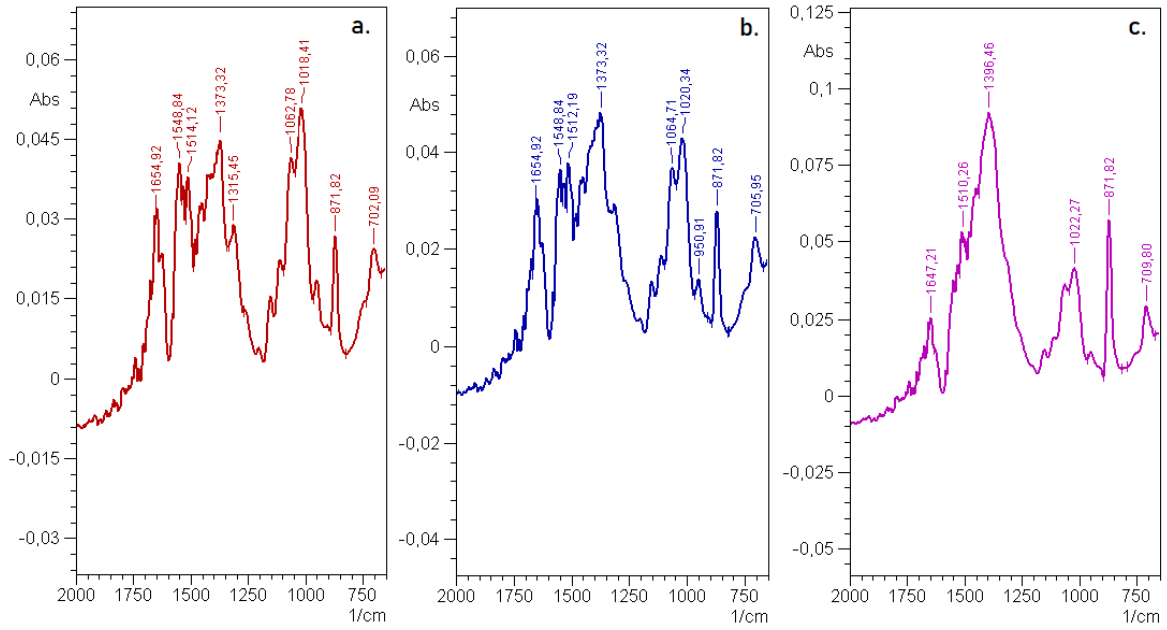

Figure 7.2 FT-IR spectra of crab-based chitin a. -40, +18 mesh, b. -60, +40 mesh, c. +60 mesh

When Figures 7.1 and 7.2 were examined, similar peaks were observed in all three mesh sizes. Stretching vibration peaks showing one or more C–H bonds were observed around 1300-1400 cm^{-1}. When these peaks were compared, it can be said that the stretching vibration in the C–H band of the chitin (1200 - 1500 cm^{-1}) was caused by the high amount of color pigment and other materials removed from the shell and it is consistent with the chemical structure of the chitin ($(C_8H_{13}O_5N)_n$).

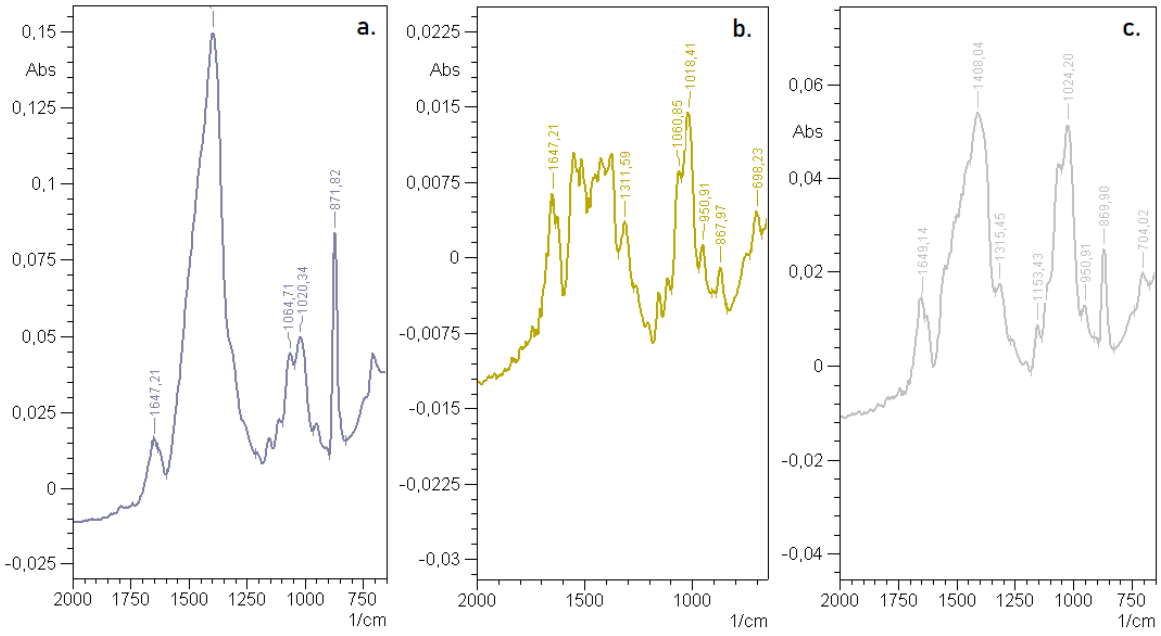

Figure 7.3 FT-IR spectra of 60°C deacetylated crab-based chitosan a. -40, +18 mesh, b. -60, +40 mesh, c. +60 mesh

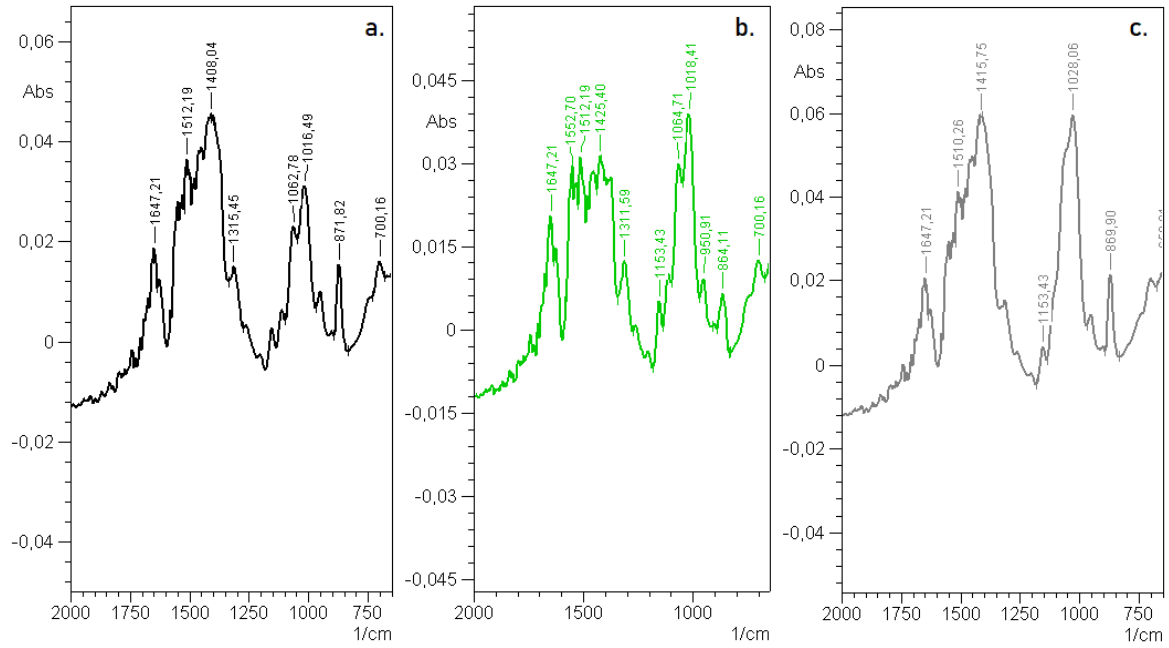

Figure 7.4 FT-IR spectra of 80°C deacetylated crab-based chitosan a. -40, +18 mesh, b. -60, +40 mesh, c. +60 mesh

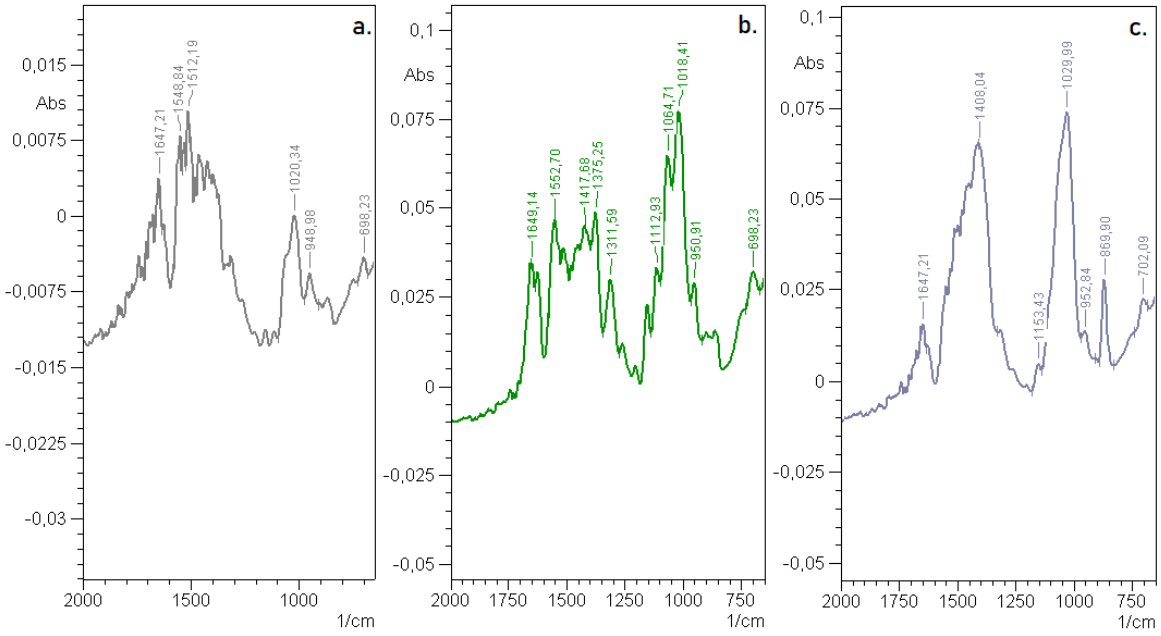

Figure 7.5 FT-IR spectra of 100°C deacetylated crab-based chitosan a. -40, +18 mesh, b. -60, +40 mesh, c. +60 mesh

Compared to Figures 7.3, 7.4, and 7.5, weaker peaks were recorded around 1200-1500 cm^{-1} in chitosan samples. It can be said that the reason for this is the acetyl group (CH_3–(C=O)) found in the shell and chitin samples and removed by deacetylation during the conversion to chitosan. When the spectra of chitin and chitosan are compared, strong stretching of amide I assigned to stretching of the C=O group hydrogen bonded to N–H of the neighboring intra-sheet chain is observed in chitin compared to chitosan. However, in the same region, chitosan samples show lower concentration of amide I (C=O stretch) due to their degree of deacetylation. Likewise, while amide II (N–H bending) and amide III (C–N stretching) bonds were detected around 1550 cm^{-1} in chitin samples, weaker peaks were observed in chitosan samples due to N–H deformation of $–NH_2$ bending.

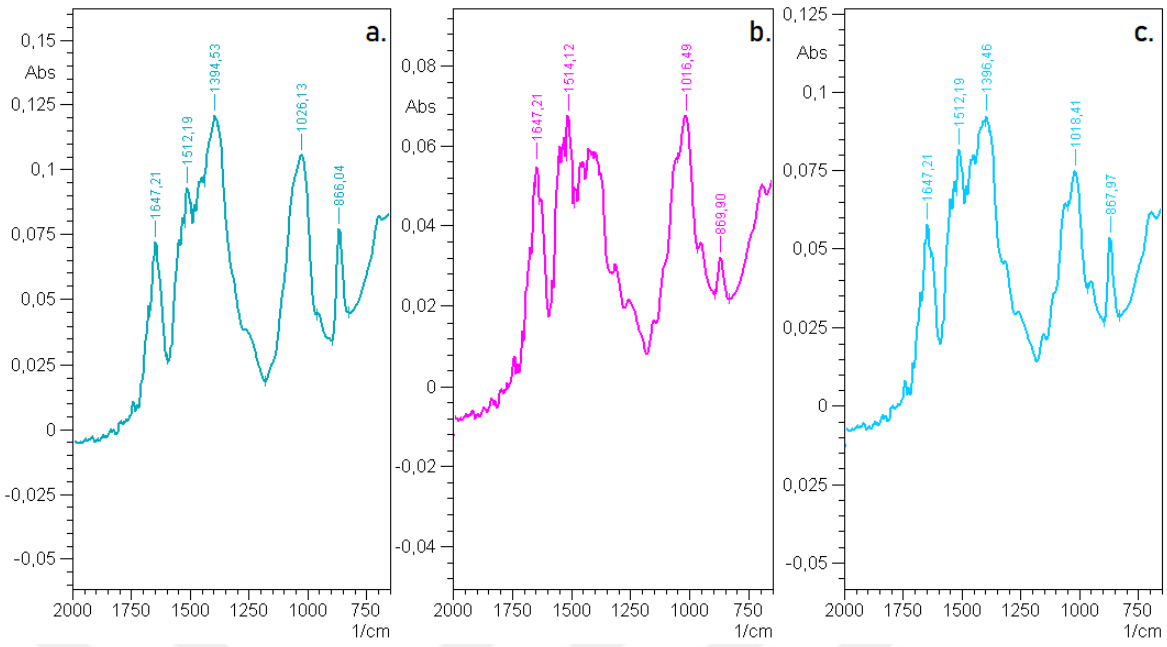

Figure 7.6 FT-IR spectra of shrimp shells a. -40, +18 mesh, b. -60, +40 mesh, c. +60 mesh

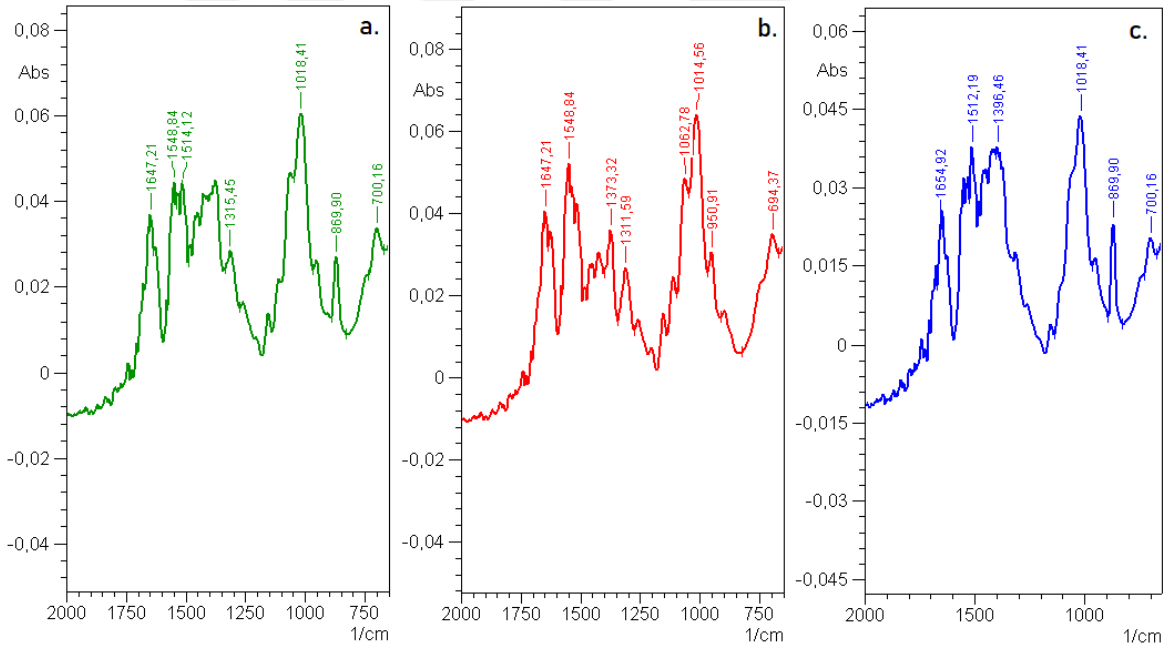

Figure 7.7 FT-IR spectra of shrimp-based chitin a. -40, +18 mesh, b. -60, +40 mesh, c. +60 mesh

When Figures 7.6 and 7.7 were examined, similar peaks were observed in all three mesh sizes. Similar to crab-based products, stretching vibration peaks showing one or more C–H bonds were observed around 1400-1600 cm^{-1}. When these peaks were compared, it can be said that the stretching vibration in the C–H band of the chitin (1200 - 1500 cm^{-1}) was caused

by the high amount of color pigment and other materials removed from the shell and it is consistent with the chemical structure of the chitin ($(C_8H_{13}O5N)_n$).

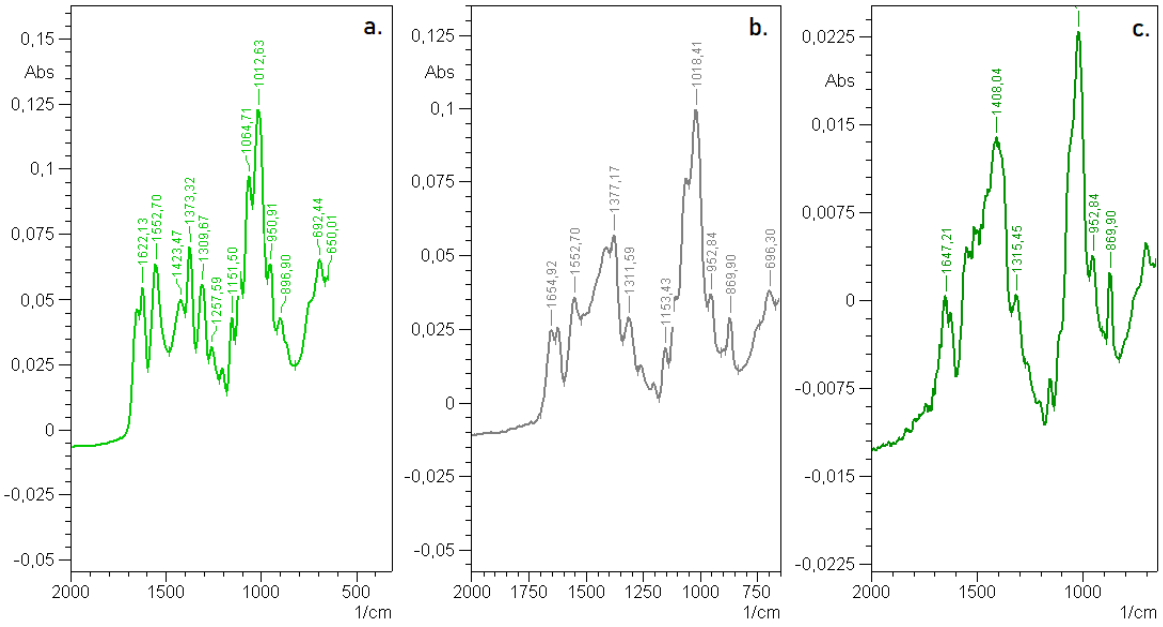

Figure 7.8 FT-IR spectra of 60°C deacetylated shrimp-based chitosan a. -40, +18 mesh, b. -60, +40 mesh, c. +60 mesh

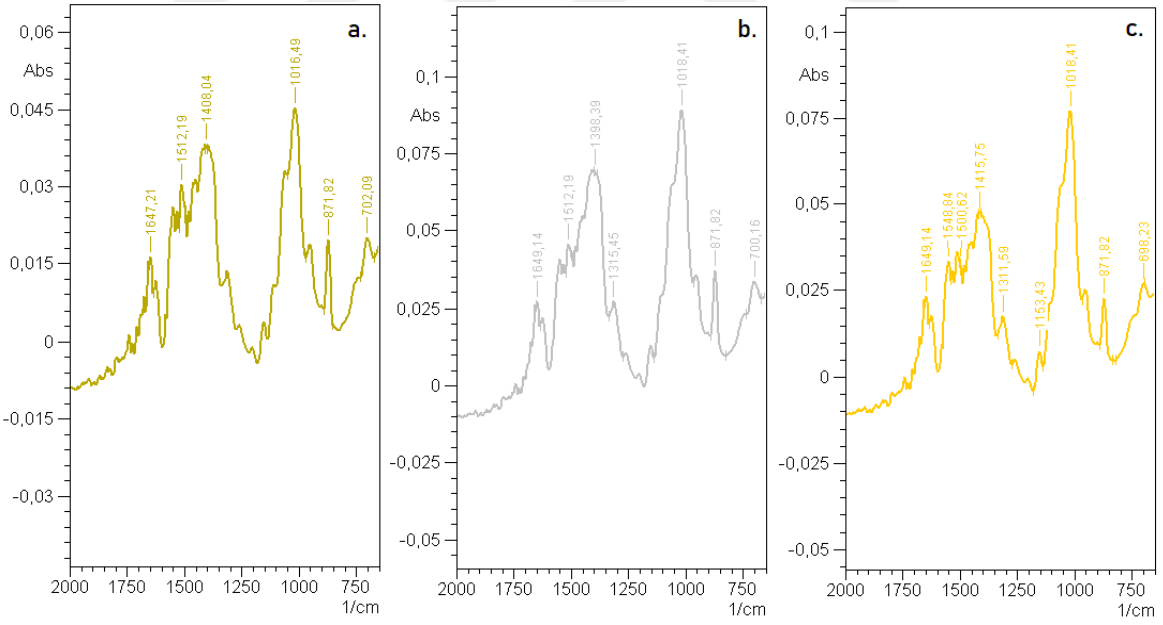

Figure 7.9 FT-IR spectra of 80°C deacetylated shrimp-based chitosan a. -40, +18 mesh, b. -60, +40 mesh, c. +60 mesh

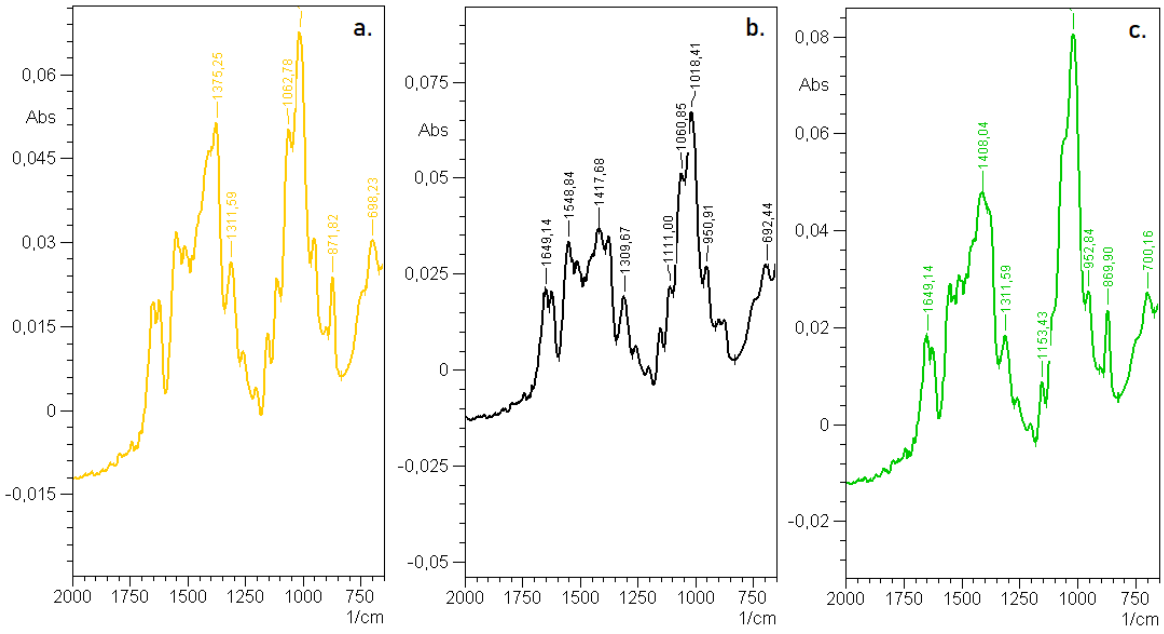

Figure 7.10 FT-IR spectra of 100°C deacetylated shrimp-based chitosan a. -40, +18 mesh, b. -60, +40 mesh, c. +60 mesh

Compared to Figures 7.8, 7.9 and 7.10, weak peaks were detected around 1200-1500 cm^{-1} due to the acetyl groups removed during the deacetylation step, as in the crab-based samples. Besides, C–O stretching and C–O–C asymmetric stretching of $–CH_2–OH$ and –CH–OH were observed between 1070 - 1020 cm^{-1}. Similar to the crab samples, the C=O group amide I peaks were detected at less depth than the chitin samples due to deacetylation in shrimp-based samples. Likewise, while amide II (N–H bending) and amide III (C–N stretching) bonds were detected around 1550 cm^{-1} in chitin samples, weaker peaks were observed in chitosan samples due to the N–H deformation of $–NH_2$ bending.

When the crab and shrimp-based samples were compared, it was determined that the observed peaks matched the chemical structure of chitosan and were similar. However, it is clearly seen that stretching vibration peaks around 1000 cm^{-1} in shrimp-based samples are more pronounced than in crab-based samples. This can be interpreted as shrimp-based samples respond better to deacetylation compared to crab-based samples.

When the effect of deacetylation temperatures was examined, it was determined that the peaks obtained at 80 and 100 °C in crab-based samples overlapped with the chemical structure of chitosan, but the structures of 60°C deacetylated samples were more like chitin chemistry. From this, it can be interpreted that the deacetylation process for crab-based samples should be carried out above 60°C. It was determined that the temperature difference

in the deacetylation stage did not show a significant chemical effect in shrimp-based samples as much as in crab.

7.1.5 Production Yield Results

The yields of different deacetylation temperatures, different sizes, and raw material sources for each step were given in the previous headings. Total yield, calculated by weight from shell to final product, is shown in Tables 7.11 and 7.12 for crab and shrimp based samples, respectively. The mentioned yield values are based on the dry weights taken at the beginning and end of the process and are inversely proportional to the purity of the product. Accordingly, an increase in the amount of protein, mineral and other organic matter removed during the conversion from the shell of crustaceans to chitosan will reduce the yield values calculated on a weight basis and will ensure that chitosan is obtained in a purer form.

Table 7.11 Total production yields of crab-based chitosan

Deacetylation Temp.	**-40, +18 mesh**	**-60, +40 mesh**	**+60 mesh**	**Average**
60°C	54.22%	51.14%	61.72%	55.71%
80°C	52.87%	47.70%	39.83%	46.76%
100°C	51.72%	48.07%	48.86%	49.54%
Average	52.94%	48.97%	50.14%	50.67%

According to Table 7.11, the total yield of crab-based chitosan production was found in 60°C deacetylated samples for -40, +18 mesh, -60, +40 mesh, and +60 mesh sizes respectively as 54.22%, 51.14%, and 61.72% and averagely as 55.71%. In 80°C deacetylated samples for -40, +18 mesh, -60, +40 mesh, and +60 mesh sizes respectively as 52.87%, 47.70%, and 39.83% and averagely as 46.76%. In 100°C deacetylated samples for -40, +18 mesh, -60, +40 mesh, and +60 mesh sizes respectively as 51.72%, 48.07%, and 48.86% and averagely as 49.54%. Moreover, average yield values were also calculated based on mesh sizes and were found to be 52.94%, 48.97%, and 50.14% for -40, +18 mesh, -60, +40 mesh, and +60

mesh sizes, respectively. For crab-based chitosan production, the final yield calculated by including all parameters from shell to chitosan was calculated as 50.67%.

Table 7.12 Total production yields of shrimp-based chitosan

Deacetylation Temp.	**-40, +18 mesh**	**-60, +40 mesh**	**+60 mesh**	**Average**
60°C	45.11%	37.94%	29.88%	37.53%
80°C	41.57%	37.62%	28.90%	35.96%
100°C	42.10%	37.35%	32.63%	37.30%
Average	42.93%	37.64%	30.47%	36.93%

According to Table 7.12, the total yield of shrimp-based chitosan production was found in 60°C deacetylated samples for -40, +18 mesh, -60, +40 mesh, and +60 mesh sizes respectively as 45.11%, 37.94%, and 29.88% and averagely as 37.53%. In 80°C deacetylated samples for -40, +18 mesh, -60, +40 mesh, and +60 mesh sizes respectively as 41.57%, 37.62%, and 28.90% and averagely as 35.96%. In 100°C deacetylated samples for -40, +18 mesh, -60, +40 mesh, and +60 mesh sizes respectively as 42.10%, 37.35%, and 32.63% and averagely as 37.30%. Moreover, average yield values were also calculated based on mesh sizes and were found to be 42.93%, 37.64%, and 30.47% for -40, +18 mesh, -60, +40 mesh, and +60 mesh sizes, respectively. For shrimp-based chitosan production, the final yield calculated by including all parameters from shell to chitosan was calculated as 36.93%.

When the weight yield values of crab and shrimp are compared, it can be said that the main reason for the difference observed is physiological differences. The fact that such crab shells contain less color pigment, have a higher density, and have less particle surface area compared to shrimp shells, caused the crab shells to lose less material than the shrimp shells, resulting in higher production efficiency in crab-based products. As a result of the size comparison, it is seen that the production yield decreases as the particle size decreases. The reason for this is the increase in the interaction surface and therefore the amount of material removed in the processes. From this point of view, it can be interpreted that the decrease in

particle size contributes to obtaining purer chitin and chitosan. Finally, when the effect of deacetylation temperature on production efficiency is examined, a decreasing trend was observed in production yields at 60, 100, and 80 °C, respectively.

Considering the complete chitosan production, it is possible to state that 80 °C deacetylated, shrimp-based, +60 mesh chitosan samples have the highest loss of substance, so the purest chitosan is obtained as a result of these parameters.

7.1.6 Color Analysis Results

The removal of color pigments expected to occur during chitosan production was investigated by color analysis. Accordingly, the color values of crab and shrimp shells, crab and shrimp-based chitin and 60, 80 and 100 °C deacetylated crab and shrimp-based chitosan samples for -40, +18 mesh, -60, +40 mesh, and +60 mesh sizes are given in Table 7.13 and Table 7.14 for crab and shrimp samples respectively. The values given in the tables are the average values of five measurements performed for each sample. The ΔE values calculated based on the crab shells from the color values obtained are also included in the stated tables.

Accordingly, when Table 7.13 is examined, the average L*, a* and b* values in crab shells were calculated as 79.28, 8.22, 11.24 for -40, +18 mesh, 80.08, 9.24, 12.71 for -60, +40 mesh, and 81.49, 9.36, 14.69 for +60 mesh samples, respectively. ΔE values were found 0 as they are calculated based on crab shells. Average L*, a* and b* values in crab-based chitin samples were calculated as 81.40, 7.19, 11.30 for -40, +18 mesh, 83.49, 7.92, 12.69 for -60, +40 mesh, and 85.47, 8.30, 14.89 for +60 meshes, respectively. The ΔE value for the crab-based chitin samples was calculated as 2.36, 3.65, and 4.12 for the -40,+18, -60,+40, and +60 mesh samples, respectively. Color removal is predicted to occur in the methods carried out in the production of chitin, hence ΔE values that deviate from 0 are expected. In addition, the fact that the ΔE values increased as the particle size decreased was interpreted as the smaller particles with a higher total surface area responded better to chemical treatments and provided more color removal.

Average L*, a* and b* values in 60 ℃ deacetylated crab-based chitosan were calculated as 85.15, 5.56, 13.02 for -40, +18 mesh, 86.62, 5.76, 12.92 for -60, +40 mesh, and 88.93, 5.40, 15.86 for +60 mesh, respectively. The ΔE value for these samples was calculated as 6.69, 7.40, and 8.50 for -40,+18, -60,+40, and +60 mesh samples, respectively. Average L*, a* and b* values in 80 ℃ deacetylated crab-based chitosan samples were calculated as 86.80, 6.25, 13.57 for -40, +18 mesh, 89.31, 6.04, 13.11 for -60, +40 mesh and 90.78, 5.19, 15.16

for +60 mesh, respectively. The ΔE value for these samples was calculated as 8.12, 9.77, and 10.19 for -40,+18, -60,+40, and +60 mesh samples, respectively. Finally, the mean L*, a* and b* values in 100 °C deacetylated crab-based chitosan samples were 86.46, 5.97, 12.85 for -40, +18 mesh, 87.39, 6.04, 13.45 for -60, +40 mesh, and 89.20, 5.72, 14.26 for +60 mesh, respectively. The ΔE value for these samples was calculated as 7.69, 8.01, and 8.53 for -40,+18, -60,+40, and +60 mesh samples, respectively.

Table 7.13 Average color values of crab-based samples

Sample	Mesh	L*	a*	b*	ΔE
Crab Shell	-40, +18	79.28	8.22	11.24	-
	-60, +40	80.08	9.24	12.71	-
	+60	81.49	9.36	14.69	-
Crab-Based Chitin	-40, +18	81.40	7.19	11.30	2.36
	-60, +40	83.49	7.92	12.69	3.65
	+60	85.47	8.30	14.89	4.12
60 °C Deacetylated Crab-Based Chitosan	-40, +18	85.15	5.56	13.02	6.69
	-60, +40	86.62	5.76	12.92	7.40
	+60	88.93	5.40	15.86	8.50
80 °C Deacetylated Crab-Based Chitosan	-40, +18	86.80	6.25	13.57	8.12
	-60, +40	89.31	6.04	13.11	9.77
	+60	90.78	5.19	15.16	10.19
100 °C Deacetylated Crab-Based Chitosan	-40, +18	86.46	5.97	12.85	7.69
	-60, +40	87.39	6.04	13.45	8.01
	+60	89.20	5.72	14.26	8.53

Table 7.14 Average color values of shrimp-based samples

	Mesh	**L***	**a***	**b***	**ΔE**
Shrimp Shell	-40, +18	78.47	10.23	18.24	-
	-60, +40	79.83	10.60	19.88	-
	+60	80.40	10.78	22.42	-
Shrimp-Based Chitin	-40, +18	79.94	7.37	21.37	4.49
	-60, +40	80.31	7.73	23.48	4.63
	+60	83.50	8.01	24.75	4.77
60 °C Deacetylated Shrimp-Based Chitosan	-40, +18	82.02	7.63	18.45	4.40
	-60, +40	83.40	7.71	19.39	4.62
	+60	84.10	8.22	23.56	4.64
80 °C Deacetylated Shrimp-Based Chitosan	-40, +18	83.06	7.82	18.64	5.20
	-60, +40	84.28	7.96	20.80	5.26
	+60	85.24	8.14	24.28	5.81
100 °C Deacetylated Shrimp-Based Chitosan	-40, +18	82.11	7.59	18.17	4.50
	-60, +40	83.64	8.18	19.30	4.55
	+60	84.47	8.33	23.18	4.82

When the ΔE values obtained with different deacetylation temperatures are examined, it is clear that the chitosan samples produced with 80 °C deacetylations had the highest total color change. This result also matches the yield data obtained throughout the crab-based chitosan production process. In these samples, it was observed that while the redness values decreased, there was an increase in the lightness and yellowness values. Furthermore, for all

deacetylation temperatures, the decrease in particle size increased the surface area where decolorization occurred, increasing ΔE values.

Accordingly, when Table 7.14 is examined, the average L*, a* and b* values in shrimp shells were calculated as 78.47, 10.23, 18.24 for -40, +18 mesh, 79.83, 10.60, 19.88 for -60, +40 mesh, and 80.40, 10.78, 22.42 for +60 mesh samples, respectively. ΔE values were found 0 as they are calculated based on shrimp shells. Average L*, a* and b* values in shrimp-based chitin samples were calculated as 79.94, 7.37, 21.37 for -40, +18 mesh, 80.31, 7.73, 23.48 for -60, +40 mesh, and 83.50, 8.01, 24.75 for +60 meshes, respectively. The ΔE value for the shrimp-based chitin samples was calculated as 4.49, 4.63, and 4.77 for the -40,+18, -60,+40, and +60 mesh samples, respectively. As in the crab samples, color removal has occurred as predicted in the production of shrimp-based chitin. Furthermore, ΔE values have also been found to increase as particle size decreases, owing to the increased surface area per unit gram of product.

Average L*, a* and b* values in 60 ℃ deacetylated shrimp-based chitosan were calculated as 82.02, 7.63, 18.45 for -40, +18 mesh, 83.40, 7.71, 19.39 for -60, +40 mesh, and 84.10, 8.22, 23.56 for +60 mesh, respectively. The ΔE value for these samples was calculated as 4.40, 4.62, and 4.64 for -40,+18, -60,+40, and +60 mesh samples, respectively. Average L*, a* and b* values in 80 ℃ deacetylated shrimp-based chitosan samples were calculated as 83.06, 7.82, 18.64 for -40, +18 mesh, 84.28, 7.96, 20.80 for -60, +40 mesh and 85.24, 8.14, 24.28 for +60 mesh, respectively. The ΔE value for these samples was calculated as 5.20, 5.26, and 5.81 for -40,+18, -60,+40, and +60 mesh samples, respectively. Finally, the mean L*, a* and b* values in 100 °C deacetylated shrimp-based chitosan samples were 82.11, 7.59, 18.17 for -40, +18 mesh, 83.64, 8.18, 19.30 for -60, +40 mesh, and 84.47, 8.33, 23.18 for +60 mesh, respectively. The ΔE value for these samples was calculated as 4.50, 4.55, and 4.82 for -40,+18, -60,+40, and +60 mesh samples, respectively. When the ΔE values obtained with different deacetylation temperatures are examined, it is clear that the chitosan samples produced with 80 °C deacetylations had the highest total color change. This result also matches the yield data obtained throughout the chitosan production process. Also, for all deacetylation temperatures, the reduction in particle size increased ΔE values as it increased the surface area at which decolorization occurred.

When the color values of crab and shrimp-based samples were compared, it was determined that more color removal was achieved in all shrimp samples as predicted. The reason for this

was interpreted as that shrimp samples contain more color pigments compared to crab samples, as well as being workable and able to respond better to chemical processes.

7.2 Heavy Metal Adsorption Results

Heavy metal adsorption experiments were carried out using antimony, aluminium and lead solutions at 20 ppm concentration and 0.1 g chitosan sample. Chitosan samples, which were subjected to 80°C deacetylation process, whose purity was determined as the highest as a result of the interpretation of yield values in the experiments, were used. The solutions obtained as a result of the experiments were subjected to ICP-OES analysis and the adsorption abilities of the produced chitosan samples for antimony, aluminium and lead were evaluated.

7.2.1 ICP – OES Analysis Results

The results of the ICP-OES analysis that was used to determine the final metal concentrations in the solutions after the adsorption procedure are shown in Tables 7.15 and 7.16 for crab and shrimp based samples, respectively.

When Table 7.15 is examined to evaluate the adsorption data of crab-based chitosan samples, the final amount of Sb in the solutions for +18, –40 mesh samples at the mixing times of 1, 2, and 3 hours were found to be 17.56 ± 0.39 m L^{-1}, 17.53 ± 0.39 m L^{-1}, and 15.62 ± 0.35 m L^{-1}, respectively. For +40, –60 mesh samples the final amount of Sb in the solutions at the mixing times of 1, 2, and 3 hours were found to be 17.94 ± 0.40 m L^{-1}, 16.69 ± 0.38 m L^{-1}, and 13.65 ± 0.31 m L^{-1}, respectively, and for +60 mesh samples the final amount of Sb in the solutions at the mixing times of 1, 2, and 3 hours were found to be 17.18 ± 0.39 m L^{-1}, 16.70 ± 0.38 m L^{-1}, and 15.12 ± 0.34 m L^{-1}, respectively.

The final amount of Al in the solutions with crab-based chitosan samples for +18, –40 mesh sizes at the mixing times of 1, 2, and 3 hours were found to be 15.250 ± 0.770 m L^{-1}, 15.250 ± 0.790 m L^{-1}, and 15.250 ± 0.770 m L^{-1}, respectively. For +40, –60 mesh samples the final amount of Al in the solutions at the mixing times of 1, 2, and 3 hours were found to be 15.200 ± 0.810 m L^{-1}, 13.190 ± 0.660 m L^{-1}, and 3.300 ± 0.170 m L^{-1}, respectively, and for +60 mesh samples the final amount of Al in the solutions at the mixing times of 1, 2, and 3 hours were found to be 4.480 ± 0.230, 3.670 ± 0.180 m L^{-1}, and 3.380 ± 0.170 m L^{-1}, respectively.

Lastly, the final amount of Pb in the solutions with crab-based chitosan samples for +18, –40 mesh sizes at the mixing times of 1, 2, and 3 hours were found to be 5.440 ± 0.290 m L^{-}

^{1}, 4.860 ± 0.260 m L^{-1}, and 3.060 ± 0.170 m L^{-1}, respectively. For +40, –60 mesh samples the final amount of Pb in the solutions at the mixing times of 1, 2, and 3 hours were found to be 5.210 ± 0.340 m L^{-1}, 5.150 ± 0.280 m L^{-1}, and 2.810 ± 0.150 m L^{-1}, respectively, and for +60 mesh samples the final amount of Pb in the solutions at the mixing times of 1, 2, and 3 hours were found to be 3.860 ± 0.210, 2.020 ± 0.110 m L^{-1}, and 1.600 ± 0.090 m L^{-1}, respectively.

Table 7.15 also shows the adsorption percentages calculated using the 20 ppm initial concentration and final concentration data of heavy metal solutions in the adsorption processes for crab-based chitosan samples. According to these data, adsorption amounts were calculated for +18, –40 mesh crab-based chitosan at mixing times of 1, 2, and 3 hours, respectively, for Sb as 12.20%, 12.35%, and 21.90%, for Al as 23.75%, 23.75%, and 23.75%, and for Pb as 72.80%, 75.70%, and 84.70%. Thus, it was observed that increasing the adsorption mixing time in +18, –40 mesh crab-based samples increased the adsorption amounts of Sb and Pb heavy metals, but the amount of Al adsorption remained the same for the mixing times.

Adsorption amounts for +40, –60 mesh crab-based chitosan at mixing times of 1, 2, and 3 hours, respectively, were calculated for Sb as 10.30%, 16.55%, and 31.75%, for Al as 24.00%, 34.05%, and 83.50%, and for Pb as 73.95%, 74.25%, and 85.95%. Thus, it was observed that increasing the adsorption mixing time in +40, –60 mesh crab-based samples increased the adsorption amounts of Sb, Al, and Pb heavy metals.

Adsorption amounts for +60 mesh crab-based chitosan at mixing times of 1, 2, and 3 hours, respectively, were calculated for Sb as 14.10%, 16.50%, and 24.40%, for Al as 77.60%, 81.65%, and 83.10%, and for Pb as 80.70%, 89.90%, and 92.00%. Thus, it was observed that increasing the adsorption mixing time in +60 mesh crab-based samples increased the adsorption amounts of Sb, Al, and Pb heavy metals.

When the adsorption study for crab-based chitosan samples was evaluated in general, the highest adsorption amounts were found in Pb, Al and Sb heavy metals in each particle size, respectively. Furthermore, when the effect of particle sizes on adsorption amounts was examined, it was observed that decreasing particle size increased the amount of adsorption due to increasing the interaction surface area. Consequently, it was discovered that the +60 mesh crab-based chitosan samples synthesized by deacetylation at 80 ℃ performed extremely well in the removal of heavy metals Pb and Al.

Table 7.15 Adsorption values of crab-based chitosan

Mesh	Time (h)	Sb (mg L^{-1})	Al (mg L^{-1})	Pb (mg L^{-1})	Sb Adsorption%	Al Adsorption%	Pb Adsorption%
+18, –40	1	17.56 ± 0.39	15.250 ± 0.770	5.440 ± 0.290	12.20	23.75	72.80
	2	17.53 ± 0.39	15.250 ± 0.790	4.860 ± 0.260	12.35	23.75	75.70
	3	15.62 ± 0.35	15.250 ± 0.770	3.060 ± 0.170	21.90	23.75	84.70
+40, –60	1	17.94 ± 0.40	15.200 ± 0.810	5.210 ± 0.340	10.30	24.00	73.95
	2	16.69 ± 0.38	13.190 ± 0.660	5.150 ± 0.280	16.55	34.05	74.25
	3	13.65 ± 0.31	3.300 ± 0.170	2.810 ± 0.150	31.75	83.50	85.95
+60	1	17.18 ± 0.39	4.480 ± 0.230	3.860 ± 0.210	14.10	77.60	80.70
	2	16.70 ± 0.38	3.670 ± 0.180	2.020 ± 0.110	16.50	81.65	89.90
	3	15.12 ± 0.34	3.380 ± 0.170	1.600 ± 0.090	24.40	83.10	92.00

N.D.: not detected.

Table 7.16 Adsorption values of shrimp-based chitosan

Mesh	Time (h)	Sb (mg L^{-1})	Al (mg L^{-1})	Pb (mg L^{-1})	Sb Adsorption%	Al Adsorption%	Pb Adsorption%
+18, –40	1	19.56 ± 0.44	8.310 ± 0.420	0.130 ± 0.100	2.20	58.45	99.35
	2	19.05 ± 0.43	2.650 ± 0.130	N.D. < 0.010	4.75	86.75	≈100
	3	14.14 ± 0.32	0.440 ± 0.020	N.D. < 0.010	29.30	97.80	≈100
+40, –60	1	19.60 ± 0.44	1.080 ± 0.050	0.072 ± 0.004	2.00	94.60	99.64
	2	18.67 ± 0.42	0.220 ± 0.010	N.D. < 0.010	6.65	98.90	≈100
	3	14.96 ± 0.34	0.097 ± 0.005	N.D. < 0.010	25.20	99.52	≈100
+60	1	18.23 ± 0.41	0.200 ± 0.010	0.052 ± 0.003	8.85	99.00	99.74
	2	18.04 ± 0.42	0.100 ± 0.010	N.D. < 0.010	9.80	99.50	≈100
	3	17.78 ± 0.40	0.050 ± 0.003	N.D. < 0.010	11.10	99.75	≈100

N.D.: not detected.

When Table 7.16 is examined to evaluate the adsorption data of shrimp-based chitosan samples, the final amount of Sb in the solutions for +18, –40 mesh samples at the mixing times of 1, 2, and 3 hours were found to be 19.56 ± 0.44 m L^{-1}, 19.05 ± 0.43 m L^{-1}, and 14.14 ± 0.32 m L^{-1}, respectively. For +40, –60 mesh samples the final amount of Sb in the solutions at the mixing times of 1, 2, and 3 hours were found to be 19.60 ± 0.44 m L^{-1}, 18.67 ± 0.42 m L^{-1}, and 14.96 ± 0.34 m L^{-1}, respectively, and for +60 mesh samples the final amount of Sb in the solutions at the mixing times of 1, 2, and 3 hours were found to be 18.23 ± 0.41 m L^{-1}, 18.04 ± 0.42 m L^{-1}, and 17.78 ± 0.40 m L^{-1}, respectively.

The final amount of Al in the solutions with shrimp-based chitosan samples for +18, –40 mesh sizes at the mixing times of 1, 2, and 3 hours were found to be 8.310 ± 0.420 m L^{-1}, 2.650 ± 0.130 m L^{-1}, and 0.440 ± 0.020 m L^{-1}, respectively. For +40, –60 mesh samples the final amount of Al in the solutions at the mixing times of 1, 2, and 3 hours were found to be 1.080 ± 0.050 m L^{-1}, 0.220 ± 0.010 m L^{-1}, and 30.097 ± 0.005 m L^{-1}, respectively, and for +60 mesh samples the final amount of Al in the solutions at the mixing times of 1, 2, and 3 hours were found to be 0.200 ± 0.010, 0.100 ± 0.010 m L^{-1}, and 0.050 ± 0.003 m L^{-1}, respectively.

Lastly, the final amount of Pb in the solutions with shrimp-based chitosan samples for +18, –40 mesh sizes at the mixing times of 1, 2, and 3 hours were found to be 0.130 ± 0.100 m L^{-1}, N.D. < 0.010 m L^{-1}, and N.D. < 0.010 m L^{-1}, respectively. For +40, –60 mesh samples the final amount of Pb in the solutions at the mixing times of 1, 2, and 3 hours were found to be 0.072 ± 0.004 m L^{-1}, N.D. < 0.010 m L^{-1}, and N.D. < 0.010 m L^{-1}, respectively, and for +60 mesh samples the final amount of Pb in the solutions at the mixing times of 1, 2, and 3 hours were found to be 0.052 ± 0.003, N.D. < 0.010 m L^{-1}, and N.D. < 0.010 m L^{-1}, respectively.

Table 7.16 also shows the adsorption percentages calculated using the 20 ppm initial concentration and final concentration data of heavy metal solutions in the adsorption processes for shrimp-based chitosan samples. According to these data, adsorption amounts were calculated for +18, –40 mesh shrimp-based chitosan at mixing times of 1, 2, and 3 hours, respectively, for Sb as 2.20%, 4.75%, and 29.30%, for Al as 58.45%, 86.75%, and 97.80%, and for Pb as 99.35%, ≈100%, and ≈100%. Adsorption amounts for +40, –60 mesh shrimp-based chitosan at mixing times of 1, 2, and 3 hours,

respectively, were calculated for Sb as 2.00%, 6.65%, and 25.20%, for Al as 94.60%, 98.90%, and 99.52%, and for Pb as 99.64%, ≈100%, and ≈100%. Adsorption amounts for +60 mesh shrimp-based chitosan at mixing times of 1, 2, and 3 hours, respectively, were calculated for Sb as 8.85%, 9.80%, and 11.10%, for Al as 99.00%, 99.50%, and 99.75%, and for Pb as 99.74%, ≈100%, and ≈100%. Thus, it was observed that increasing the adsorption mixing time in each mesh shrimp-based samples increased the adsorption amounts of Sb, Al, and Pb heavy metals.

When the adsorption study for shrimp-based chitosan samples was evaluated in general, the highest adsorption amounts were found in Pb, Al, and Sb heavy metals in each particle size, respectively. Additionally, it was observed that decreasing particle size increased the amount of adsorption due to increasing the interaction surface area. In particular, the fact that Pb heavy metal was able to reduce the amount of heavy metal below detectable amounts after 1 hour of mixing for each mesh sample shows that almost all of this metal was adsorbed by the produced chitosan samples. In addition, the detection of Al metal adsorption amounts close to 100% for +40, -60 and +60 mesh samples show that shrimp-based chitosan is a very effective adsorbent for Al, as well as Pb.

When the adsorption performances of crab and shrimp-based chitosan samples were compared, it was determined that shrimp-based samples showed a significantly better adsorption performance. In addition, it was observed that the heavy metal adsorbed at the highest rate in both crab and shrimp samples was Pb, followed by Al and Sb metals, respectively. In terms of particle sizes, it was determined that the adsorption rates decreased from +60 to +18, -40 mesh samples. Hence it was concluded the adsorption rate is inversely proportional to the particle size, as it was proportional to the surface area.

7.3 Conclusion and Future Work

In this study, the adsorption amounts of various heavy metals in the aquatic environment of chitosan samples derived from shrimp and crab shells with various production parameters were investigated. Three sieve sizes and three deacetylation temperatures were applied as production parameters. Material loss at each stage of production was used to compute percentage production yield. Furthermore, FT-IR analysis was performed with the shells, chitin and chitosan samples that were produced. These analyzes carried out for each sample were evaluated in comparison with each other and the conversions of

the shells to chitin and chitosan, respectively, were followed. In this approach, it was determined whether chitosan production was successful. Color analysis was performed on shells and produced chitin and chitosan in each sieve size to monitor color changes expected during the production process. The adsorption process was carried out by mixing selected chitosan samples with antimony, aluminium and lead solutions for 1, 2 and 3 hours. At the end of the process, the filtrates of the solutions were subjected to ICP-OES analyzes and the heavy metal amounts remaining in the solution were determined and the amounts and percentages of heavy metal adsorbed by chitosan samples were calculated. It has been interpreted that the samples with the most substance removal from the weight loss results obtained after the production stage are more successful than the ones that are closer to the desired purity. Accordingly, chitosan samples produced with 80 °C deacetylation, the most successful product, were selected to be used in adsorption experiments. In the raw material and size comparisons, it was observed that the reduction in particle size increased the material loss and the shrimp shells experienced more material loss than the crab shells since they were softer and deformable. In the FT-IR analysis results, stretching vibration peaks of C-H bonds were identified in the shells, while weaker peaks were observed in the chitin samples due to color and organic matter removal. In chitosan samples, unlike the ones observed in the shells and chitin samples, amino groups were read instead of acetyl groups, which was interpreted as a successful deacetylation process. As a result of the color analyzes performed, the total color changes in shrimp samples, which are known to contain more color pigments, were higher than the crab samples. Furthermore, the amount of color removal rose as the particle size reduced, and the samples that had deacetylation at 80 °C had the highest color removal. When the adsorption results were examined, it was determined that the shrimp-based chitosan samples performed much more successfully than the crab-based samples, and the amount of adsorption increased as the particle size decreased. In addition, quite high adsorption rates were achieved in lead and aluminium metals, respectively, but the produced chitosan samples were found to be insufficient for antimony adsorption.

In the light of the data provided in the thesis, it is planned to make changes in production parameters, examine the chitosan samples to be produced with different analyzes and determine their suitability for adsorption processes, and improve heavy metal removal by differentiating the adsorption parameters.

REFERENCES

Abd El-Hack, M. E., El-Saadony, M. T., Shafi, M. E., Zabermawi, N. M., Arif, M., Batiha, G. E., Khafaga, A. F., Abd El-Hakim, Y. M., & Al-Sagheer, A. A. (2020). Antimicrobial and antioxidant properties of chitosan and its derivatives and their applications: A review. *International journal of biological macromolecules*, *164*, 2726–2744. https://doi.org/10.1016/j.ijbiomac.2020.08.153

Akpomie, K. G., & Conradie, J. (2020). Banana peel as a biosorbent for the decontamination of water pollutants. A review. *Environmental Chemistry Letters*, *18*(4), 1085-1112. https://doi.org/10.1007/s10311-020-00995-x

Alabi, O. A., & Adeoluwa, Y. M. (2020). Production usage and potential public health effects of aluminum cookware: a review. *Ann Sci Technol*, *5*(1), 20-30. https://doi.org/10.2478/ast-2020-0003

Alasfar, R. H., & Isaifan, R. J. (2021). Aluminum environmental pollution: the silent killer. Environmental science and pollution research international, 28(33), 44587–44597. https://doi.org/10.1007/s11356-021-14700-0

Al-Ghouti, M. A., & Da'ana, D. A. (2020). Guidelines for the use and interpretation of adsorption isotherm models: A review. *Journal of hazardous materials*, *393*, 122383. https://doi.org/10.1016/j.jhazmat.2020.122383

Ali, A., & Ahmed, S. (2018). A review on chitosan and its nanocomposites in drug delivery. International journal of biological macromolecules, 109, 273–286. https://doi.org/10.1016/j.ijbiomac.2017.12.078

Aluminium. (2022, May 30) *Wikipedia*. Retrieved June 2, 2022, from https://en.wikipedia.org/wiki/Aluminium

Andonegi, M., Heras, K. L., Santos-Vizcaíno, E., Igartua, M., Hernandez, R. M., de la Caba, K., & Guerrero, P. (2020). Structure-properties relationship of chitosan/collagen films with potential for biomedical applications. Carbohydrate polymers, 237, 116159. https://doi.org/10.1016/j.carbpol.2020.116159

Antimony. (2022, May 19) *Wikipedia*. Retrieved June 2, 2022, from https://en.wikipedia.org /wiki/Antimony

Aouini, F., Trombini, C., Volland, M., Elcafsi, M., & Blasco, J. (2018). Assessing lead toxicity in the clam Ruditapes philippinarum: Bioaccumulation and biochemical responses. *Ecotoxicology and environmental safety*, *158*, 193–203. https://doi.org/10.1016/j.ecoenv.2018.04.033

Aranaz, I., Alcántara, A. R., Civera, M. C., Arias, C., Elorza, B., Heras Caballero, A., & Acosta, N. (2021). Chitosan: An Overview of Its Properties and Applications. *Polymers*, *13*(19), 3256. https://doi.org/10.3390/polym13193256

Ayawei, N., Ebelegi, A. N., & Wankasi, D. (2017). *Modelling and interpretation of adsorption isotherms*. *Journal of chemistry*, *2017*. https://doi.org/10.1155/2017/3039817

Azizian, S., & Eris, S. (2021). Adsorption isotherms and kinetics. In *Interface Science and Technology* (Vol. 33, pp. 445-509). Elsevier. https://doi.org/10.1016/B978-0-12-818805-7.00011-4

Azra, M. N., Okomoda, V. T., Tabatabaei, M., Hassan, M., & Ikhwanuddin, M. (2021). The contributions of shellfish aquaculture to global food security: Assessing its characteristics from a future food perspective. *Frontiers in Marine Science*, *8*, 365. https://doi.org/10.3389/fmars.2021.654897

Bagherifam, S., Brown, T. C., Fellows, C. M., & Naidu, R. (2019). Derivation methods of soils, water and sediments toxicity guidelines: a brief review with a focus on antimony. *Journal of Geochemical Exploration*, *205*, 106348. https://doi.org/10.1016/j.gexplo.2019.106348

Bakshi, P. S., Selvakumar, D., Kadirvelu, K., & Kumar, N. S. (2020). Chitosan as an environment friendly biomaterial - a review on recent modifications and applications. *International journal of biological macromolecules*, *150*, 1072–1083. https://doi.org/10.1016/j.ijbiomac.2019.10.113

Bhattacharya S. (2019). Probiotics against alleviation of lead toxicity: recent advances. *Interdisciplinary toxicology*, *12*(2), 89–92. https://doi.org/10.2478/intox-2019-0010

Boreiko, C. J., & Rossman, T. G. (2020). Antimony and its compounds: Health impacts related to pulmonary toxicity, cancer, and genotoxicity. *Toxicology and applied pharmacology*, *403*, 115156. https://doi.org/10.1016/j.taap.2020.115156

Briffa, J., Sinagra, E., & Blundell, R. (2020). Heavy metal pollution in the environment and their toxicological effects on humans. Heliyon, 6(9), e04691. https://doi.org/10.1016/j.heliyon.2020.e04691

Britannica, T. Editors of Encyclopaedia (2020, October 23). Aluminum. Encyclopedia Britannica. Retrieved October 27, 2021, from https://www.britannica.com/science/aluminum

Britannica, T. Editors of Encyclopaedia (2021, August 29). Lead. Encyclopedia Britannica. Retrieved October 27, 2021, from https://www.britannica.com/science/lead-chemical-element

Britannica, T. Editors of Encyclopaedia (2022, January 5). Antimony. Encyclopedia Britannica. Retrieved October 27, 2021, from https://www.britannica.com/science/antimony

Caridea. (2022, March 27). *Wikipedia*. Retrieved June 2, 2022, from https://en.wikipedia.org/wiki/Caridea

Chai, W. S., Cheun, J. Y., Kumar, P. S., Mubashir, M., Majeed, Z., Banat, F., â€¦ Show, P. L. (2021). A review on conventional and novel materials towards heavy metal adsorption in wastewater treatment application. *Journal of Cleaner Production*, 296, 126589. https://doi.org/10.1016/j.jclepro.2021.126589

Chakraborty, M., Hasanuzzaman, M., Rahman, M., Khan, Md. A. R., Bhowmik, P., Mahmud, N. U., Tanveer, M., & Islam, T. (2020). Mechanism of Plant Growth Promotion and Disease Suppression by Chitosan Biopolymer. *Agriculture*, *10*(12), 624. https://doi.org/10.3390/agriculture10120624

Charoenvuttitham, P., Shi, J., & Mittal, G. S. (2006). Chitin extraction from black tiger shrimp (Penaeus monodon) waste using organic acids. *Separation science and technology*, *41*(06), 1135-1153. https://doi.org/10.1080/01496390600633725

Chauhan, D. K., Yadav, V., Vaculík, M., Gassmann, W., Pike, S., Arif, N., Singh, V. P., Deshmukh, R., Sahi, S., & Tripathi, D. K. (2021). Aluminum toxicity and aluminum stress-induced physiological tolerance responses in higher plants. Critical reviews in biotechnology, 41(5), 715–730. https://doi.org/10.1080/07388551.2021.1874282

Chen, A., Shang, C., Shao, J., Lin, Y., Luo, S., Zhang, J., Huang, H., Lei, M., & Zeng, Q. (2017). Carbon disulfide-modified magnetic ion-imprinted chitosan-Fe (III): a novel adsorbent for simultaneous removal of tetracycline and cadmium. Carbohydrate polymers, 155, 19-27. https://doi.org/10.1016/j.carbpol.2016.08.038

Chen, P. Y., Lin, A. Y., McKittrick, J., & Meyers, M. A. (2008). Structure and mechanical properties of crab exoskeletons. *Acta biomaterialia*, *4*(3), 587–596. https://doi.org/10.1016/j.actbio.2007.12.010

Cheung, R. C., Ng, T. B., Wong, J. H., & Chan, W. Y. (2015). Chitosan: An Update on Potential Biomedical and Pharmaceutical Applications. *Marine drugs*, *13*(8), 5156–5186. https://doi.org/10.3390/md13085156

Chitin. (2022, April 27). *Wikipedia*. Retrieved June 2, 2022, from https://en.wikipedia.org/wiki/chitin

Chitosan. (2022, May 18). *Wikipedia*. Retrieved June 2, 2022, from https://en.wikipedia.org/wiki/chitosan

Ciosek, Ż., Kot, K., Kosik-Bogacka, D., Łanocha-Arendarczyk, N., & Rotter, I. (2021). The Effects of Calcium, Magnesium, Phosphorus, Fluoride, and Lead on Bone Tissue. *Biomolecules*, *11*(4), 506. https://doi.org/10.3390/biom11040506

Crini, G., & Lichtfouse, E. (2019). Advantages and disadvantages of techniques used for wastewater treatment. *Environmental Chemistry Letters*, *17*(1), 145-155. https://doi.org/10.1007/s10311-018-0785-9

Dai, Y., Sun, Q., Wang, W., Lu, L., Liu, M., Li, J., Yang, S., Sun, Y., Zhang, K., Xu, J., Zheng, W., Hu, Z., Yang, Y., Gao, Y., Chen, Y., Zhang, X., Gao, F., & Zhang, Y. (2018). Utilizations of agricultural waste as adsorbent for the removal of contaminants: A review. *Chemosphere*, *211*, 235–253. https://doi.org/10.1016/j.chemosphere.2018.06.179

Dave, D., Liu, Y., Pohling, J., Trenholm, S., & Murphy, W. (2020). Astaxanthin recovery from Atlantic shrimp (Pandalus borealis) processing materials. *Bioresource Technology Reports*, *11*, 100535. https://doi.org/10.1016/j.biteb.2020.100535

Davie, P. J., Guinot, D., & Ng, P. K. (2015). Anatomy and functional morphology of Brachyura. *Treatise on Zoology-Anatomy, Taxonomy, Biology. The Crustacea, Volume 9 Part C (2 vols)*, 11-163. https://doi.org/10.1163/9789004190832_004

de Souza, I. D., de Andrade, A. S., & Dalmolin, R. (2018). Lead-interacting proteins and their implication in lead poisoning. *Critical reviews in toxicology*, *48*(5), 375–386. https://doi.org/10.1080/10408444.2018.1429387

Demir, E., & Yalçin, H. (2014). Adsorbentler: sınıflandırma, özellikler, kullanım ve öngörüler. Türk Bilimsel Derlemeler Dergisi, 7(2), 70-79.

Diarte-Plata, G., & Escamilla-Montes, R., (Eds.). (2020). *Crustacea*. IntechOpen. https://doi.org/10.5772/intechopen.78108

Eivazzadeh-Keihan, R., Radinekiyan, F., Asgharnasl, S., Maleki, A., & Bahreinizad, H. (2020). A natural and eco-friendly magnetic nanobiocomposite based on activated chitosan for heavy metals adsorption and the in-vitro hyperthermia of cancer therapy. Journal of Materials Research and Technology, 9(6), 12244-12259. https://doi.org/10.1016/j.jmrt.2020.08.096

El Knidri, H., Belaabed, R., Addaou, A., Laajeb, A., & Lahsini, A. (2018). Extraction, chemical modification and characterization of chitin and chitosan. International journal of biological macromolecules, 120(Pt A), 1181–1189. https://doi.org/10.1016/j.ijbiomac.2018.08.139

El-Dessouky, H. T., & Ettouney, H. M. (2002). *Fundamentals of salt water desalination*. Elsevier. 409-437. https://doi.org/10.1016/B978-044450810-2/50009-9

El-Sayed, A. F. M. (2021). Use of biofloc technology in shrimp aquaculture: a comprehensive review, with emphasis on the last decade. *Reviews in Aquaculture*, *13*(1), 676-705. https://doi.org/10.1111/raq.12494

FAO. (2021). FAO yearbook. Fishery and Aquaculture Statistics 2019/FAO annuaire. Statistiques des pêches et de l'aquaculture 2019/FAO anuario. Estadísticas de pesca y acuicultura 2019. Rome/Roma.

Fast, A. W., & Lester, L. J. (Eds.). (2013). *Marine shrimp culture: principles and practices*. Elsevier. ISBN:9781483291048

Feng, R., Lei, L., Su, J., Zhang, R., Zhu, Y., Chen, W., Wang, L., Wang, R., Dai, J., Lin, Z., Li, Y., Liu, B., Fan, Z., Liu, H., & Rensing, C. (2020). Toxicity of different forms of antimony to rice plant: Effects on root exudates, cell wall components, endogenous hormones and antioxidant system. *The Science of the total environment*, *711*, 134589. https://doi.org/10.1016/j.scitotenv.2019.134589

Filella, M., Williams, P. A., & Belzile, N. (2009). Antimony in the environment: knowns and unknowns. *Environmental Chemistry*, *6*(2), 95-105. https://doi.org/10.1071/EN09007

Fulcher's Brand Royal Red Shrimp. (n.d.). *Fulcher's Seafood*. Retrieved May 5, 2022, from https://fulchers.com/products/shrimp-royal-red/

Gedam, A. H., & Dongre, R. S. (2015). Adsorption characterization of Pb (II) ions onto iodate doped chitosan composite: equilibrium and kinetic studies. *RSC advances*, 5(67), 54188-54201. https://doi.org/10.1039/C5RA09899H

Guerao, G., & Rotllant, G. (2009). Post-larval development and sexual dimorphism of the spider crab Maja brachydactyla (Brachyura: Majidae). Scientia Marina, 73(4), 797–808. https://doi.org/10.3989/scimar.2009.73n4797

Gzyra-Jagieła, K., Pęczek, B., Wiśniewska-Wrona, M. and Gutowska, N. (2019). Physicochemical Properties of Chitosan and its Degradation Products. In *Chitin and Chitosan* (eds L. A. Broek and C. G. Boeriu). https://doi.org/10.1002/9781119450467.ch3

Harnedy, P. A., & FitzGerald, R. J. (2012). Bioactive peptides from marine processing waste and shellfish: A review. *Journal of functional foods*, *4*(1), 6-24. https://doi.org/10.1016/j.jff.2011.09.001

He, M., Wang, X., Wu, F., & Fu, Z. (2012). Antimony pollution in China. The Science of the total environment, 421-422, 41–50. https://doi.org/10.1016/j.scitotenv.2011.06.009

Hobbs H. H. III., White, W. B., & Culver, D. C. (Eds.). (2012). Crustacea. *Encyclopedia of Caves* (Second Edition), Academic Press, Amsterdam, 177-194, https://doi.org/10.1016/B978-0-12-383832-2.00027-X

Hou, X., Lv, S., Chen, Z., & Xiao, F. (2018). Applications of Fourier transform infrared spectroscopy technologies on asphalt materials. *Measurement*, 121, 304-316. https://doi.org/10.1016/j.measurement.2018.03.001

Hu, Z., & Gänzle, M. G. (2019). Challenges and opportunities related to the use of chitosan as a food preservative. Journal of applied microbiology, 126(5), 1318–1331. https://doi.org/10.1111/jam.14131

Hunter L, a, b Color Space. (n.d.) *Hunter Lab*. Retrieved March 10, 2022, from https://support.hunterlab.com/hc/en-us/categories/201319586-Color-Theory

Hunter, R. S., & Harold, R. W. (1987). *The measurement of appearance*. John Wiley & Sons.

IARC (International Agency for Research on Cancer). (2019). *Agents Classified by the IARC Monographs*, Volumes 1–123. Retrieved June 2, 2022 from https://monographs.iarc.fr/agents-classified-by-the-iarc/

Igberase, E., Osifo, P., & Ofomaja, A. (2014). The adsorption of copper (II) ions by polyaniline graft chitosan beads from aqueous solution: equilibrium, kinetic and desorption studies. *Journal of environmental chemical engineering*, 2(1), 362-369. https://doi.org/10.1016/j.jece.2014.01.008

Jayaswal, K., Sahu, V., & Gurjar, B. R. (2018). Water pollution, human health and remediation. In *Water remediation* (pp. 11-27). Springer, Singapore. https://doi.org/10.1007/978-981-10-7551-3_2

Jeong, C. H., Kwon, H. C., Kim, D. H., Cheng, W. N., Kang, S., Shin, D. M., Yune, J. H., Yoon, J. E., Chang, Y. H., Sohn, H., & Han, S. G. (2020). Effects of Aluminum on the Integrity of the Intestinal Epithelium: An in Vitro and in Vivo Study. Environmental health perspectives, 128(1), 17013. https://doi.org/10.1289/EHP5701

Kaisler, M., van den Broek, L. A., & Boeriu, C. G. (2019). Chitin and Chitosan as Sources of Bio-Based Building Blocks and Chemicals. *Chitin and chitosan: properties and applications*, 229-244. https://doi.org/10.1002/9781119450467.ch9

Kapahi, M., & Sachdeva, S. (2019). Bioremediation Options for Heavy Metal Pollution. Journal of health & pollution, 9(24), 191203. https://doi.org/10.5696/2156-9614-9.24.191203

Keshvardoostchokami, M., Majidi, M., Zamani, A., & Liu, B. (2021). A review on the use of chitosan and chitosan derivatives as the bio-adsorbents for the water treatment: Removal of nitrogen-containing pollutants. Carbohydrate polymers, 273, 118625. https://doi.org/10.1016/j.carbpol.2021.118625

Klein G. L. (2019). Aluminum toxicity to bone: A multisystem effect?. Osteoporosis and sarcopenia, 5(1), 2–5. https://doi.org/10.1016/j.afos.2019.01.001

Kou, S. G., Peters, L. M., & Mucalo, M. R. (2021). Chitosan: A review of sources and preparation methods. International journal of biological macromolecules, 169, 85–94. https://doi.org/10.1016/j.ijbiomac.2020.12.005

Kritchenkov, A. S., Egorov, A. R., Kurasova, M. N., Volkova, O. V., Meledina, T. V., Lipkan, N. A., Tskhovrebov, A. G., Kurliuk, A. V., Shakola, T. V., Dysin, A. P., Egorov, M. Y., Savicheva, E. A., & Dos Santos, W. M. (2019). Novel non-toxic high efficient antibacterial azido chitosan derivatives with potential application in food coatings. Food chemistry, 301, 125247. https://doi.org/10.1016/j.foodchem.2019.125247

Kucukgulmez, A., Celik, M., Yanar, Y., Sen, D., Polat, H., & Kadak, A. E. (2011). Physicochemical characterization of chitosan extracted from Metapenaeus stebbingi shells. *Food Chemistry*, *126*(3), 1144-1148. https://doi.org/10.1016/j.foodchem.2010.11.148

Kumar, A., Kumar, A., M M S, C. P., Chaturvedi, A. K., Shabnam, A. A., Subrahmanyam, G., Mondal, R., Gupta, D. K., Malyan, S. K., S Kumar, S., A Khan, S., & Yadav, K. K. (2020). Lead Toxicity: Health Hazards, Influence on Food Chain, and Sustainable Remediation Approaches. International journal of environmental research and public health, 17(7), 2179. https://doi.org/10.3390/ijerph17072179

Kumar, S., Ye, F., Dobretsov, S., & Dutta, J. (2019). Chitosan nanocomposite coatings for food, paints, and water treatment applications. *Applied Sciences*, *9*(12), 2409. https://doi.org/10.3390/app9122409

Kumaraswamy, R. V., Kumari, S., Choudhary, R. C., Pal, A., Raliya, R., Biswas, P., & Saharan, V. (2018). Engineered chitosan based nanomaterials: Bioactivities, mechanisms and perspectives in plant protection and growth. International journal of biological macromolecules, 113, 494–506. https://doi.org/10.1016/j.ijbiomac.2018.02.130

Kumari, S., & Rath, P. K. (2014). Extraction and characterization of chitin and chitosan from (Labeo rohit) fish scales. *Procedia Materials Science*, *6*, 482-489. https://doi.org/10.1016/j.mspro.2014.07.062

Kyzas, G. Z., & Deliyanni, E. A. (2013). Mercury (II) removal with modified magnetic chitosan adsorbents. *Molecules*, 18(6), 6193-6214. https://doi.org/10.3390/molecules18066193

Lead. (2022, May 29) *Wikipedia*. Retrieved June 2, 2022, from https://en.wikipedia.org/wiki/Lead

Levchuk, I., Rueda Márquez, J. J., & Sillanpää, M. (2018). Removal of natural organic matter (NOM) from water by ion exchange - A review. Chemosphere, 192, 90–104. https://doi.org/10.1016/j.chemosphere.2017.10.101

Li, J., Zheng, B., He, Y., Zhou, Y., Chen, X., Ruan, S., Yang, Y., Dai, C., & Tang, L. (2018). Antimony contamination, consequences and removal techniques: A review. Ecotoxicology and environmental safety, 156, 125–134. https://doi.org/10.1016/j.ecoenv.2018.03.024

Liu, C., Wang, B., Deng, Y., Cui, B., Wang, J., Chen, W., & He, S. Y. (2015). Performance of a new magnetic chitosan nanoparticle to remove arsenic and its separation from water. Journal of Nanomaterials, 2015. https://doi.org/10.1155/2015/191829

Liu, L., Li, C., Bao, C., Jia, Q., Xiao, P., Liu, X., & Zhang, Q. (2012). Preparation and characterization of chitosan/graphene oxide composites for the adsorption of Au (III) and Pd (II). *Talanta*, 93, 350-357. https://doi.org/10.1016/j.talanta.2012.02.051

Lopes, C. D. C. A., Limirio, P. H. J. O., Novais, V. R., & Dechichi, P. (2018). Fourier transform infrared spectroscopy (FTIR) application chemical characterization of enamel, dentin and bone. *Applied Spectroscopy Reviews*, 53(9), 747-769. https://doi.org/10.1080/05704928.2018.1431923

Lyons-Weiler, J., & Ricketson, R. (2018). Reconsideration of the immunotherapeutic pediatric safe dose levels of aluminum. Journal of trace elements in medicine and biology : organ of the Society for Minerals and Trace Elements (GMS), 48, 67–73. https://doi.org/10.1016/j.jtemb.2018.02.025

Majd, M., Kordzadeh-Kermani, V., Ghalandari, V., Askari, A., & Sillanpää, M. (2022). Adsorption isotherm models: A comprehensive and systematic review (2010-2020). The Science of the total environment, 812, 151334. https://doi.org/10.1016/j.scitotenv.2021.151334

Malien-Aubert, C., Dangles, O., & Amiot, M. J. (2001). Color stability of commercial anthocyanin-based extracts in relation to the phenolic composition. Protective effects by intra-and intermolecular copigmentation. *Journal of agricultural and food chemistry*, *49*(1), 170-176. https://doi.org/10.1021/jf000791o

Mani, M. S., Kabekkodu, S. P., Joshi, M. B., & Dsouza, H. S. (2019). Ecogenetics of lead toxicity and its influence on risk assessment. Human & experimental toxicology, 38(9), 1031–1059. https://doi.org/10.1177/0960327119851253

Mazhar, R., & Ilyas, N. (2019). Heavy Metal Toxicity in Plants and Its Mitigation. In *Approaches for Enhancing Abiotic Stress Tolerance in Plants* (pp. 171-178). CRC Press.

Mitiku, A. A. (2020). A review on water pollution: causes, effects and treatment methods. *Int J Pharm Sci Rev Res*, *60*(2), 94-101.

Mohamed, M. A., Jaafar, J., Ismail, A. F., Othman, M. H. D., & Rahman, M. A. (2017). Fourier transform infrared (FTIR) spectroscopy. In *Membrane Characterization* (pp. 3-29). Elsevier. https://doi.org/10.1016/B978-0-444-63776-5.00001-2

Mohtashami, R., & Shang, J. Q. (2019). Electroflotation for treatment of industrial wastewaters: a focused review. *Environmental processes*, *6*(2), 325-353. https://doi.org/10.1007/s40710-019-00348-z

Moovendhan, M., Seedevi, P., Vairamani, S., & Shanmugam, A. (2019). Exploring the chemical composition and anticancer potential of oil from squid (Loligo duvauceli) liver waste from fish processing industry. *Waste and Biomass Valorization*, *10*(10), 2967-2973. https://doi.org/10.1007/s12649-018-0304-z

Morin-Crini, N., Lichtfouse, E., Torri, G., & Crini, G. (2019). Applications of chitosan in food, pharmaceuticals, medicine, cosmetics, agriculture, textiles, pulp and paper,

biotechnology, and environmental chemistry. *Environmental Chemistry Letters*, *17*(4), 1667-1692. https://doi.org/10.1007/s10311-019-00904-x

N'diaye, A. D., & Kankou, M. S. A. (2020). Modeling of adsorption isotherms of pharmaceutical products onto various adsorbents: A short review. *J. Mater. Environ. Sci*, *11*(8), 1264-1276.

Nasrollahzadeh, M., Sajjadi, M., Iravani, S., & Varma, R. S. (2021). Starch, cellulose, pectin, gum, alginate, chitin and chitosan derived (nano)materials for sustainable water treatment: A review. Carbohydrate polymers, 251, 116986. https://doi.org/10.1016/j.carbpol.2020.116986

Nguyen, V. B., Nguyen, D. N., Nguyen, A. D., Ngo, V. A., Ton, T. Q., Doan, C. T., Pham, T. P., Tran, T., & Wang, S. L. (2020). Utilization of Crab Waste for Cost-Effective Bioproduction of Prodigiosin. Marine drugs, 18(11), 523. https://doi.org/10.3390/md18110523

Nirmal, N. P., Santivarangkna, C., Rajput, M. S., & Benjakul, S. (2020). Trends in shrimp processing waste utilization: An industrial prospective. *Trends in Food Science & Technology*, *103*, 20-35. https://doi.org/10.1016/j.tifs.2020.07.001

Nishad, P. A., & Bhaskarapillai, A. (2021). Antimony, a pollutant of emerging concern: A review on industrial sources and remediation technologies. *Chemosphere*, *277*, 130252. https://doi.org/10.1016/j.chemosphere.2021.130252

Njati, S. Y., & Maguta, M. M. (2019). Lead-based paints and children's PVC toys are potential sources of domestic lead poisoning - A review. *Environmental pollution (Barking, Essex: 1987)*, *249*, 1091–1105. https://doi.org/10.1016/j.envpol.2019.03.062

Oladzadabbasabadi, N., Mohammadi Nafchi, A., Ariffin, F., Wijekoon, M., Al-Hassan, A. A., Dheyab, M. A., & Ghasemlou, M. (2022). Recent advances in extraction, modification, and application of chitosan in packaging industry. *Carbohydrate polymers*, *277*, 118876. https://doi.org/10.1016/j.carbpol.2021.118876

Ozyalcin, Z. O., & Kipcak, A. S. (2022). The Ultrasound Effect on the Drying Characteristics of Loligo vulgaris by the Methods of Oven and Vacuum-oven. *Journal of Aquatic Food Product Technology*, 1-13. https://doi.org/10.1080/10498850.2021.2024634

Piccin, J. S., Vieira, M. L. G., Gonçalves, J. O., Dotto, G. L., & Pinto, L. A. D. A. (2009). Adsorption of FD&C Red No. 40 by chitosan: Isotherms analysis. *Journal of Food Engineering*, *95*(1), 16-20. https://doi.org/10.1016/j.jfoodeng.2009.03.017

Pohling, J., Dave, D., Liu, Y., Murphy, W., & Trenholm, S. (2022). Two-step demineralization of shrimp (Pandalus Borealis) shells using citric acid: an environmentally friendly, safe and cost-effective alternative to the traditional approach. *Green Chemistry*, *24*(3), 1141-1151. https://doi.org/10.1039/D1GC03140F

Rebouças, J., Oliveira, F., Araujo, A., Gouveia, H. L., Latorres, J. M., Martins, V. G., Prentice Hernández, C., & Tesser, M. B. (2021). Shellfish industrial waste reuse. *Critical reviews in biotechnology*, 1–17. Advance online publication. https://doi.org/10.1080/07388551.2021.2004989

Ripley, G., & Dana, C. A. (Eds.). (1859). *The new American cyclopaedia: A popular dictionary of general knowledge* (Vol. 6). D. Appleton.

Routray, W., Dave, D., Cheema, S. K., Ramakrishnan, V. V., & Pohling, J. (2019). Biorefinery approach and environment-friendly extraction for sustainable production of astaxanthin from marine wastes. *Critical reviews in biotechnology*, *39*(4), 469–488. https://doi.org/10.1080/07388551.2019.1573798

Ruethers, T., Taki, A. C., Johnston, E. B., Nugraha, R., Le, T., Kalic, T., McLean, T. R., Kamath, S. D., & Lopata, A. L. (2018). Seafood allergy: A comprehensive review of fish and shellfish allergens. *Molecular immunology*, *100*, 28–57. https://doi.org/10.1016/j.molimm.2018.04.008

Sah, A. K., Dewangan, M., & Suresh, P. K. (2019). Potential of chitosan-based carrier for periodontal drug delivery. *Colloids and surfaces. B, Biointerfaces*, *178*, 185–198. https://doi.org/10.1016/j.colsurfb.2019.02.044

Saheed, I. O., Da Oh, W., & Suah, F. B. M. (2021). Chitosan Modifications For Adsorption Of Pollutants–A Review. *Journal of Hazardous Materials*, 408, 124889. https://doi.org/10.1016/j.jhazmat.2020.124889

Shahid, M., Khalid, S., & Saleem, M. (2021). Unrevealing arsenic and lead toxicity and antioxidant response in spinach: A human health perspective. *Environmental Geochemistry and Health*, 1-10. https://doi.org/10.1007/s10653-021-00818-0

Shahraki, S., Delarami, H. S., Khosravi, F., & Nejat, R. (2020). Improving the adsorption potential of chitosan for heavy metal ions using aromatic ring-rich derivatives. Journal of Colloid and Interface Science, 576, 79-89. https://doi.org/10.1016/j.jcis.2020.05.006

Shariatinia, Z. (2019). Pharmaceutical applications of chitosan. *Advances in colloid and interface science*, *263*, 131-194. https://doi.org/10.1016/j.cis.2018.11.008

Shellfish. (2022, May 16) *Wikipedia*. Retrieved June 2, 2022, from https://en.wikipedia.org/wiki/Shellfish

Shetty, R., Vidya, C. S., Prakash, N. B., Lux, A., & Vaculík, M. (2021). Aluminum toxicity in plants and its possible mitigation in acid soils by biochar: A review. *The Science of the total environment*, *765*, 142744. https://doi.org/10.1016/j.scitotenv.2020.142744

Shrimp. (2022, March 7) *Wikipedia*. Retrieved June 2, 2022, from https://en.wikipedia.org/wiki/Shrimp

Sieg, H., Braeuning, C., Kunz, B. M., Daher, H., Kästner, C., Krause, B. C., Meyer, T., Jalili, P., Hogeveen, K., Böhmert, L., Lichtenstein, D., Burel, A., Chevance, S., Jungnickel, H., Tentschert, J., Laux, P., Braeuning, A., Gauffre, F., Fessard, V., Meijer, J., … Lampen, A. (2018). Uptake and molecular impact of aluminum-containing nanomaterials on human intestinal caco-2 cells. *Nanotoxicology*, *12*(9), 992–1013. https://doi.org/10.1080/17435390.2018.1504999

Singh, J., Yadav, P., Pal, A. K., & Mishra, V. (2020). Water pollutants: Origin and status. In *Sensors in water pollutants monitoring: Role of material* (pp. 5-20). Springer, Singapore. https://doi.org/10.1007/978-981-15-0671-0_2

Soltaninejad, K., & Shadnia, S. (2018). Lead Poisoning in Opium Abuser in Iran: A Systematic Review. *International journal of preventive medicine*, *9*, 3. https://doi.org/10.4103/ijpvm.IJPVM_22_17

Sowmya, R., Rathinaraj, K., & Sachindra, N. M. (2011). An autolytic process for recovery of antioxidant activity rich carotenoprotein from shrimp heads. *Marine biotechnology (New York, N.Y.)*, *13*(5), 918–927. https://doi.org/10.1007/s10126-010-9353-4

Srinivasan, H., Kanayairam, V., & Ravichandran, R. (2018). Chitin and chitosan preparation from shrimp shells Penaeus monodon and its human ovarian cancer cell line, PA-1. *International Journal of Biological Macromolecules*, *107*, 662-667. https://doi.org/10.1016/j.ijbiomac.2017.09.035

Stahl, T., Taschan, H., & Brunn, H. (2011). Aluminium content of selected foods and food products. *Environmental Sciences Europe*. 23, 37. https://doi.org/10.1186/2190-4715-23-37

Sundar, S., & Chakravarty, J. (2010). Antimony toxicity. *International journal of environmental research and public health*, *7*(12), 4267–4277. https://doi.org/10.3390/ijerph7124267

Teli, M. D., & Sheikh, J. (2012). Extraction of chitosan from shrimp shells waste and application in antibacterial finishing of bamboo rayon. *International journal of biological macromolecules*, *50*(5), 1195-1200. https://doi.org/10.1016/j.ijbiomac.2012.04.003

Tian, B., & Liu, Y. (2020). Chitosan-based biomaterials: From discovery to food application. *Polymers for Advanced Technologies*, *31*(11), 2408-2421. https://doi.org/10.1002/pat.5010

Tietz, T., Lenzner, A., Kolbaum, A. E., Zellmer, S., Riebeling, C., Gürtler, R., Jung, C., Kappenstein, O., Tentschert, J., Giulbudagian, M., Merkel, S., Pirow, R., Lindtner, O., Tralau, T., Schäfer, B., Laux, P., Greiner, M., Lampen, A., Luch, A., Wittkowski, R., … Hensel, A. (2019). Aggregated aluminium exposure: risk assessment for the general population. *Archives of toxicology*, *93*(12), 3503–3521. https://doi.org/10.1007/s00204-019-02599-z

Touir, J., Kitanou, S., Zait, M., Belhamidi, S., Belfaquir, M., Tahaikt, M., Taky, M. & Elmidaoui, A. (2021). The Comparison of Electrodialysis and Nanofiltration in Nitrate Removal from Groundwater. *Indonesian Journal of Science and Technology*, *6*(1), 17-30. https://doi.org/10.17509/ijost.v6i1.31477

Umar, M., Roddick, F., & Fan, L. (2015). Recent advancements in the treatment of municipal wastewater reverse osmosis concentrate—an overview. *Critical Reviews in Environmental Science and Technology*, *45*(3), 193-248. https://doi.org/10.1080/10643389.2013.852378

Vardhan, K. H., Kumar, P. S., & Panda, R. C. (2019). A review on heavy metal pollution, toxicity and remedial measures: Current trends and future perspectives. *Journal of Molecular Liquids*, *290*, 111197. https://doi.org/10.1016/j.molliq.2019.111197

Vareda, J. P., Valente, A., & Durães, L. (2019). Assessment of heavy metal pollution from anthropogenic activities and remediation strategies: A review. *Journal of*

environmental management, *246*, 101–118. https://doi.org/10.1016/j.jenvman.2019.05.126

Vasudevan, S., & Oturan, M. A. (2014). Electrochemistry: as cause and cure in water pollution—an overview. *Environmental chemistry letters*, *12*(1), 97-108. https://doi.org/10.1007/s10311-013-0434-2

Venugopal, V., & Gopakumar, K. (2017). Shellfish: Nutritive Value, Health Benefits, and Consumer Safety. *Comprehensive reviews in food science and food safety*, *16*(6), 1219–1242. https://doi.org/10.1111/1541-4337.12312

Wang, C., Li, T., Yu, G., & Deng, S. (2021). Removal of low concentrations of nickel ions in electroplating wastewater by combination of electrodialysis and electrodeposition. *Chemosphere*, *263*, 128208. https://doi.org/10.1016/j.chemosphere.2020.128208

Wang, G., Liu, J., Wang, X., Xie, Z., & Deng, N. (2009). Adsorption of uranium (VI) from aqueous solution onto cross-linked chitosan. *Journal of hazardous materials*, *168*(2-3), 1053–1058. https://doi.org/10.1016/j.jhazmat.2009.02.157

Wang, J., & Guo, X. (2020). Adsorption isotherm models: Classification, physical meaning, application and solving method. *Chemosphere*, *258*, 127279. https://doi.org/10.1016/j.chemosphere.2020.127279

Wang, L., Peng, H., Liu, S., Yu, H., Li, P., & Xing, R. (2012). Adsorption properties of gold onto a chitosan derivative. *International journal of biological macromolecules*, 51(5), 701-704. https://doi.org/10.1016/j.ijbiomac.2012.06.010

Wang, W., Xue, C., & Mao, X. (2020). Chitosan: Structural modification, biological activity and application. *International journal of biological macromolecules*, *164*, 4532–4546. https://doi.org/10.1016/j.ijbiomac.2020.09.042

Whole Cooked Male Crab. (n.d.) *The Berwick Shellfish Co.* Retrieved May 5, 2022, from https://berwickshellfish.com/products/live-brown-crab.

Xu, Z., Yang, Z., Zhu, T., & Shu, W. (2021). Toxicity of soil antimony to earthworm Eisenia fetida (Savingy) before and after the aging process. *Ecotoxicology and environmental safety*, *207*, 111278. https://doi.org/10.1016/j.ecoenv.2020.111278

Yan, H., Dai, J., Yang, Z., Yang, H., & Cheng, R. (2011). Enhanced and selective adsorption of copper (II) ions on surface carboxymethylated chitosan hydrogel beads. *Chemical Engineering Journal*, 174(2-3), 586-594. https://doi.org/10.1016/j.cej.2011.09.064

Yan, N., & Chen, X. (2015). Sustainability: Don't waste seafood waste. *Nature*, *524*(7564), 155–157. https://doi.org/10.1038/524155a

Zafar-Ul-Hye, M., Tahzeeb-Ul-Hassan, M., Abid, M., Fahad, S., Brtnicky, M., Dokulilova, T., Datta, R., & Danish, S. (2020). Potential role of compost mixed biochar with rhizobacteria in mitigating lead toxicity in spinach. *Scientific reports*, *10*(1), 12159. https://doi.org/10.1038/s41598-020-69183-9

Zhu, C. Q., Zhang, J. H., Sun, L. M., Zhu, L. F., Abliz, B., Hu, W. J., Zhong, C., Bai, Z. G., Sajid, H., Cao, X. C., & Jin, Q. Y. (2018). Hydrogen Sulfide Alleviates Aluminum Toxicity via Decreasing Apoplast and Symplast Al Contents in Rice. *Frontiers in plant science*, *9*, 294. https://doi.org/10.3389/fpls.2018.00294

PUBLICATIONS FROM THE THESIS

Papers

Kipcak, A. S., and Ozyalcin, Z. O., Antimony adsorption study of chitosan produced from Caridea and Brachyura shells. Journal of The Indian Chemical Society, vol.97, no.10, pp.2097-2100, 2020 (Journal Indexed in SCI Expanded).

Projects

Kipçak A. S. , Özyalçın Z. Ö. , Project Supported by Higher Education Institutions, Caridea ve Brachyura Kabuklarından Elde Edilen Kitosan ile Atık Sulardan Ağır Metal Giderimi, 2020